Uncovering the Structural Determinants of DNA Replication Stress Induced by Topoisomerase Inhibition.

Dissertation
zur
Erlangung der naturwissenschaftlichen Doktorwürde
(Dr. sc. nat.)

vorgelegt der

Mathematisch-naturwissenschaftlichen Fakultät

der

Universität Zürich

von

Arnab Ray Chaudhuri

aus
Indien

Promotionskomitee

Prof. Michael Hengartner
Prof. Massimo Lopes (Vorsitz und Leitung der Dissertation)
Dr. Angelos Constantinou
Dr. Vincenzo Costanzo

Zürich, 2011

- to my parents -

ZUSAMMENFASSUNG

Das Enzym Topoisomerase I (TopI) baut durch Relaxation torsionalen Stress während der Replikation und der Transkription der DNS ab. Die TopI Inhibitoren Camptothecin (CPT), sowie seine Derivate Irinotecan und Topotecan (TPT), sind anerkannte Chemotherapeutika. Die Toxizität dieser TopI- Inhibitoren wurde bisher auf die Bildung des sogenannten „TopI cleavage complex“ (Top1cc) auf der DNA, und die replikationsabhängige Konvertierung des mit dem Top1cc einhergehenden Einzelstrangbruches in einen Doppelstrangbruch (DSB) zurückgeführt. Neuere Untersuchungen haben aber gezeigt, dass die genannten Inhibitoren auch die Relaxation durch Top1 verhindern und dadurch zur Ansammlung von positivem „Supercoiling“, d.h. superhelikalen Windungen der DNS führen, ohne allerdings den Mechanismus genauer zu erklären.

Durch biochemische und genetische Methoden und Analyse einzelner Moleküle mittels Mikroskopie in *S. Cerevisiae*, Säugerzellen und Extrakten aus *Xenopus*-Eiern zeigen wir, dass Inhibition von Top1 innerhalb kurzer Zeit Replikationsgabeln verlangsamt und deren „Umkehrung“ bewirkt, und dies weitgehend unabhängig von der Bildung von DSB. Poly (ADP-ribose) polymerase (PARP) Aktivität ist notwendig für die effektive Umkehrung der Replikationsgabeln und die Verhinderung von DSB, die DSB-Reparatur dagegen ist nicht notwendig für die Replikation und die Aktivierung der zellulären Antwort auf die Schädigung der DNS. Diese Ergebnisse zeigen, dass die Umkehrung von Replikationsgabeln eine Strategie der Zelle auf replikativen Stress ist, mit dem Ziel, Brüche der Chromosomen zu vermeiden, und erklärt die molekularen Grundlagen der Zytotoxizität von Top1-Inhibitoren. Darüber hinaus erklären unsere Daten den synergistischen Effekt von Top1 und PARP-Inhibitoren, deren klinisches Potential in Kombinationstherapie derzeit untersucht wird.

Als nächstes möchten wir folgende Fragen beantworten: 1) Ist die Umkehrung von Replikationsgabeln eine allgemeine, physiologische Reaktion auf Probleme bei der

Replikation? 2) Welche molekularen Mechanismen liegen dieser Umkehrung zugrunde? 3) Welche zellulären Faktoren sind an der Bildung, Auflösung oder Prozessierung von umgekehrten Replikationsgabeln beteiligt, die durch Top1-Inhibition und andere Formen von replikativem Stress verursacht werden?

SUMMARY

Topoisomerase I (Top1) releases torsional stress during DNA replication and transcription and is selectively inhibited by camptothecin (CPT) and by its derivatives, irinotecan and topotecan (TPT), approved anticancer drugs. Top1 inhibitor cytotoxicity has been consistently linked to Top1 trapping on the nicked intermediate (Top1 cleavage complex, Top1cc) and conversion of Top1cc to toxic DSB in replicating cells. Recent findings showed that these drugs impair also Top1 relaxation activity, inducing accumulation of positive supercoiling and calling for further mechanistic insight in their cytotoxicity. Our single molecule, biochemical and genomic studies in *S. cerevisiae*, mammalian cells and *Xenopus* egg extracts show that Top1 poisons rapidly induce replication fork slowing and reversal, which can be largely uncoupled from DSB formation at clinically relevant doses. Poly (ADP-ribose) polymerase (PARP) activity is required for effective fork reversal and limits DSB formation, making DSB processing dispensable for bulk DNA replication and checkpoint activation. These data identify fork reversal as a cellular strategy to prevent chromosome breakage upon exogenous replication stress and uncover the molecular events preceding fork collapse upon Top1 poisoning. Moreover, they provide a new mechanistic basis to explain the observed synergistic effects of Top1 and PARP inhibitors, under promising clinical development for combinatorial anticancer treatments. Ongoing and prospective experiments aim to: 1) elucidate whether fork reversal is a general, physiological response to replication stress, 2) understand the molecular mechanisms leading to fork reversal, and 3) identify cellular factors involved in mediating, resolving or processing reversed forks upon Top1 poisoning, as well as other kinds of DNA replication stress.

1. INTRODUCTION

1.1 DNA replication

1.1.1 General concepts of chromosome replication

During the process of growth and division, eukaryotic cells duplicate their genomes with remarkable precision. The fidelity of this process depends on stringent regulatory mechanisms that couple DNA replication to cell cycle progression. Eukaryotic genomes are large, ranging from 10^7 to $>10^9$ base pairs (bp), and are organized into multiple chromosomes. Errors that result in under or over-replication of the genome in any cell cycle have catastrophic consequences and can result in a variety of human genetic diseases, including cancer, birth defects and developmental abnormalities (DePamphlis 2006). Many regulatory mechanisms are in place to ensure that the genome is replicated and then segregated equally to the resultant daughter cells. Sequential assembly and reorganization of complex arrays of proteins are crucial for the coordinated execution of initiation, elongation and termination processes of DNA replication. The progression of the replication fork is monitored strictly to ensure complete replication of the entire genome. These controls ensure that each DNA segment in the genome is duplicated in a timely manner exactly once per cell cycle. Additionally, DNA replication must be coordinated with the other events of the cell cycle, ensuring strict alternation of DNA replication and cell division.

Finally, eukaryotic cells have evolved additional control mechanisms, called checkpoints, which limit the normal course of cell cycle progression in response to potentially genotoxic events, such as DNA damage or perturbations of DNA synthesis. These and the other regulatory mechanisms function together to maintain genome integrity during the replication process (Kelly and Brown, 2000).

1.1.2. Initiation of DNA replication

In eukaryotic cells, DNA replication is initiated from multiple sites on chromosomes, called "origins". In *Saccharomyces cerevisiae* the origins exist as short, well-defined sequences of about 150 bp. These origins, termed as autonomously replicating sequences (ARS) for their ability to confer autonomous replication to plasmids, fire asynchronously during S-phase in order to ensure efficient replication of the chromosomes (Friedman et al., 1995). In the fission yeast *Schizosaccharomyces pombe*, however, the origins are more complex, lack a clear consensus sequence and consist of an AT-rich 500-1000 bp region (Chuang and Kelly, 1999; Kim and Huberman, 1998). In metazoans an even more complex picture emerges, as the origins of replication seem to be heterogeneous in size. In mammalian cells, characterization of sequence elements required for replication initiation has identified AT rich sequences (Paixao et al., 2004; Wang et al., 2004), dinucleotide repeats) and asymmetrical purine-pyrimidine sequences (Wang et al., 2004). Other factors, like topology of the DNA and presence of binding sites for transcription factors, concur in the selection of specific segments on the genome as initiation sites for DNA replication (Houchens et al., 2008; Minami et al., 2006; Remus et al., 2004).

Although the origins of replication have been difficult to define in metazoans, all eukaryotes utilize similar proteins and a conserved mechanism to drive initiation of DNA replication. DNA synthesis is initiated by the binding of initiator proteins to the origins of replication. In *S. cerevisiae* a multi-subunit protein called the origin recognition complex (ORC) binds specifically to ARS sequences (Bell and Stillman, 1992)(Fig.1.1). This complex consists of six proteins, Orc1-Orc6. Similar multi-subunit complexes have been identified in *S. pombe*, *Xenopus* and *Drosophila melanogaster* (Chesnokov et al., 1999; Gavin et al., 1995; Moon et al., 1999; Tugal et

al., 1998). In *S. cerevisiae*, the ORC complex is bound to origins in all stages of the cell cycle (Diffley et al., 1994; Liang and Stillman, 1997) and forms the core of the origin complex to which other components are loaded in a step-wise manner.

The next step in the process is to load the MCM helicase on to the origin. This is brought about by at least two proteins, Cdc6 and Cdt1. This process is like a "clamp loading" procedure in which a clamp loader loads a ring shaped molecule onto the DNA by opening the ring. Cdc6 is an AAA+-ATPase, which is required to load the MCM helicase in G1 phase and has been proposed to act as a clamp loader (Randell et al., 2006). Cdt1, like Cdc6 is also required to load the MCM helicase during G1 phase in eukaryotes. The Cdc6 ATPase activity has been shown to be required for binding of Cdt1 to the origins in vitro (Randell et al., 2006). Hence it has been proposed that Cdt1-MCM complex is loaded onto the ORC-Cdc6 complex during the initiation step. The assembly of these four factors is known altogether as the "pre-replicative complex" (pre-RC)(Fig.1.1).

The transition from G1 to S phase requires the conversion of pre-RCs into active replication forks. Initiation requires origin unwinding, stabilization of single stranded DNA, and loading of the replicative polymerases. These processes need the function of a second set of replication factors and the activities of at least two kinases – Cyclin dependent kinases (CDKs and) the Dbf4 dependent kinase (DDK). Unlike pre-RCs, which form at early and late origins simultaneously, these factors are temporally regulated throughout S phase, being associated with origins at the time of activation. Therefore, mechanisms influencing origin choice and timing probably regulate the targeting of these factors to origins (Takeda and Dutta, 2005).

Origin licensing is blocked during S, G2 and M phases of the cell cycle to prevent rereplication by many redundant levels of regulation. The CDKs mediate most of

these regulations. These include degradation or relocalization of the components of the pre-RC. For example, in yeast Cdc6 is degraded, while in mammals Cdc6 is exported from the nucleus after CDK phosphorylation (Delmolino et al., 2001; Drury et al., 2000). Another level of regulation to prevent rereplication takes place via Geminin. This factor has been shown to bind and inhibit Cdt1, which in turn prevents replication licensing by preventing the loading of MCM helicase to the origins (McGarry and Kirschner, 1998; Wohlschlegel et al., 2000).

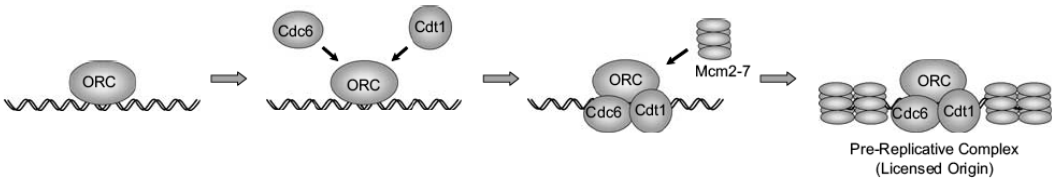

Fig.1.1. Model for the formation of the Pre-Replicative complex (preRC). Modified from Takeda and Dutta, 2005

1.1.3 Origin activation and chain elongation.

Upon initiation, The MCM complex moves away from the origins as part of the replication machinery. Data suggests that the MCM2-7 complex is a ring shaped hexameric complex and could be the putative replicative helicase (Masai et al., 2010). All 6 members of the gene family are essential in both budding and fission yeast. They are AAA+ ATPases with similarity to DNA helicases. The MCM proteins form several stable sub complexes. Characterization of the MCM4-6-7 subcomplex revealed it has ATPase and helicase activities. The helicase activity of this complex was also enhanced by the presence of T-rich regions on the DNA, which is found near replication origins (Masai et al., 2006). A recent study has shown that the MCM2-7 complex is loaded onto the DNA as double hexamer and DNA runs through a central channel in the double hexamer (Remus et al., 2009).

There are several hypothetical models on the mechanism by which the MCM helicase

separates the nascent DNA strands to allow DNA replication. In one of the models known as the "ploughshare model", the MCM double hexamer is loaded onto the origin (Fig.1.2A). After activation, single hexamers translocate in opposite directions along the dsDNA with a ploughshare protein helping to keep the ssDNA unwound as it emerges from behind the helicase (Takahashi et al., 2005). Another model known as "pump-in-ring" or steric exclusion model (Kaplan et al., 2003), suggests that each hexamer also moves bidirectionally on the DNA, but displaces the opposite strand due to the steric hindrance from meeting the dsDNA at the fork (Fig.1.2B). Finally, the "rotary pump" model has different hexamers twisting the DNA at a distance from the origin, resulting in topological strain and unwinding in the center (Laskey and Madine, 2003) (Fig.1.2C). The latter model is based on data showing that MCM2–7 proteins are not located at replication foci in the nucleus (Madine et al., 1995).

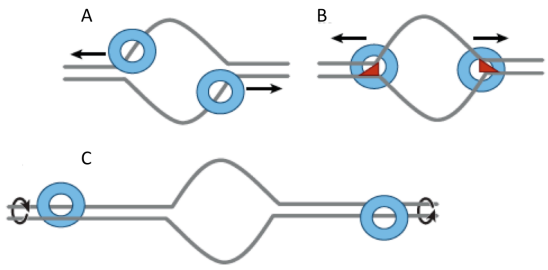

Fig.1.2. Hypothetical models suggested for the unwinding of DNA by MCM helicase: (A) Pump in ring model; (B) Ploughshare model; (C) Rotary pump model. Modified from Sclafani and Holzen, 2007

The transition from pre-RC to replication fork complex requires CDK and DDK activity. These kinases promote the binding of other factors like Cdc45, GINS, Sld3, Sld2 and Dpb11 to replication origins, all of which are essential for origin firing. Firstly, along with CDK and DDK activity, Mcm10 loading is required for the recruitment of Cdc45 (Gregan et al., 2003; Sawyer et al., 2004). Cdc45 recruitment is essential for the subsequent origin unwinding (Masuda et al., 2003; Mimura et al., 2000; Walter and Newport, 2000) and loading of the replicative polymerases (Mimura

and Takisawa, 1998; Uchiyama et al., 2001; Zou and Stillman, 2000). Secondly, Mcm10 facilitates DDK phosphorylation of Mcm2–7 by physically interacting with both complexes (Lee et al., 2003). Mcm10's function in elongation may be related to its ability to retain Cdc45 on elongating forks. Mcm10 also interacts with the elongation factors DNA polymerase δ, DNA polymerase ε and DNA2 (Kawasaki et al., 2000), and has been shown to activate the primase activity of DNA polymerase α in vitro (Fien et al., 2004). Elongating forks pause at unfired pre-RCs in a Mcm10 mutant in *S. cerevisiae* (Homesley et al., 2000), suggesting that assembled pre-RCs may present a barrier to fork progression that is overcome though the action of Mcm10.

In budding yeast, Sld2 and Sld3, which are targeted for phosphorylation by Cdc45, are required for origin firing. Sld3 is essential for the interaction between the MCM complex and Cdc45 (Kamimura et al., 2001)(Fig.1.3). It has also been shown to be targeted by the checkpoint to prevent late origin firing in yeast during replication stress (Zegerman and Diffley, 2010). Another important factor known to be associated with the replisome is the GINS complex. This is a stable, four-factor complex comprising Sld5, Psf1, Psf2 and Psf3, which is essential for DNA replication in both yeast and Xenopus egg extracts (Kubota et al., 2003; Takayama et al., 2003). GINS is necessary for the engagement of Cdc45 with the nascent replisome (Fig.1.3). It is also required for continued association between Cdc45 and MCM complex during S-phase progression (Kanemaki and Labib, 2006; Labib and Gambus, 2007). The GINS complex may be involved in coordinating the progression of the MCM helicase and priming events at the replication fork (Marinsek et al., 2006).

The replisome is assumed to comprise not only factors essential for replication, but also factors involved in other chromosome transactions and chromatin regulation.

These are referred to as "replisome progression complexes" (RPC), which are composed of more than 20 replication related proteins (Gambus et al., 2006). In addition to Cdc45, MCM complex and GINS (referred to as the CMG complex), The RPC contains MRC1, Tof1 and Csm3 (Claspin, Timeless and Tipin in mammalian cells), that are considered fork stabilization factors (Calzada et al., 2005).

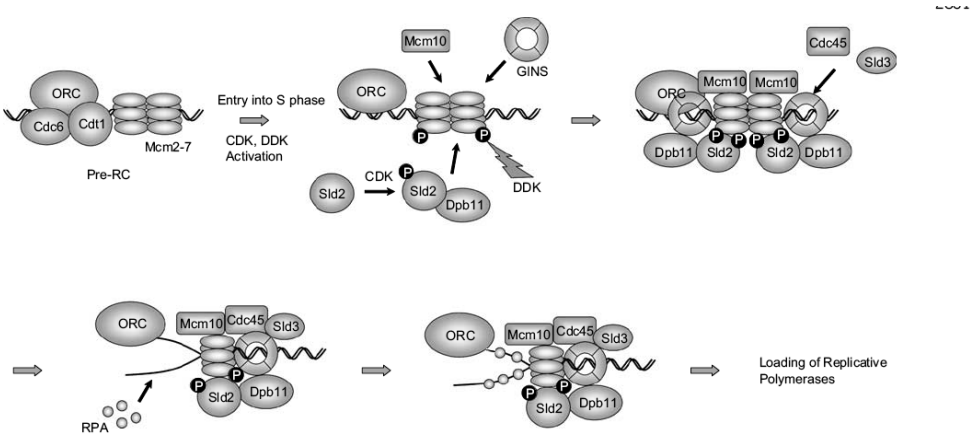

Fig.1.3. Model for the activation of pre-RC by the recruitment of the proteins composing the Replisome Progression Complex (RPC) . Modified from Takeda and Dutta, 2005

Once the duplex DNA at the origin is unwound by the MCM helicase, replication on both the leading and the lagging strands is initiated. Since DNA consists of anti-parallel strands, DNA polymerases must use a 3'-OH of a nucleoside as a primer and synthesize DNA in the 5'-3' direction. Both strands of the DNA helix are copied differently, with one strand synthesized continuously (leading strand) and the opposite strand copied in short - approximately 200 bp - segments (Okazaki fragments), which are joined together postreplicatively (lagging strand). Both the leading strand and every Okazaki fragment on the lagging strand are primed by a short RNA that is synthesized *de novo* by a specialized RNA polymerase called primase, which in eukaryotes is part of the Pol α polymerase complex, known as Pol α–primase (Stillman, 2008). This tetrameric complex comprises two subunits of Pol α together with two primase subunits. Primase acts by synthesizing a short (approx. 10 nt) RNA

primer. The 3' end of the nascent strand then translocates from the primase active site to the polymerase active site to allow synthesis of about 20 nucleotides of DNA (Fig.1.4). After this initiation event, the clamp loader complex replication factor C (RFC) loads the sliding clamp and processivity factor PCNA onto double-stranded DNA (Garg and Burgers, 2005). Either Pol δ or Pol ε is then loaded on to the PCNA–primer– template ternary complex. The sliding clamp encircles the double-stranded DNA and tethers Pol δ and Pol ε to the template to increase enzyme processivity, although the mechanism by which this occurs is not clear. Pol ε has been shown to be the polymerase responsible for leading strand synthesis (Pursell et al., 2007)(Fig.1.4). It is a highly processive enzyme. Lagging strand synthesis on the other hand requires Pol δ (Fig.1.4). It is thought to proceed in several discrete stages, *i.e.*, initiation by DNA primase, limited elongation of the RNA primer by Pol α, a switch of the primer terminus from Pol α to Pol δ proposed to be brought about by RFC, elongation by Pol δ, and maturation of the completed Okazaki fragment in conjunction with Fen1 and DNA ligase1. Each transition is believed to be mediated by a specific protein or protein complex and has to occur with very high efficiency (Garg and Burgers, 2005).

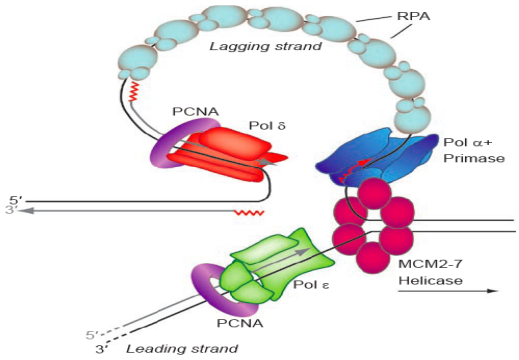

Fig.1.4. Model of a eukaryotic replication fork, depicting the main factors involved in DNA synthesis. Modified from McCulloch and Kunkel, 2008

Unwinding of the DNA helix during replication by the replicative helicase leads to the generation of topological stress in the form of supercoiling on the DNA, which needs

to be resolved for proper fork progression. DNA topoisomerases are enzymes that control and modify the topological state of DNA. By transiently breaking a DNA strand and passing another strand through the transient break (type I topoisomerases), or by transiently breaking a pair of complementary strands and passing another double-stranded segment (type II topoisomerases), these enzymes can catalyze many types of interconversions between DNA topological isomers (topoisomers) (Wang, 2002).

Topoisomerase 1 (Top1) tends to be concentrated in supercoiled regions of chromatin, mostly associated with ongoing transcription or replication (Wang, 2002). It has been shown that Top1 encircles the DNA tightly like a clamp (Stewart et al., 1998) and creates a nick. The relaxation of the supercoils takes place in a stepwise manner which does not allow free rotation of the DNA. It is brought about by a swivel mechanism which involves friction between the rotating DNA and the enzyme cavity and controls the speed of rotation (Koster et al., 2005). Once the relaxation is achieved, the DNA is religated back by Top1 activity in a manner that requires reversing its covalent binding. The religation step requires the 5'-OH group at the DNA end to be aligned with the tyrosine DNA phosphodiester bond which is formed between a tyrosine in the active site of Top1 and DNA during the nicking reaction. Under normal conditions, the cleavage intermediates are transient and religation is favored over cleavage (Pommier, 2006)(Fig.1.5). A recent study showed that deletion of Top1 in human and yeast cells results in slow progression of the replication forks and formation of double stranded breaks (DSB) upon collision of the replication and the transcription machinery (Tuduri et al., 2009). Topoisomerase 1 is a target for chemotherapeutics of the class of camptothecins, the details of which will be discussed later in this Introduction.

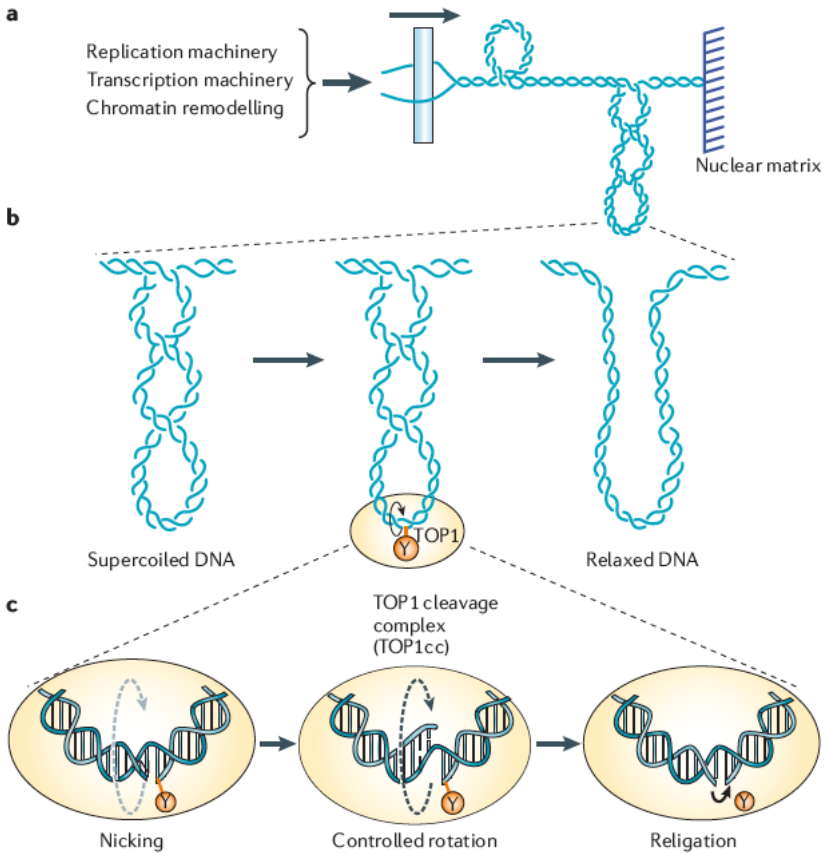

Fig. 1.5. A model for the mechanism of Topoisomerase1 action. Modified from Pommier,2006

1.1.3 Termination of DNA replication

Termination of replication occurs when two opposing replication forks meet and the nascent DNA from the two forks is ligated together. In prokaryotes, which have circular chromosomes as genetic material, termination occurs at sequence specific termini called Ter sites. Such sites (also known as Replication fork barriers or replication termination sites) are also present in specific regions of the eukaryotic chromosomes like the non-transcribed spacers of ribosomal DNA from yeast to man (Rothstein et al., 2000). These replication fork barriers (RFB) are specific DNA sequences that arrest further progress of a replication fork. In these specific regions, termination is achieved by arresting the first fork that enters the termination region,

forcing it to wait there for the inevitable collision with the fork coming from the opposite direction. The best-characterized blocks to eukaryotic replication due to RFBs is the ribosomal DNA repeats of budding yeast on chromosome XII. The RFB is bound by a protein called Fob1 (Brewer et al., 1992; Linskens and Huberman, 1988; Mohanty and Bastia, 2004), but the mechanism by which Fob1 prevents replication fork progression is still elusive. It is thought that the Fob1-RFB complex inhibits the passage of the replicative MCM helicase thus stalling the fork, allowing the fork from the other direction to come in terminate. A recent study in yeast has identified and characterized 71 chromosomal termination regions (TER) in budding yeast. Interestingly, almost all the TERs were shown to contain pausing elements, such as transcription clusters or centromeric regions, that determine the position of fork merging, thus suggesting pausing of the 1st fork as a general mechanism for replication termination. Furthermore, the

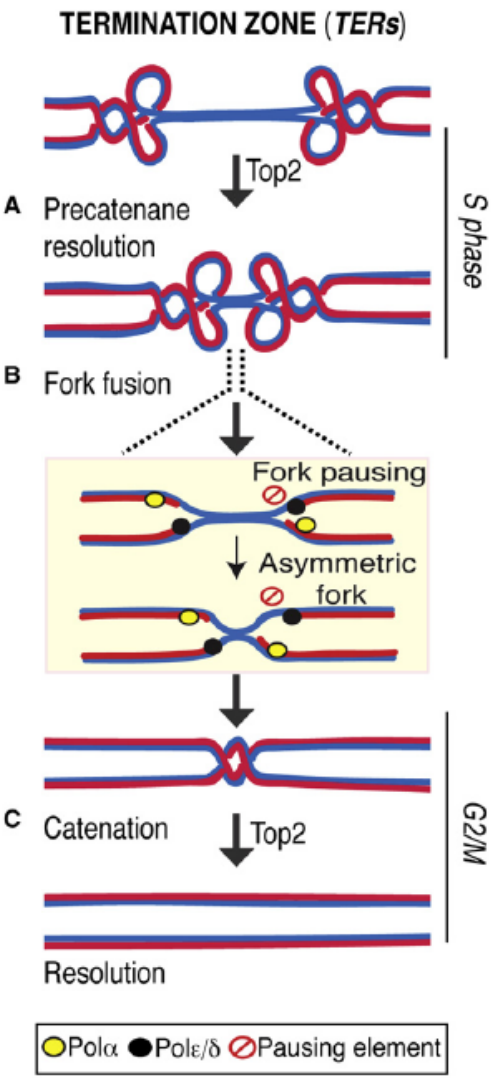

Fig.1.6. Model for replication fork termination
Modified from Fachinetti et al., 2010

DNA helicase Rrm3 was shown to assist fork progression across TERs. Top2 was also shown to bind TERs during S-phase and G2/M to facilitate fork fusion and prevent DNA breakage (Fachinetti et al., 2010)(Fig.1.6).

1.2 DNA damage and repair mechanisms.

1.2.1. DNA damage and consequences.

Cell survival depends on the faithful and accurate transmission of genetic information during cell division. To reach this goal, cells require not only high fidelity DNA replication and precision in chromosome segregation, but also the ability to survive both environmental and endogenous sources of damage which cause a number of different types of lesions on the DNA. Alkylating and oxidizing agents, UV, and ionizing radiation, are among the agents that can result in such lesions.

If these lesions are converted in mutations - either by means of faulty repair or replication errors - the changes are permanent and have their effects in the daughter cells. One of the possible outcomes of mutations is the loss of tumor-suppressor genes and the improper activation of oncogenes, which trigger uncontrolled cellular proliferation and the development of malignant cells. Indeed, genome instability is the hallmark of all forms of cancer (Bartek and Lukas, 2007). Besides these permanent changes to DNA sequence, the epigenome (modifications of DNA bases and of associated histones) can also be subjected to time-dependent, semi-permanent changes; growing evidence suggests that epigenetic changes significantly contribute to cancer (Esteller, 2007).

DNA integrity is compromised mainly from three sides. 1) Spontaneous reactions (mostly hydrolysis) intrinsic to the chemical nature of DNA in an aqueous solution create abasic sites and cause deamination (Lindahl, 1993). 2) Cellular metabolism generates reactive oxygen and nitrogen species, lipid peroxidation products, endogenous alkylating agents, estrogen and cholesterol metabolites, and reactive carbonyl species (De Bont R, 2004), all of which potentially damage DNA. Reactive oxygen and nitrogen species alone generate several kinds of single-strand breaks and

more than 70 oxidated base and sugar products in DNA. 3) DNA is damaged by exogenous physical and chemical agents like UV and carcinogens present in different chemicals. DNA in a cell can be exposed to up to 10^4 endogenous lesions per day (Lindahl, 1993). A single day in the sun can induce up to 10^5 UV photo- products in each exposed keratinocyte, and inflammation can cause high levels of oxidative damage locally (Hoeijmakers, 2009).

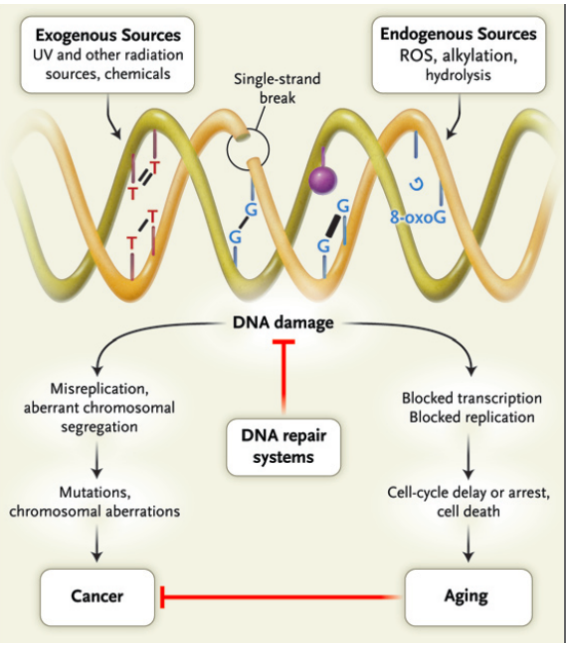

Fig.1.7. Model depicting the sources and the consequences of DNA damage. Modifed from Hoijemakers, 2009

Different types of DNA injury can induce mutations that may finally result in cancer, cell death or senescence, and may also contribute to aging (Fig.1.7). Some lesions are primarily mutagenic, others mainly cytotoxic or cytostatic. Many DNA lesions lead to both types of outcomes in different ratios, depending on the location and number of lesions, cell type, and stage in the cell cycle and differentiation. For example, a well-known mutagenic injury is 8-oxoguanine, an oxidative lesion that on DNA replication pairs equally well with the cytosine (normal pairing) and adenine (abnormal pairing), causing GC→TA transversions (Akbari and Krokan, 2008). In contrast, double strand breaks that are induced by ionizing radiation or that occur during the processing of

interstrand cross-links are primarily cytotoxic or cytostatic.

1.2.2 DNA damage repair mechanisms

To cope with damages in the genetic material, evolution has endowed cells with an array of DNA repair pathways (Fig.1.8). These include systems that repair or replace damaged bases, restore the integrity of the DNA backbone, and allow tolerance of DNA damage. Furthermore, cells have the possibility to activate checkpoints that arrest or attenuate cell cycle progression to allow for repair to take place. Characteristic features of the main DNA repair pathways will be briefly discussed in this chapter.

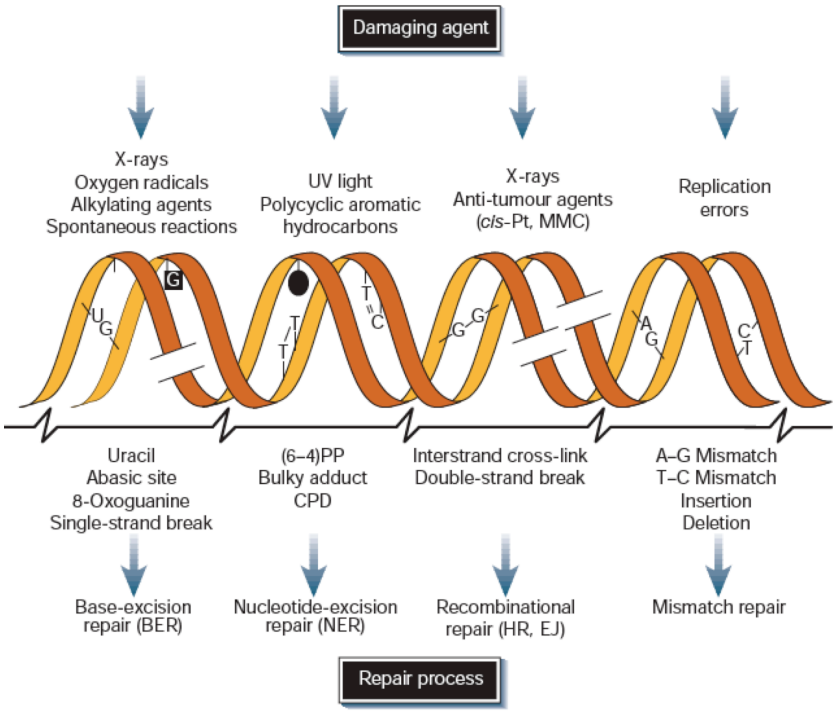

Fig.1.8. Schematics on different DNA damage sources and repair mechanisms. Modified from Hoijemakers 2001.

1.2.2.1 Base Excision Repair

Base excision repair is the primary pathway responsible for the repair of DNA bases from a variety of damage that arise due to oxidation, alkylation, deamination and depurination/depyrimidination. BER repairs the damaged DNA by two general pathways: short patch and long patch BER. The short patch repair pathway is used to repair a single damaged nucleotide, whereas the long patch pathway is used in the repair process of at least two nucleotides. (Robertson et al., 2009). The core BER repair pathway requires the function of at least four proteins which include a DNA glycosylase, an AP endonuclease or AP DNA lyase, a DNA polymerase and a DNA ligase (Kubota et al., 1996). The first step in BER is the recognition of the damaged base by a DNA glycosylase which catalyses the cleavage of an N-glycosidic bond, removing the damaged base and creating an apurinic or apyrimidinic site (AP site)(Fig.1.9). In addition to catalyzing the cleavage of N-glycosidic bonds, some glycosylases are bifunctional having additional AP lyase activity (O'Connor et al., 1989). 11 different mammalian glycosylases have been characterized so far (Robertson et al., 2009). One of the glycosylases, OGG1, can effectively catalyze the cleavage of an N-glycosidic bond between a deoxyribose sugar and the damaged base 8-oxoguanine (8-oxoG), which results from the oxidative damage of a guanosine base. 8-oxoG can base pair with adenine as well as cytosine resulting in G- to -T transversion mutation.

The next step in the process is the cleavage of the DNA backbone by an AP endonuclease or a DNA AP lyase - the activity of which might be present in some glycosylases. There are two different activities capable of cleaving DNA at the AP site. The AP nuclease activity incises the DNA 5'to the AP site creating a sugar

moiety, which must be processed by a DNA polymerase to allow DNA ligation (Fig.1.9). Alternatively, an AP lyase activity in combination with a glycosylase creates a DNA nick containing a 3' sugar moiety, which requires further processing by a polymerase to provide a suitable substrate for a DNA ligase.

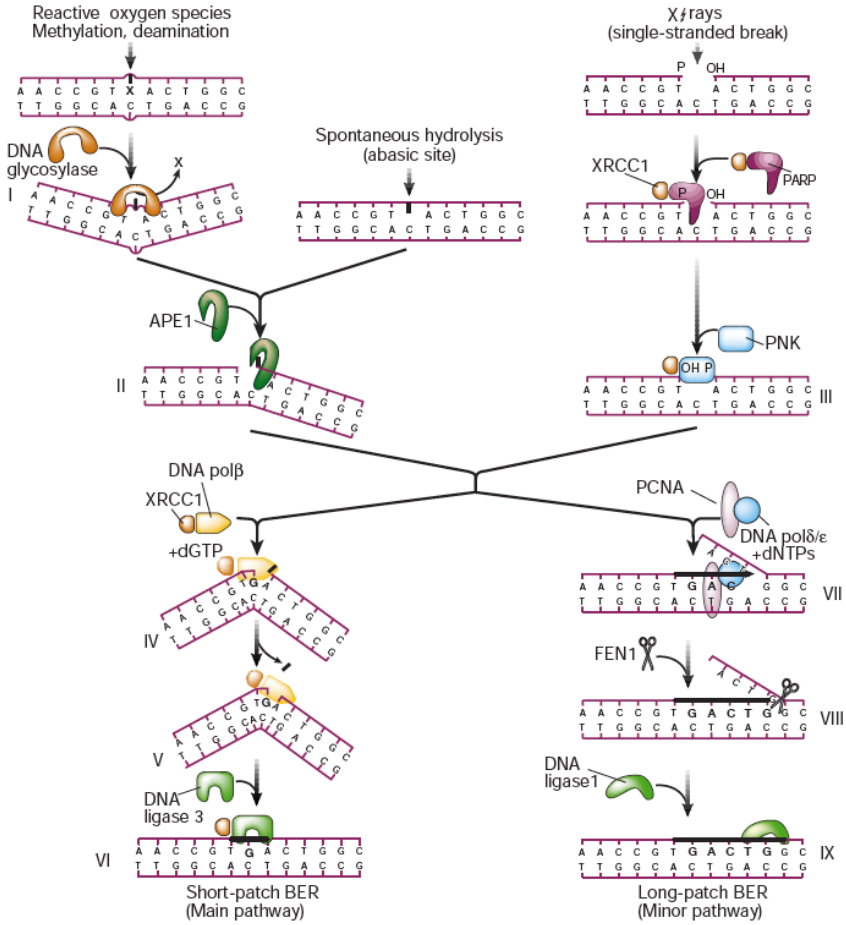

Fig.1.9. Model depicting the mechanism of BER. Modified from Hoijemakers, 2001.

After the cleavage of the DNA backbone, a DNA polymerase fills the gap with the correct nucleotide. For short patch BER DNA polymerase β catalyses this reaction that requires XRCC1 which acts as a scaffold for the recruitment of the ligase as well (Kubota et al., 1996). On the other hand gap filling in Long patch BER is thought to require Polδ and /or Polε, which in turn requires the processivity factor PCNA for its activity (Frosina et al., 1996)(Fig.1.9).

Finally a DNA ligase completes the repair process and restores the integrity of the helix by sealing the nick. The one-nucleotide short patch BER pathway is completed by the action of DNA ligase III (Kubota et al., 1996). Completion of the Long patch BER requires the activity of the replicative DNA ligase I. In addition, long patch BER also requires the activity of flap structure-specific endonuclease1 (Fen1) since strand displacement by polymerase produces a flapped substrate, which is refractory to ligation. Fen1 resolves this problem by removing this flapped substrate (Robertson et al., 2009)(Fig.1.9).

1.2.2.2 Nucleotide Excision repair

NER is involved in the removal of lesions that distort the DNA double helix, interfere in base pairing and block DNA replication and transcription. The most common among these lesions are the cyclobutane pyrimidine dimers (CPDs) and the 6-4 photoproducts (6-4PPs), the most common injuries inflicted by ultraviolet (UV) light and many other kinds of adducts induced by chemical agents. Deficiency in the NER pathway leads to many human diseases such as Xeroderma Pigmentosum, Cockayne's syndrome and trichothiodystrophy (Costa et al., 2003).

There are two pathways for NER : 1) Transcription coupled repair (TCR), selective for lesions present in the transcribed strand of expressed genes and 2) the Global genome NER (GGR) that acts over the rest of the genome.

The first step of NER is the recognition of the DNA lesion by the repair machinery. This step is considerably different for TCR and GGR. The crucial step for damage recognition in GGR is brought about by the XPC-hHR23B complex (Sugasawa et al., 1998)(Fig.1.10). The presence of unpaired bases is a key factor for specific DNA binding by XPC. It poorly recognizes certain types of lesions that induce only a subtle

helix distortion, unless they are combined with a mismatched sequence. For instance, many oxidative base lesions are not highly distorting, so that they are usually detected and handled by base excision repair rather than NER. Another relevant example is the UV-induced CPD where the two affected pyrimidines continue to have a hydrogen bond with the opposite purines, causing minimal helix distortions and thus poor recognition by XPC (Kim et al., 1995). These lesions can be recognized by the UV-DDB complex, which consists of two subunits, DDB1 and DDB2. This complex is thought to promote XPC recruitment to certain type of UV lesions thus facilitating (Sugasawa, 2010)(Fig.1.10).

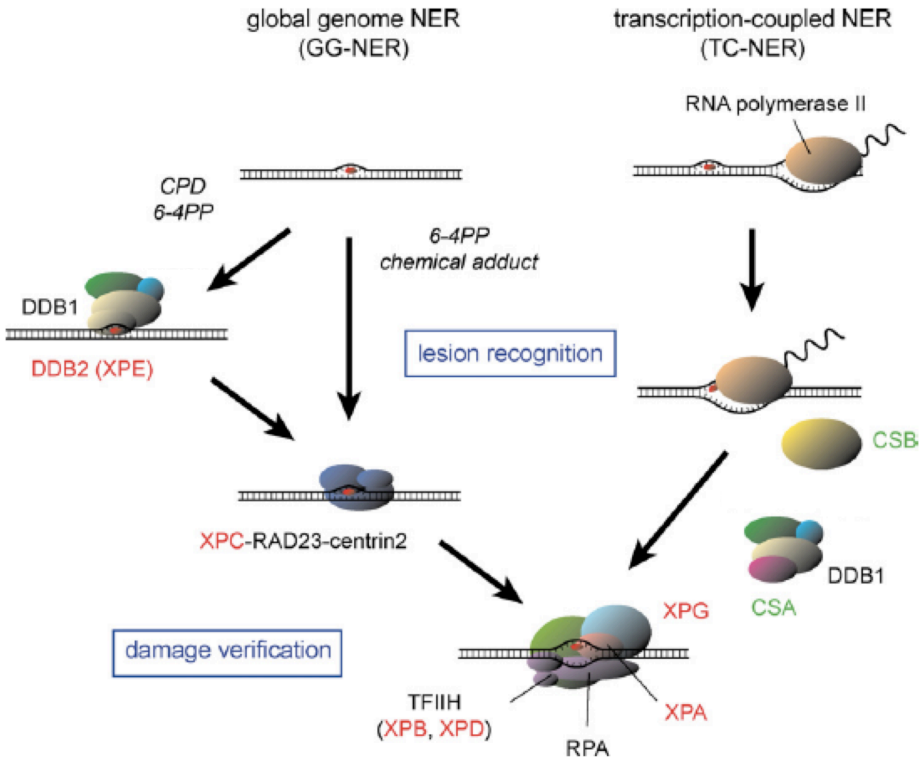

Fig.1.10. Model depicting the mechanism of NER. Modified from Sugasawa, 2010

On the other hand, the XPC-hHR23B complex is dispensable for TCR. For this pathway, the first signal for repair activity is the blockage of transcription elongation by RNA polymerase II in front of DNA lesions (Costa et al., 2003)(Fig.1.10). The stalled polymerase must be displaced to make the injury accessible for repair (Le Page

et al., 2000), and this requires at least two TCR-specific factors: CSB and CSA. The subsequent stages of GG-NER and TCR may be identical. The XPB and XPD helicases of the multi-subunit transcription factor TFIIH open ~30 base pairs of DNA around the damage. XPA then confirms the presence of damage by probing for abnormal backbone structure (Buschta-Hedayat et al., 1999). If the damage is absent the NER process is aborted (Sugasawa et al., 2001). The single-stranded-binding protein RPA (replication protein A) stabilizes the open intermediate by binding to the undamaged strand (Fig.1.10). The use of subsequent factors, each with limited capacity for lesion detection, still allows very high damage specificity (Sugasawa et al., 1998). The XPG and ERCC1/XPF, respectively cleave (Houtsmuller et al., 1999) the borders of the opened stretch only in the damaged strand, generating a 24–32-base oligonucleotide containing the lesion. The regular DNA replication machinery then completes the repair by filling the gap. In total, 25 or more proteins participate in NER. *In vivo* studies indicate that the NER machinery is assembled in a step-wise fashion from individual components at the site of a lesion. After a single repair event the entire complex is disassembled (Houtsmuller et al., 1999).

1.2.2.3 Mismatch Repair

Mismatch repair (MMR) is responsible for several genetic stabilization functions, like correction of DNA biosynthetic errors, ensuring the fidelity of genetic recombination, and participation in the earliest steps of checkpoint and apoptotic responses to several classes of DNA damage (Jiricny, 2006; Kunkel and Erie, 2005). Defects in this pathway are the cause of typical and atypical hereditary nonpolyposis colon cancer, but may also play a role in the development of 15–25% of sporadic tumors that occur in a number of tissues (Modrich, 2006). Mismatch repair-deficient tumor cells are

resistant to certain cytotoxic chemotherapeutic drugs (Iyer et al., 2006; Jiricny, 2006), a manifestation of its involvement in the DNA damage response.

The human genome contains multiple MutS and MutL complex, heterodimeric proteins complexes which are essential for MMR. The functions of the MutS and MutL complex are discussed in Table1.1.

Complex	Components	Function
MutSα	MSH2, MSH6	Recognition of base–base mismatches and small IDLs
MutSβ	MSH2, MSH3	Recognition of IDLs
MutLα	MLH1, PMS2	Forms a ternary complex with mismatch DNA and MutSα; increases discrimination between heteroduplexes and homoduplexes; also functions in meiotic recombination
MutLβ	MLH1, PMS1	Unknown
MutLγ	MLH1, MLH3	Primary function in meiotic recombination; backup for MutLα in the repair of base–base mismatches and small IDLs

Table1.1. Functions of MutL and MutL complexes in MMR. Adapted from Jiricny 2006

The MutSα can initiate the repair of different kinds of mismatches and insertions/deletions (IDLs) of up to 8 unpaired nucleotides. MutSβ is able to repair even larger IDLs , but cannot recognize mispairs. MutLα supports repair initiated by MutSα and MutSβ, whereas the other two heterodimers, MutLβ and MutLγ play only a secondary role in MMR.

The repair is initiated by MutSα recognition of a mismatch. Once the complex is bound, a conformational change is brought about by ATP allowing the complex to diffuse along the DNA in both the directions. The MutSα-ATP complex along with MutLα, searches for a strand discontinuity (Fig.1.11). When a nick is found, Exonuclease1 (Exo1) degrades the DNA in a 5'-3' direction and excises the mismatch. The single strand binding protein RPA binds the complementary strand and protects the ssDNA against endonucleolytic cleavage (Jiricny, 2006). On the other hand, PCNA and RFC are needed for initiating the latent endonucleolytic activity of MutLα

if a 3' nick is found. MutLα nicks the DNA 5' of the mismatch, which then allows Exo1 mediated strand degradation in the 5'-3' direction. Finally the gap is filled by the action of Polδ and the nick sealed by DNA ligase I (Jiricny, 2006)(Fig.1.11).

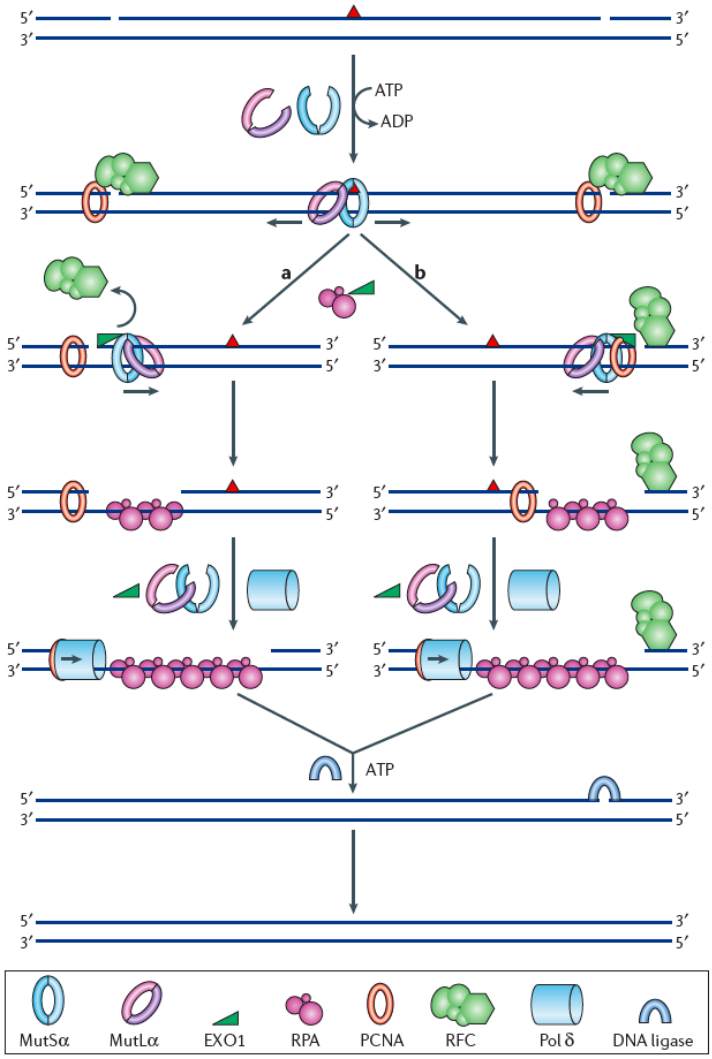

Fig.1.11. Model for MMR. Adapted from Jiricny, 2006

1.2.2.4 Homologous Recombination Repair

Homologous recombination (HR) constitutes a key repair and tolerance pathway for complex DNA damage, which includes DNA double-stranded breaks (DSB), interstrand crosslinks (ICL) and DNA gaps. In addition, recombination and replication are intimately linked, as recombination recovers stalled and broken replication forks. Defects in HR lead to genomic instability and elevated cancer

predisposition, indicating a clear cellular need for this process (Heyer et al., 2010)

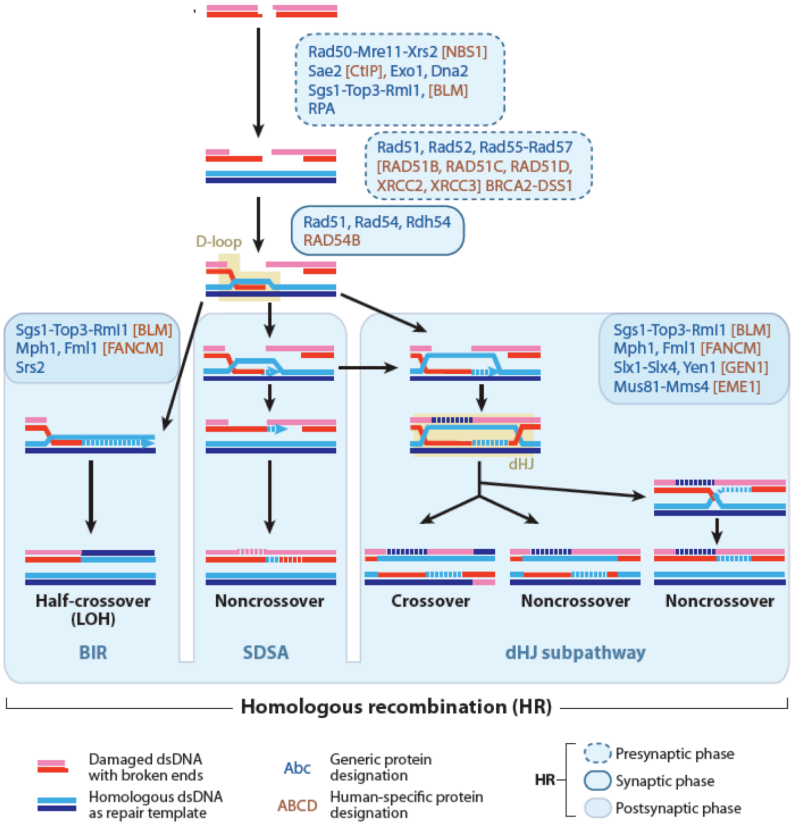

Fig.1.12. Model for HR. Modified from Heyer et al., 2006

The HR process can be divided into 3 stages: presynapsis, synapsis and post synapsis (Fig.1.12). In presynapsis, the DNA damage is processed to form extended regions of single stranded DNA (ssDNA) which is bound by the ssDNA binding protein RPA. For DSBs in mammalian cells, this step involves 4 different nucleases - the MRN complex (Mre11, Rad50, NBS1), Exo1, DNA2 and CtIP (Mimitou and Symington, 2009) - as well as the helicase activity of BLM (Fig.1.12). RPA then binds to the ssDNA. inhibiting formation of secondary structures, which is needed for the proper assembly of Rad51 filaments. RPA bound to ssDNA also forms a kinetic barrier against Rad51 filament assembly, making it necessary for mediator proteins to allow timely Rad51 filament formation on RPA-covered ssDNA. Three different classes of mediators have been described, but their mechanisms of action and the interplay

between them is poorly understood. The Rad51 paralogs constitute a first group and comprise five proteins in mammals (RAD51B, RAD51C, RAD51D, XRCC2, XRCC3). A second class is typified by the Rad52 protein, which performs two independent roles: its mediator function, and a second, later function in strand annealing of RPA-bound ssDNA (Heyer et al., 2010). A third class of mediator proteins is BRCA2, the human breast and ovarian cancer tumor suppressor protein. Human BRCA2 contains ssDNA binding motifs, a double-stranded DNA (dsDNA) binding motif and a number of Rad51 binding sites (Yang et al., 2005). Recent biochemical studies have shown that BRCA2 binds RAD51 and potentiates recombinational DNA repair by promoting assembly of RAD51 onto single-stranded DNA (ssDNA). It acts by targeting RAD51 to ssDNA over double-stranded DNA, enabling RAD51 to displace replication protein-A (RPA) from ssDNA and stabilizing RAD51–ssDNA filaments by blocking ATP hydrolysis. BRCA2 does not anneal ssDNA complexed with RPA, implying it does not directly function in repair processes that involve ssDNA annealing, but acts as a mediator protein (Jensen et al.). During synapsis, the Rad51 filament performs homology search and DNA-strand invasion, generating a displacement loop (D-loop), within which the invading strand primes DNA synthesis. The Rad54 motor protein is required for stabilizing the Rad51 filament and enhancing D-loop formation by Rad51. It is also required for promoting the transition from DNA strand invasion to DNA synthesis by dissociating Rad51 from heteroduplex DNA (Heyer et al., 2006). Finally, in postsynapsis, the three sub pathways of HR are distinguished, each with specific enzymatic requirements (Heyer et al., 2010)(Fig.1.12). The D-loop represents the branching point for the multiple sub-pathways of HR. In the absence of a second end, the D-loop may become a full-fledged replication fork in a process termed break-induced replication (BIR).

Although this process restores the integrity of the chromosome, it can lead to loss-of-heterozygosity of all genetic information distal to the DSB. In the presence of a second end, the predominant pathway for DSB repair in somatic cells appears to be synthesis-dependent strand annealing (SDSA), in which the extended D-loop is reversed, leading to annealing of the newly synthesized strand with the resected strand of the second end (Paques and Haber, 1999). This pathway inherently avoids crossovers, which reduces the potential for genomic rearrangements. While generation of crossovers by double Holliday junction (dHJ) formation is typical of meiotic recombination in germ cells, recently dHJs have also been identified as an intermediate in recombinational DNA repair in somatic cells (Bzymek et al.). dHJ formation involves capture of the second end, a process that is actively blocked by the Rad51 protein in vitro, suggesting an inherent mechanistic bias toward SDSA (Wu et al., 2008). The dHJ intermediate could be resolved by endonucleases like Mus81-Eme1 or Gen1, but the exact mechanisms and identity of proteins involved remain under debate. Alternatively, dHJs can be dissolved by a complex mechanism involving a RecQ-family DNA motor protein (*S. cerevisiae* Sgs1 or human BLM), TopoisomeraseIII (Top3), and cofactors. The two junctions are migrated toward each other, leading to a hemicatenane that is eliminated by Top3 (Fig.1.12). Genetically, the end point of dissolution is always a noncrossover, avoiding the potential for rearrangements associated with crossovers (Wu et al., 2008). Crossovers are defined as recombination events that lead to the exchange of flanking markers generating deletions, inversions, or translocation when non-allelic, repeated DNA sequences are involved.

1.2.2.5 Non Homologous End joining

Non-homologous end joining (NHEJ) is a pathway that specifically repairs DSBs in DNA. NHEJ is referred to as "non-homologous" because the break ends are directly ligated without the need for a homologous template, in contrast to homologous recombination, which requires a homologous sequence to guide repair.

Both HR and NHEJ play a role in DSB repair in mammalian cells. The most important factor determining the choice of repair pathway is probably the cell cycle stage. Whereas HR depends on the use of a template — that can be found on a sister chromatid during S and G2 cell cycle phase — NHEJ brings the DNA termini together in a protein–DNA complex and joins them without the need for homology. This pathway is mainly functional during G0, G1 and early S-phase (Weterings and van Gent, 2004).

The first step of NHEJ is generally considered to be recognition of a DSB, which requires association of DNA termini with the Ku70/80 heterodimer (Fig.1.13). Once the Ku ring is bound to DNA ends, it facilitates recruitment to the DSB of the DNA-dependent protein kinase catalytic subunit (DNA-PKcs). The simultaneous and specific binding of both Ku and DNA-PKcs to DNA ends activates the serine/threonine kinase activity of DNA-PKcs. This leads to phosphorylation of XRCC4, p53 and Artemis. DNA-PKcs also phosphorylates the Ku70, Ku80 and DNA-PKcs subunits of the DNA-PK holo-enzyme itself. The autophosphorylation of DNA-PKcs causes a conformational change in the protein that regulates access by other NHEJ proteins (Uematsu et al., 2007). This conformational change in DNA-PKcs may also alter the conformation of Artemis which can function as a 5'- or 3'-endonuclease at overhangs (Ma et al., 2002) and process DNA termini which have non-ligatable ends. Finally XRCC4/Ligase 4 is recruited, which promotes the

religation of the broken ends with the help of the stimulatory factor XLF (Mahaney et al., 2009) (Fig.1.13).

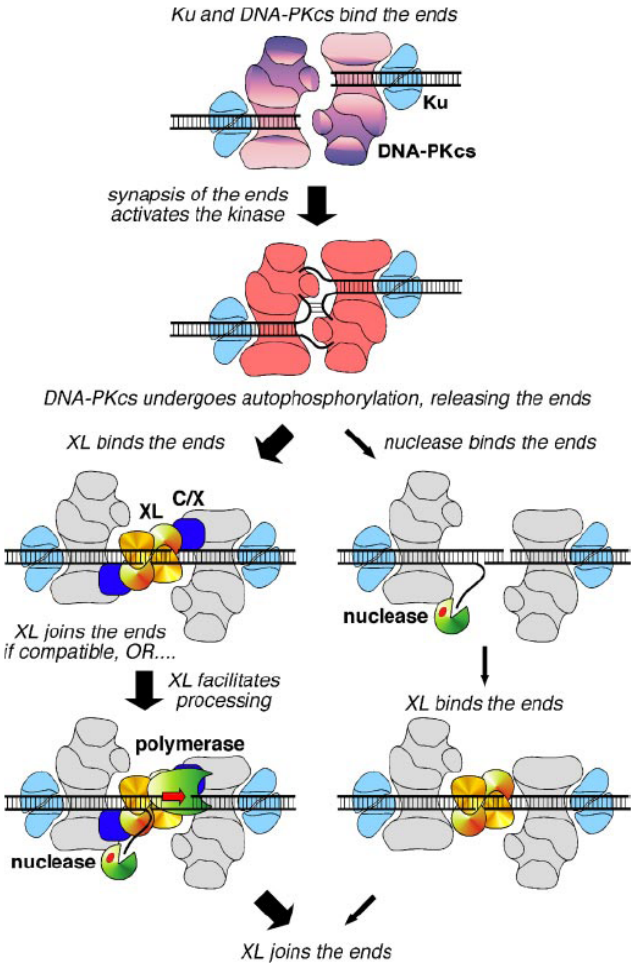

Fig.1.13. Model depicting protein-DNA interactions during NHEJ. Modified from Budman et al., 2007.

1.2.3. DNA damage tolerance mechanisms

1.2.3.1 Translesion synthesis

Although the cells have evolved elaborate repair mechanisms to counteract DNA damage, the repair processes are in some cases slow and incomplete. In these circumstances, the cell is forced to replicate DNA containing persisting damage. It is generally not possible for the replicative polymerases to accommodate damaged base in their active site due to high stringency and fidelity. For this reasons, replication past lesions requires the use of specialized DNA polymerases which have been adapted for this specific function. These polymerases have lower stringency than the replicative polymerase and their active sites are more open and can therefore accommodate damaged bases. There is a growing number of DNA polymerases recently found to mediate DNA synthesis across specific damages. The four main players of this family in human cells are polη, polι, polκ, Rev1 and Polλ. Each one is able to carry out TLS past different lesions in vitro.

It has been suggested that for UV induced lesions like CPDs, translesion synthesis (TLS) with polη is most efficient, inserting the correct nucleotide opposite the damaged base (Masutani et al., 2000). In its absence, a less efficient and more error-prone pathway is brought into play leading to UV induced hypermutations in the DNA. It has been shown that polη localizes to the nucleus, and that during S phase it accumulates in nuclear foci at sites of DNA synthesis (Kannouche et al., 2001). The mechanism by which polη is thought to be recruited to the replication forks upon UV damage is by monoubiquitination of PCNA by Rad6 and Rad18 (Kannouche et al., 2004) which increases the affinity of PCNA for polη. This increased affinity for polη brings about the " polymerase switch" where polδ is replaced by polη at the damaged

replication fork. polη then carries out replication past the CPD. After the lesion is bypassed, polη dissociates and chain extension is taken over by the more processive polδ (Lehmann, 2005)(Fig.1. 4).

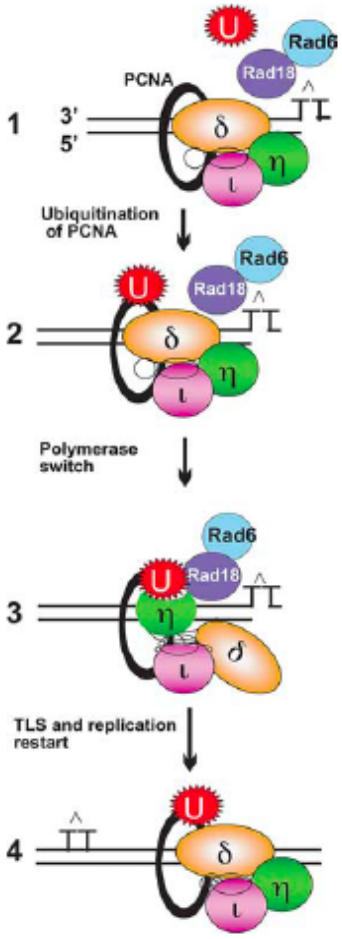

Fig.1.14 Model for TLS in mammalian cells. Modified from Lehmann 2005.

Polι on the other hand can inserts correct bases opposite different kinds of lesions (Tissier et al., 2000), but cannot complete the bypass thus requiring another polymerase to carry out TLS past different lesions. In support to ist role in TLS, it has also been shown to interact strongly with polη (Kannouche et al., 2003)(Fig.1.14).

Another TLS polymerase, polκ, is able to bypass benzo[a]-pyrene (BaP)-guanine adducts quite efficiently and accurately and could also participate in bypass of UV lesions, although its molecular role has not been elucidated (Ogi et al., 2002).

Rev1, though structurally a member of the Y-family of polymerases, is a dCMP

transferase, rather than a DNA polymerase. Little is known about its mechanism of action, but it appears to have a role in the prevention of mutagenesis after DNA damage (Gibbs et al., 2000). It has been shown to interact with the other TLS polymerases and also with Rev7 suggesting its role in TLS (Lehmann, 2005). It has also been speculated to act as a platform for the switch between TLS polymerases (Kannouche and Stary, 2003).

Finally, Pol λ has also been implicated in the bypass of 8-oxoguanine lesions, which are formed on the DNA by the production of free radicals. This bypass process requires the presence of PCNA and Replication protein A (RPA) (Maga et al., 2007).

1.2.3.2 Template switching mechanisms

Template switching has evolved as an important mechanism to promote fork restart, gap-filling and damage bypass. Among damage tolerance mechanisms, template switching contributes largely to error-free bypass and opposes the undesirable effects associated with mutagenesis. The template switching pathway is mainly controlled by RAD5–MMS2–UBC13 genes encoding ubiquitin ligases and ubiquitin conjugating enzymes that mediate PCNA polyubiquitylation (Hoege et al., 2002) and is hypothesized to involve a switch of templates in which the blocked nascent strand uses the undamaged newly replicated strand of the sister chromatid as a temporary replication template (Xiao et al., 2000)(Fig.1.15). One of the models suggested for lesion bypass requires the formation of a reversed fork intermediate, without any requirement for recombination proteins (Higgins et al., 1976). Although the ATPase Rad5 can promote fork reversal *in vitro* (Blastyak et al., 2007; Johnson et al., 1994), whether the reversed fork intermediate promotes error-free bypass of lesions *in vivo* remains a matter of debate. Another mechanism of error free lesion bypass proposes a

recombination-like invasion event, in which the blocked nascent chain invades the opposite homologous duplex and uses the sister chromatid as a template (Minca and Kowalski)(Fig.1.15). It has been suggested that template switching behind the fork leads to X- shaped structures that contain ssDNA, and in which the sister chromatids are linked (Branzei, 2010). These template switch intermediates may also contain Holliday Junctions (HJs) (Mankouri et al., 2011)(Fig.1.15). Whereas the reversed fork model restricts these events to the fork, the recombination-like invasion mechanism can theoretically occur either at the fork or behind the fork.

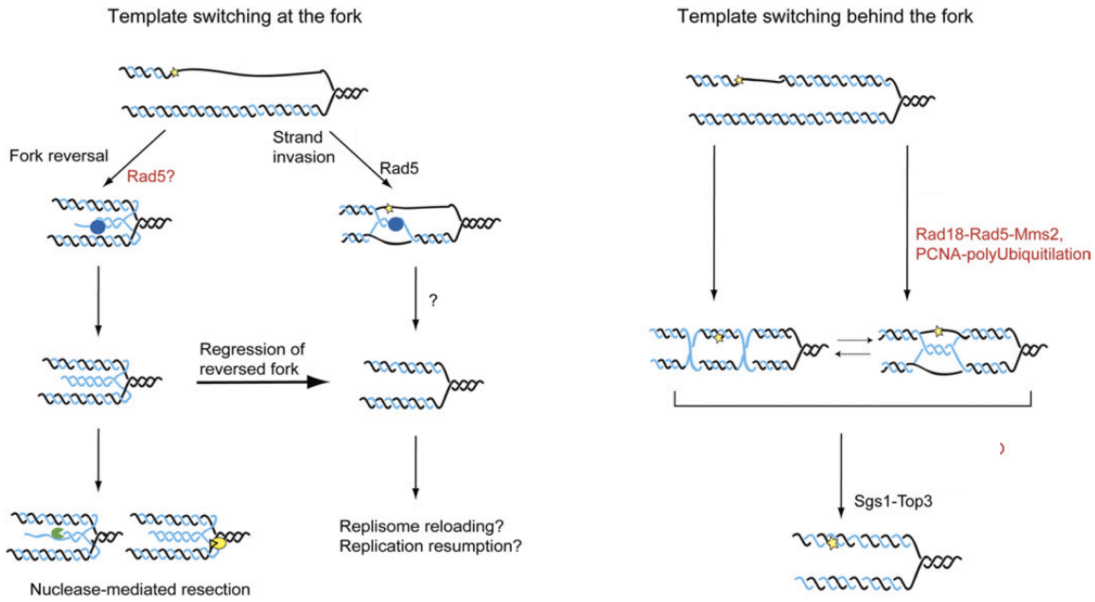

Fig.1.15 A model depicting template switch mechanisms. Modified from Branzei 2011.

The error-free template switch bypass is controlled by the E3 ligase Rad5 that stimulates the E2 ubiquitin conjugating activity of the Mms2–Ubc13 complex to polyubiquitinilate PCNA (Hoege et al 2002). PCNA polyubiquitylation and error-free Rad5–Mms2–Ubc13 complex are required for gap-filling damage tolerance (Branzei et al 2004). They are also required for the formation of damage-dependent sister chromatid junctions behind replication forks (Branzei et al 2008)(Fig.1.15).

The template switch intermediates need to be resolved in order to restore a normal

replication fork and chromosomal structure. Several resolvases have been identified in eukaryotic cells but little is known about their regulation and coordination with one another. Resolution of damage-induced template switch intermediates has been shown to require RecQ helicase Sgs1 (BLM in humans) and Topoisomerase3 (Liberi et al., 2005; Mankouri and Hickson, 2006)suggesting that Sgs1–Top3 represents the major activity involved in template switch intermediate resolution.

1.3 Checkpoint signaling in DNA Damage.

Cells have evolved multiple mechanisms to sense DNA lesions and signal their presence thus activating specific repair pathways. The DNA damage response (DDR) pathway is a signal transduction pathway consisting of sensors, transducers and effectors, which form a network of interacting pathways that together execute the response. The DDR results in the induction of DNA damage checkpoints. These checkpoints halt the proliferating cell in its cell cycle progression, providing more time to the DNA damage repair machinery to repair the lesion. The main players in the checkpoint-signaling cascade are proteins of the Phosphoinositol 3 (PI3) kinases, ATM and ATR. The DNA damage checkpoint can be broadly activated by two kinds of stress: 1) DNA double strand breaks (DSB), which is mediated by the ATM pathway and 2) Replication associated stress, mediated by the ATR pathway. Although the two types of stress response pathways are distinguished, considerable amount of crosstalk exists between them.

DSB are considered the most lethal among DNA insults and can be caused by both intracellular and extracellular agents such as reactive oxygen radicals, ionizing radiation or radiomimetic drugs. DSB induce a robust DDR mechanism, which has been widely studied in eukaryotes. The first step in DDR is the sensing of the DSB. Multiple signals that arise from DSB could lead to crosstalking downstream events. One of these signals is chromatin decondensation, which in turn leads to ATM activation, chromatin association of 53BP1 which acts as a mediator and recruitment of Rad51 repair complex (Su, 2006)(Fig.1.16). The association of the Mre11-Rad50-NBS1 complex to the DNA has also been implicated in DSB sensing (Lee and Paull, 2005) (Fig.1.16). This occurs independently of ATM/ATR and leads to the recruitment and activation of ATM. BRCA1 was proposed to act as a mediator in this

process, because it binds DSB independently of ATM activation and can recruit ATM to the damage (Kruhlak et al., 2006).

On the other hand, the generation of ssDNA formed at stalled replication forks leads to activation of the ATR checkpoint pathway. ssDNA formation leads to the binding of RPA and subsequent recruitment of the ATR-ATRIP, and the 9-1-1 (Rad9-Rad1-Hus1) and Rad17 complexes. Another mediator protein that is recruited and is required DNA replication and checkpoint signaling is TopBP1. TopBP1 has been shown to bind the 9-1-1 complex and also contains a domain that can bind ATRIP and stimulate ATR activity (Kumagai et al., 2006). ATR is also activated by ssDNA generated during DSB resection by the Mre11-CtIP complex leading to the downstream recruitment of additional proteins as described above.

Events downstream of damage-sensing strengthen the initial interaction and recruit additional proteins to the sites of the DNA damage. At the site of DNA damage, the variant histone H2AX gets phosphorylated at serine 139 by ATM, ATR and DNA PK (Rogakou et al., 1998). This phosphorylation then directly recruits Mdc1, which in turn acts to amplify H2AX phosphorylation over megabases of DNA possibly by tethering ATM or preventing H2AX dephosphorylation (Stucki and Jackson, 2006). Mdc1 and H2AX also allow the recruitment to sites of damage of many additional factors - like 53BP1, p53 etc. - driving the repair process (Fig.1.16). Mdc1 phosphorylation also leads to ubiquitination events at the sites of DSBs, which further acts as a signal to assemble repair proteins. Phosphorylation of Mdc1 leads to the recruitment of an E3 ubiquitin ligase UBC13-RNF8 which ubiquitinates H2AX and possibly other proteins, in order to recruit 53BP1 (Huen et al., 2007; Kolas et al., 2007).

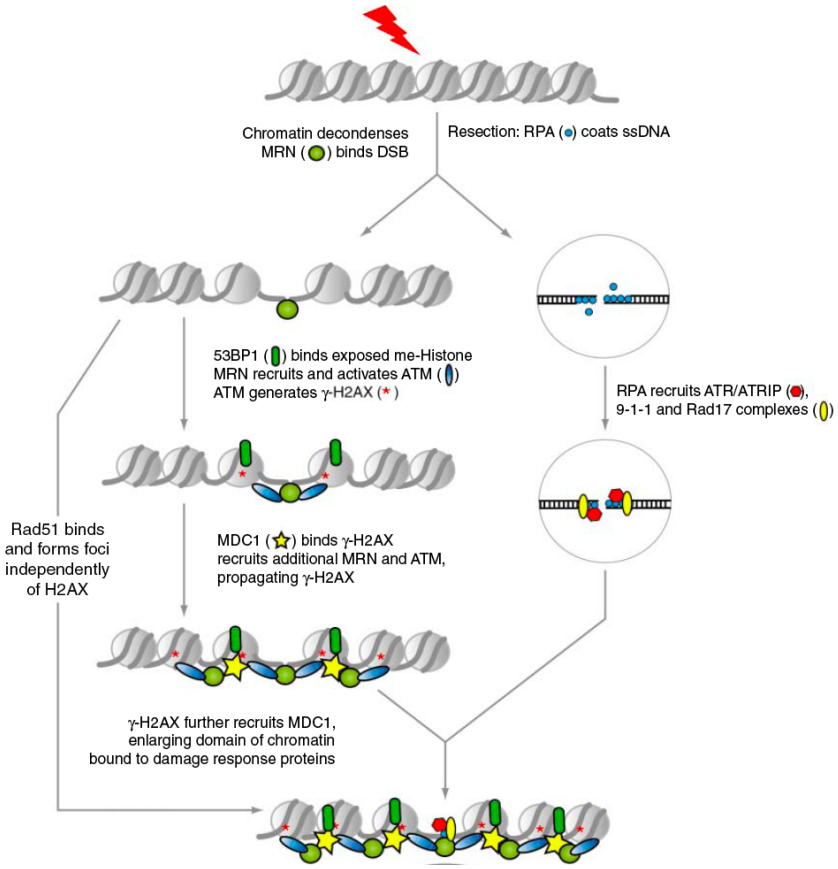

Fig.1.16. Model for the activation of DDR in response to DSB. Adapted from Su, 2006

Signals initiated by the sensors very rapidly transduce to ATM and ATR kinases, which are both extremely large proteins that phosphorylate a great number of substrates. In humans, mutations in ATM cause ataxia telangiectesia, a rare autosomal recessive disease characterized by cerebellar degeneration, immunodeficiency, genome instability, clinical radiosensitivity and predisposition to cancer (Shiloh, 1997). The protein kinase activity of ATM is minimal or low but can be stimulated in vivo by agents that induce DSBs in vivo and by linear DNA in vitro. Activated ATM phosphorylates many proteins, including BRCA1 (Cortez et al., 1999), NBS1 (Lim et al., 2000), Chk2 and p53 (Banin et al., 1998; Canman et al., 1998), as well as itself (Bakkenist and Kastan, 2003) in the sequence context of SQ or TQ. ATM under unstressed conditions exists as a homodimer in which tight intermolecular binding to

a protein domain at around Ser1981 physically blocks the kinase domain. DSBs cause a conformational change in the ATM protein that stimulates the kinase to phosphorylate Ser1981 by intermolecular autophosphorylation, resulting in dissociation of the homodimer. The conformational change does not appear to require binding to the site of DNA damage, but results from some change in the higher-order chromatin structure. Such chromatin changes can be sensed at some distance away from the DSB site. ATM kinase activity is also regulated by binding to Mre11 that enhances its ability to phosphorylate substrates in vitro (Lee and Paull, 2005). Thus ATM activity is likely to be regulated by two distinct events, one being the intermolecular autophosphorylation of ATM and dissociation of its homodimer induced by unknown chromatin changes, and the other, recruitment of the activated ATM to the kinase substrates.

ATR is the initiator of the checkpoint response to a wide variety of agents that cause replication forks to stall. As discussed above, it is also required for the response to DSB, by getting recruited to ssDNA generated by DSB resection. The gene encodes a protein of 303 kDa with a C-terminal kinase domain and regions of homology to other PIKK family members. ATR deficiency in mice results in early embryonic death (Brown and Baltimore, 2000) and mutations causing a partial loss of its activity have been reported to be associated with the human autosomal recessive disorder Seckel syndrome (O'Driscoll et al., 2003). As with ATM, ATR is capable of specifically phosphorylating serine or threonine residues in SQ/TQ sequences. Unlike ATM, however, there is no measurable change in the kinase activity of ATR, suggesting that it may be constitutively ready to phosphorylate substrates but that its functions may be largely dependent on its subcellular localization. In human cells, ATR exists in a stable complex with ATRIP (Cortez et al., 2001). Given that RPA, an ssDNA-binding

protein, stimulates *in vitro* binding of ATRIP to ssDNA (Zou and Elledge, 2003), it is possible that the ATR–ATRIP complex is recruited at sites of DNA damage by means of the binding of ATRIP to RPA. ATR is thought to have a pivotal function in the normal cell cycle because, differently from ATM, it is essential for embryonic development. The observation that RPA is involved in DNA replication (Dutta and Stillman, 1992) and a component of the DNA replication fork led to a model in which ATR–ATRIP localizes to sites of this fork, monitoring the progression of DNA replication. Once the active ATR is translocated to DNA replication foci, it can phosphorylate and activate Chk1. This model is consistent with the observation that Chk1 is also essential for embryonic cell viability (Liu et al., 2000; Takai et al., 2000). Also, it has been reported that ATR regulates late origin firing of DNA replication (Shechter et al., 2004). Therefore, ATR appears to be a multi-functional kinase that regulates several distinct events from S phase to M phase.

Among the prominent substrates of the apical checkpoint kinases ATM and ATR are the two serine/threonine checkpoint effector kinases CHK2 and CHK1 (Fig1.17). Although there is some cross-talk between ATM and CHK1, in general the ATM and ATR mediated phosphorylations trigger preferentially the activation of CHK2 and CHK1 respectively (Bartek and Lukas, 2003). Phosphorylation of CHK2 renders it freely diffusible in the nucleoplasm, spreading DDR signaling by phosphorylating its substrates throughout the nucleoplasm (Lukas et al., 2003). Similarly, once CHK1 is activated by phosphorylation, mainly by ATR but also by ATM, it is not retained at DNA lesions and diffuses throughout the nucleus (Bekker-Jensen et al., 2006). Ultimately, checkpoint enforcement results from multiple, often redundant, signaling pathways that converge on key decision-making factors, such as p53 and the CDC25 phosphatases (Fig.1.17). DNA damage induced CDC25 inactivation causes a rapid

cell-cycle arrest, as these phosphatases are essential for proliferation (Mailand et al., 2000). In contrast, slower p53 induction following phosphorylation by DDR kinases (Turenne et al., 2001) leads to its stabilization and enhancement of its ability to induce the transcription of p21, a cyclin-dependent kinase inhibitor (Deng et al., 1995), which triggers a stable cell-cycle arrest.

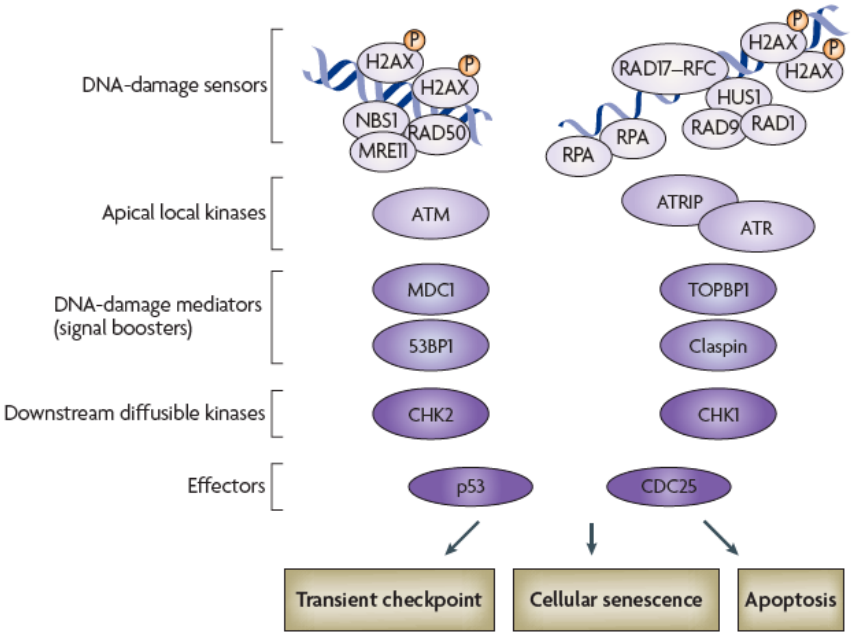

Fig.1.17. Model for the signal transduction cascade during checkpoint signaling. Modified from Fabrizio d'Adda di Fagagna 2008

1.4 DNA damaging agents as chemotherapeutics

Cancer chemotherapy comprises a wide range of treatments for cancer patients, aiming at killing cancer cells more effectively than normal tissue cells. Therapies therefore need to exploit specific molecular and cellular features of the cancer cells they are aiming to eliminate. Cancer cells proliferate more rapidly than their normal counterparts, so most cancer drugs target factors required for cell cycle. The most common means of targeting the cell cycle is to exploit the effect of DNA-damaging drugs. DNA damage causes cell-cycle arrest and cell death either directly or following DNA replication during the S phase of the cell cycle. Cellular attempts to replicate damaged DNA can cause increased cell killing, thus making DNA-damaging treatments more toxic to replicating cells than to non-replicating cells. However, the toxicity of DNA-damaging drugs can be reduced by the activities of several DNA repair pathways that remove lesions before they become toxic. Since the efficacy of DNA damage-based cancer therapy can be boosted by specific defects in DNA repair pathways, synthetic lethal approaches are becoming increasingly popular for the treatment of specific cancers in which one of the DNA repair pathways is compromised. Synthetic lethality arises when inactivation of a specific cellular function leads to cell death in combination with another genetic defects or treatments, whereas each of this events is per se compatible with life. A typical example of "synthetic lethality"-approach for chemotherapy - i.e. the use of PARP inhibitors for treatment of cancers where HR is compromised - will be discussed below. Thus, more in general, DNA repair mechanisms constitute promising targets for novel cancer treatments.

Many anti-cancer drugs employed in the clinic are highly efficient in killing proliferating cells. High levels of DNA damage cause cell-cycle arrest and cell death.

Also, DNA lesions that occur in S phase of the cell cycle can impede replication fork progression, resulting in the formation of replication-associated DSB, considered to be the most toxic of all DNA lesions. Common types of DNA damage that interfere with the DNA replication process are chemical modifications (adducts) of DNA bases, created by reactive drugs that covalently bind DNA either directly or after being metabolized in the body (Fig.1.18). These alkylating agents are grouped in two categories: 1) monofunctional alkylating agents with one active moiety that modifies single bases (alkyl sulfonates, Nitrosourea compounds and Temozolomide) and 2) bifunctional alkylating agents that have two reactive sites and crosslink DNA with proteins or, alternatively, cause DNA intra-strand crosslinks and inter-strand crosslinks (Nitrogen Mustard, Mitomycin C and Cisplatin). Inter-strand crosslinks pose a severe block to replication forks and the mechanisms for replication completion in the presence of these adducts are still largely elusive. Antimetabolites, such as 5-fluorouracil (5FU) and thiopurines, resemble nucleotides, nucleotide precursors or cofactors required for nucleotide biosynthesis and act by inhibiting nucleotide metabolism pathways, thus depleting cells of dNTPs. They can also impair replication fork progression by becoming incorporated into the DNA (Swann et al., 1996). In general, the molecular mechanisms through which anti-metabolites induce cell death are poorly understood.

Another means of interfering with replication is to exploit DNA strand breaks that arise naturally during the process of DNA synthesis (Fig.1.16). Topoisomerases resolve torsional strains imposed on the double helix during DNA replication or during termination by creating single stranded nicks or double stranded breaks. Resealing of these breaks can be prevented by the use of topoisomerase poisons that trap the enzymes in complex with the DNA. The nature of the damage that is caused

depends on which type of enzyme is targeted. Top2 poisons like Etoposide cause DSBs during late replication or during mitosis, while Top1 poisons like Camptothecin have been thought to cause replication-associated DSBs during replication elongation (Hsiang et al., 1985; Markovits et al., 1987). The cytotoxicity associated with this treatment is discussed in more details below and is the subject of study in this thesis.

Ionizing radiation and radiomimetic agents such as bleomycin cause replication independent DSBs that can kill non-replicating cells (Fig.1.16). In addition, such treatments can also rapidly prevent DNA replication by activation of cell-cycle checkpoints to avoid formation of toxic DNA replication lesions.

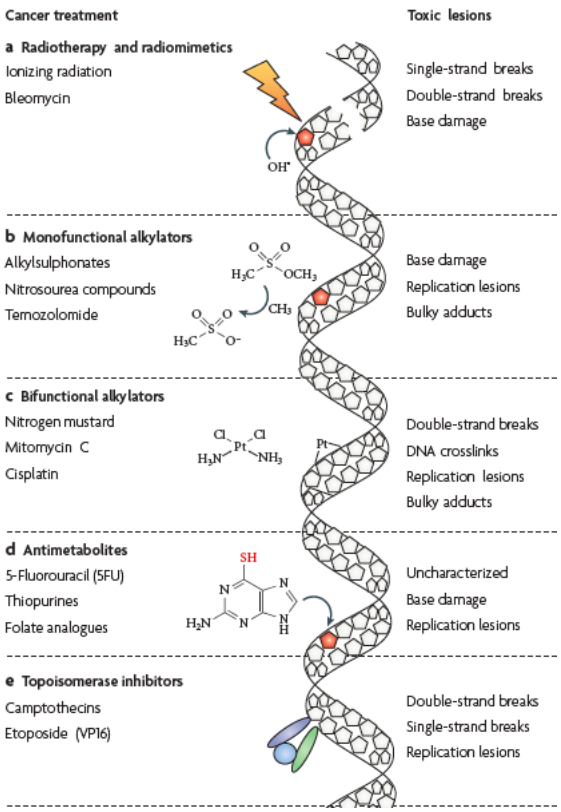

Fig.1.18. Schematics showing the different types of chemotherapeutics used. Modified from Helleday et al., 2008

1.4.1 Topoisomerase inhibition

DNA undergoes conformational and topological changes during many cellular processes such as replication and transcription. Topoisomerases have evolved to solve these conformational and topological changes in DNA. They perform their functions by introducing transient protein-bridged DNA breaks on one (type I) or both DNA strands (type II). Both types of topoisomerases have been isolated from mammalian cells. While Top1 can relax supercoiled DNA, only Top2 can unlink two intertwined DNA circles via its strand-passing activity (Liu, 1989). Inhibition of topoisomerase activity has been frequently used in cancer chemotherapy.

Top1 enzymes are particularly vulnerable to inhibitors like Camptothecin (CPT) during their transient cleavage step (cleavage complex). Top1 cleavage complexes (Top1ccs) are normally transient, but CPT and its derivatives specifically and reversibly trap these complexes. The religation of TOP1ccs requires nucleophilic attack of the tyrosyl-DNA-phosphodiester bond by the free DNA end (the 5′-hydroxyl end). It requires perfect alignment of the 5′-hydroxyl-DNA end with the tyrosyl-phosphodiester bond to be religated back, a step inhibited by the formation of stable Top1ccs by CPT.

Replication-fork collision with the Top1ccs has been proposed to be the primary cytotoxic mechanism for Top1 inhibitors in dividing cells (Holm et al., 1989). This hypothesis is known as the " Replication run-off "theory as the leading strand is thought to be replicated up to the last nucleotide at the 5′ end of the Top1cc (Fig.1.19). This hypothesis has been supported by data implicating the role of DNA damage markers like H2AX phosphorylation and homologous recombination factors in CPT induced cytotoxicity (Pommier, 2006).

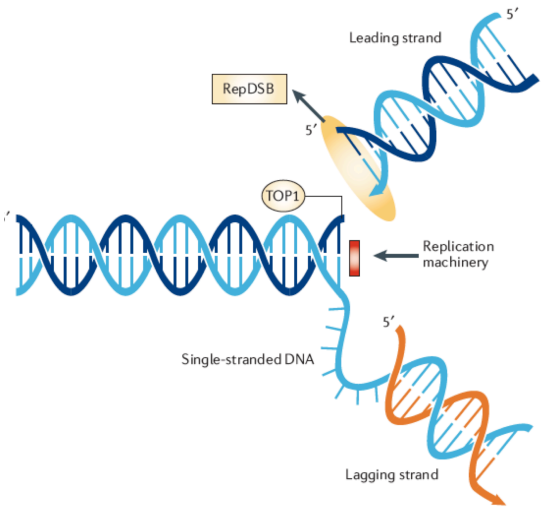

Fig.1.19. Model depicting the Replication run-off theory. Modified from Pommier, 2006.

A recent report has however challenged this hypothesis, by showing that Top1 inhibitors also prevent the relaxation activity of Top1, thus leading to the accumulation of positive supercoiling on the DNA, which may contribute to Top1 poison-mediated cytotoxicity (Fig.1.20). The cytotoxic potential of increased topological stress induced by Top1 inhibitors during DNA replication is the main subject of this PhD thesis.

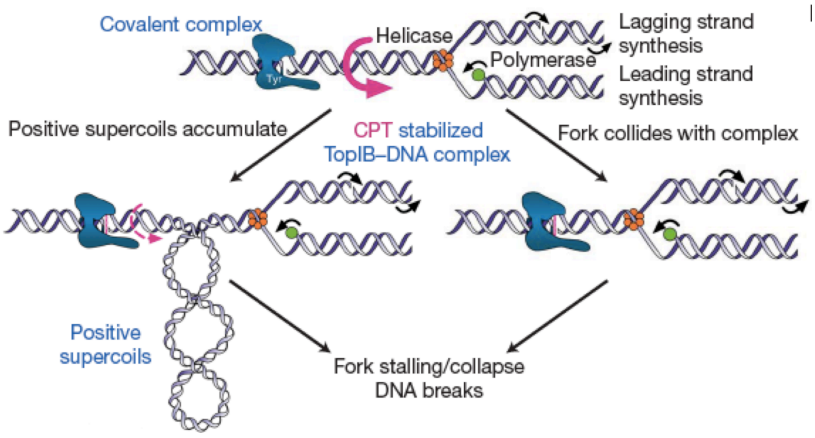

Fig.1.20. Model showing the accumulation of positive supercoils in response to Top1 inhibition and its potential contribution to cytotoxicity. Modified from Koster et al., 2007

Top1ccs can however be removed from the DNA by the tyrosyl-DNA-phosphodiesterase (TDP1) excision pathway, which involves the XRCC1 and base

excision repair (BER) complex. TDP1 was identified as an enzyme that hydrolyses a tyrosyl residue from the 3′ end of DNA in yeast (Pouliot et al., 1999). In humans, mutations inactivating TDP1 are responsible for the autosomal recessive disease spino-cerebellar ataxia with axonal neuropathy (SCAN1)(Takashima et al., 2002). TDP1 forms macromolecular complexes with the BER complex including XRCC1, which has been proposed to repair the lesion formed by the Top1ccs. In addition, Top1 needs to be proteolytically degraded or denatured for efficient Tdp1 activity (Interthal et al., 2005). This appears to be mediated by ubiquitination events, as Top1 ubiquitination and degradation have also been observed following camptothecin treatment (Desai et al., 1997).

Top2 plays a major role in removing the intertwining of the two newly replicated strands (precatanes) generated behind the replication fork (Zechiedrich and Cozzarelli, 1995). It has also been shown to assist the completion of DNA replication by its enrichment at termination zones (Fachinetti et al., 2010). In contrast to Top1 inhibitors, Top2 inhibitors, such as etoposide and ICRF 193, act late during replication or during mitosis. The cytotoxicity induced by etoposide treatment has been attributed to the formation of stable cleavage complex of the drug with Top2, inhibiting the religation step and thus resulting in DSB (Bromberg et al., 2003). ICRF 193 treated cells on the other hand have problems to progress beyond mitosis, with defects in chromosome segregation leading to hyper-catenated DNA which elicits a checkpoint response (Baxter and Diffley, 2008).

1.4.2 PARP inhibition.

PARP is a nuclear protein responsible for the detection and signaling of single strand DNA breaks (SSB) to the enzymatic machinery involved in the SSB repair. PARP activation is an immediate cellular response to metabolic, chemical, or radiation-induced DNA SSBs or DSBs. Once PARP detects a DNA damage it binds to the DNA, and, after a structural change, begins the synthesis of a poly(ADP-ribose)chains (PAR) as a signal for other DNA repair enzymes (Fig.1.19). Some of the factors recruited to the damage include proteins of the BER pathway such as DNA ligase III, DNA polβ and scaffolding proteins such as XRCC1. After repair, the PAR chains are degraded via PAR glycohydrolase (PARG). NAD+ is required as substrate for generating ADP-ribose monomers (Rouleau et al., 2010). In addition to its role in BER described above, PARP is involved in several other nuclear processes. It has recently been observed that rapid recruitment of Mre11 and ATM, crucial components of the homologous recombination machinery, to DNA DSBs is dependent on PAR synthesis (Haince et al., 2007; Haince et al., 2008), which suggests that PARP acts as a facilitator of homologous recombination. Studies in mammalian cells indicate that recruitment of Mre11 to assist replication fork restart is also dependent on PARP (Bryant et al., 2009). *In vitro* studies have also implicated the role of PARP in NHEJ (Audebert et al., 2004). Although PARP is spontaneously recruited to sites of DSBs, it does not seem to play a direct role in DSB repair (Yang et al., 2004). PARP1 can also regulate transcription by modulating chromatin structure, altering DNA methylation patterns, acting as a co-regulator of transcription factors and interacting with chromatin insulators (Caiafa and Zlatanova, 2009).

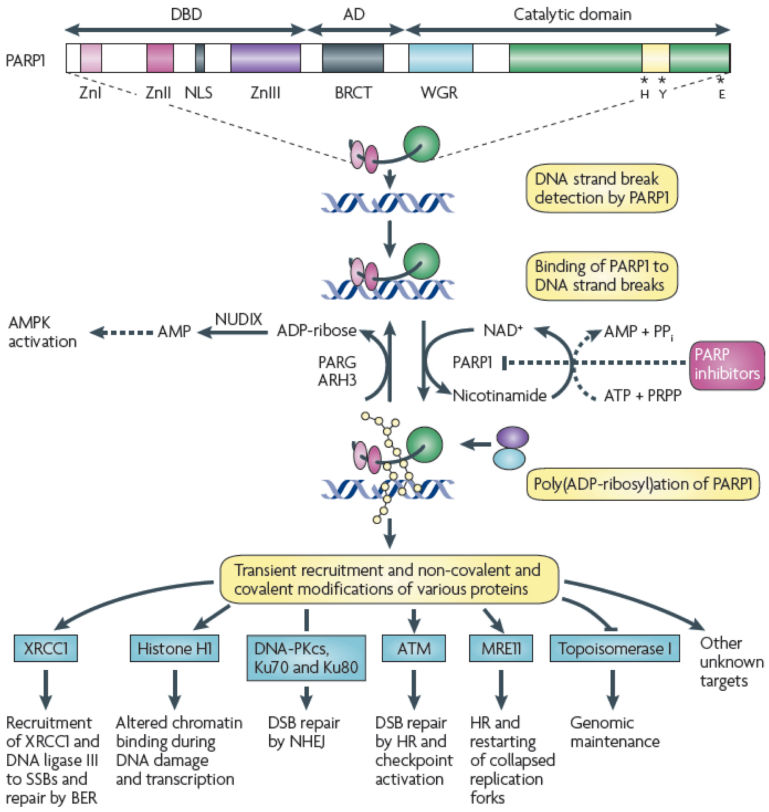

Fig1.20. Model suggesting the role of PARP in DNA repair. Modified from Rouleau et al 2010.

Recently, small molecule inhibitors of PARP have been developed as chemotherapy sensitizers for the treatment of cancer. It has been demonstrated that BRCA1-deficient and BRCA2-deficient cells, when compared with matched wild-type cells, are profoundly sensitive to PARP inhibitors (Bryant et al., 2005). In some cases, BRCA2-deficient cells were more than 1000 times more sensitive to nanomolar concentrations of PARP inhibitor (Farmer et al., 2005), suggesting the possibility of a highly selective therapy. It is likely that PARP inhibitors target the HR deficiency in BRCA-deficient cells. PARP is documented to be crucial for the repair of single-strand DNA breaks (SSBs) and PARP inhibitors cause an increase in persistent SSBs (Boulton et al., 1999). It was shown that PARP inhibition also increases nuclear Rad51 foci (Schultz et al., 2003), a marker of ongoing HR repair. Taken together, these different

lines of evidence suggest that PARP inhibition could lead to accumulated SSBs and resultant collapsed replication forks/DSBs. In face of this thread, HR-defective cells (frequent in certain types of cancer) would be unable to maintain genome integrity and show markedly increased sensitivity to PARP inhibition. Consistent with the HR defect in BRCA-deficient cells being the primary cause of PARP inhibitor sensitivity, cells with deficiencies in a number of other HR proteins are also sensitive to PARP inhibitors (McCabe et al., 2006).

Drug	Company	Biophysical parameters	Synergizes with (*in vitro*)	Clinical trials*	Phase*
ABT-888	Abbott	K_i = 5.2 nM (PARP1) K_i = 2.9 nM (PARP2) EC_{50} = 2 nM (C41 cells)	Temozolomide Platins Cyclophosphamide Ionizing radiation MNNG Topoisomerase I poisons	Glioblastoma multiforme (with temozolomide)	Phase II
				Solid tumours and leukaemia (various combinations)	Phase I
				BRCA1- or BRCA2-mutant tumours	Phase I
AG014699	Pfizer	K_i = 1.4 nM (PARP1)	Temozolomide Ionizing radiation Topotecan	BRCA1- or BRCA2-mutant tumours	Phase II
AZD2281 (olaparib)	AstraZeneca	IC_{50} = 5 nM (PARP1) IC_{50} = 1 nM (PARP2) IC_{50} = 1.5 μM (tankyrase 1)	Temozolomide Platins MMS Ionizing radiation (with and without 17-AAG)	Platin-sensitive ovarian cancer	Phase II
				BRCA1- or BRCA2-mutant tumours (with carboplatin)	Phase II
				Triple-negative breast cancer (single-agent or with carboplatin)	Phase II
				Other solid tumours	Phase I/II
BSI-201	Sanofi-Aventis	ND	Ionizing radiation Oxaliplatin Gemcitabine and carboplatin Topotecan	Triple-negative breast cancer (with gemcitabine and carboplatin)	Phase III
				Ovarian cancer, glioblastoma multiforme and uterine cancer (various combinations)	Phase II
				BRCA2-mutant pancreatic cancer (various combinations)	Phase Ib
				Other solid tumours	Phase I/II
CEP-8983/ CEP-9722 (prodrug)	Cephalon	IC_{50} = 20 nM (PARP1) IC_{50} = 6 nM (PARP2)	Temozolomide Topoisomerase I poisons	Solid tumours (with temozolomide)	Phase I
MK-4827	Merck	IC_{50} = 3.2 nM (PARP1) IC_{50} = 4 nM (PARP2)		Solid tumours and ovarian cancer	Phase I

Table1.2. Table showing different PARP inhibitors, their combination with DNA damaging drugs and the ongoing clinical trials eploiting these treatments. Modified from Rouleau et al., 2010

An alternate approach for PARP mediated chemotherapy has been the use of a combination of DNA damaging agents along with PARP inhibitors. The DNA damaging agents that showed marked chemosensitization in combination with PARP inhibitor include Methylating agents, Topoisomerase1 inhibitors, DNA crosslinkers and ionizing radiation (Rouleau et al., 2010)(Table1.2). Phase I and Phase II trials of several PARP inhibitors in combination with DNA damaging agents are ongoing and

might offer new important perspectives to cancer chemotherapeutic approaches (Rouleau et al., 2010).

2. RESULTS

2.1 Top1 inhibition results in slow fork progression in yeast.

To address the effects of CPT induced Top1 poisoning in vivo in yeast, we monitored replication kinetics along the chromosomes by ChIP-chip and Bromodoeoxyuridine (BrdU) incorporation in synchronized *S. cerevisiae* cells (Katou et al., 2003). We compared length and distribution of BrdU tracks in yeast cells, released from a G1 block in presence or absence of CPT. The cells were pre-synchronized in S-phase by the addition of α-factor and released at 16°C by media replacement in the presence of

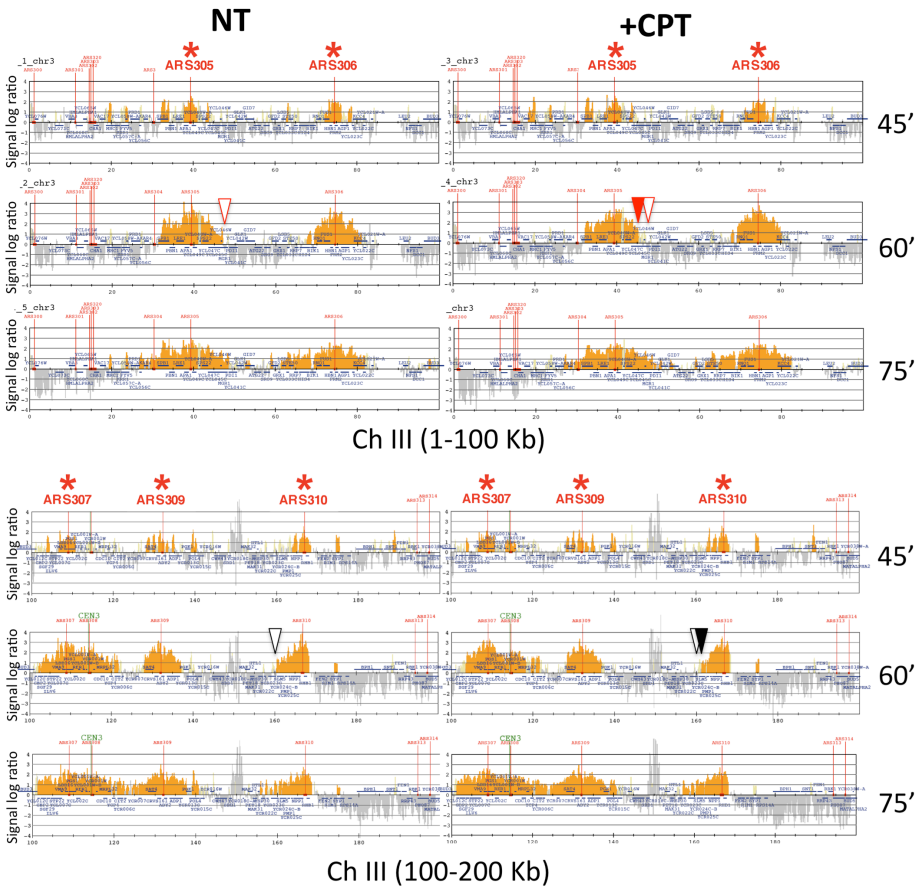

Fig.2.1. Representative BrdU replication profiles (ChrIII, 1-200kb) in presence or absence of 50μM CPT. Genome wide BrdU incorporation maps were obtained at different time points (45, 60 and 75 min) after release from G1 block at 16°C in the presence (right) or absence (left, NT) of 50μM CPT. Representative data are shown here for Chromosome III (1-100kb; 100-200kb). For genome-wide analysis of fork progression, we focused on a mid-S phase time point (60 min), where the highest number of replicons could be simultaneously analyzed. The position of left and right tails of each BrdU peak was compared in presence and absence of CPT and only distances above 1kb were considered significant, as exemplified by the red, full (+CPT) and empty (NT) arrowheads. An example of fork delay considered "non-significant" is marked by black (full, +CPT; empty, NT) arrowheads.

Pronase. To follow the origin firing and progression of replication forks, a kinetic analysis was performed at 45, 60 and 75 min time points after G1 release. Small BrdU peaks were visible and comparable in width at all early replication origins (*) at the earliest time point (45 min) in presence and absence of CPT, showing that CPT treatment does not affect timing and distribution of origin firing (Fig.2.1). We then focused our analysis on a mid-S phase time point, where the highest number of replicons could be simultaneously analyzed. BrdU track extension was measured as reliable read out of fork progression in presence or absence of CPT. While we never found a CPT treated fork moving

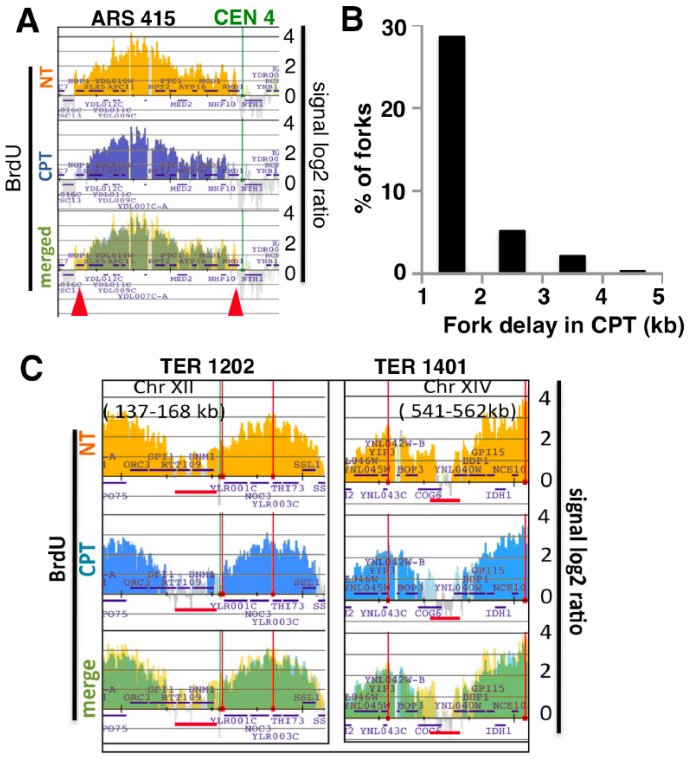

Fig.2.2. CPT-treated *S. cerevisiae* cells have slower fork progression (A) Examples of fork movement across a region of chromosome IV, monitored by BrdU incorporation. CPT-induced fork delay (red arrow heads) was scored measuring the distance between BrdU track tails in presence and absence of 50μM CPT (see also Table 2.1 at the end of the results section). (B) Graphical representation of the percentage of delayed (kb) forks upon CPT treatment. (C) Examples of termination zones showing impaired fork progression upon CPT treatment. Horizontal red bars indicate recently characterized TERs (Fachinetti et al., 2010).

faster than the untreated counterpart, we did find ≈35% of all active forks (119/350) showing a delay of at least 1kb in presence of CPT (Fig.2.2A and 2.2B). A small fraction of forks (≈10%) was delayed by more than 2kb (Fig.2.2B). Two chromosomal features previously linked to fork pausing - centromeres and termination zones (Fachinetti et al., 2010; Greenfeder and Newlon, 1992) - were also analyzed for CPT-induced delay in fork progression. 5 of the 8 (62%) centromeres

undergoing replication at the timepoint chosen for analysis were delayed in replication upon CPT treatment (Fig.2.2A and Table 2.1, at the end of this Results session). Similarly, we could also detect delayed replication termination at 12 of 16 (75%) recently characterized termination regions (TERs) (Fachinetti et al., 2010)showing converging forks in our experiment (Fig.2.2C).

An independent experiment revealed a similar proportion of delayed forks (107/350; 30.5%). Despite the unavoidable, subtle variability in the kinetic of S phase entry in the two experiments, 53 forks (49.5%) were found to be delayed at identical chromosomal positions.

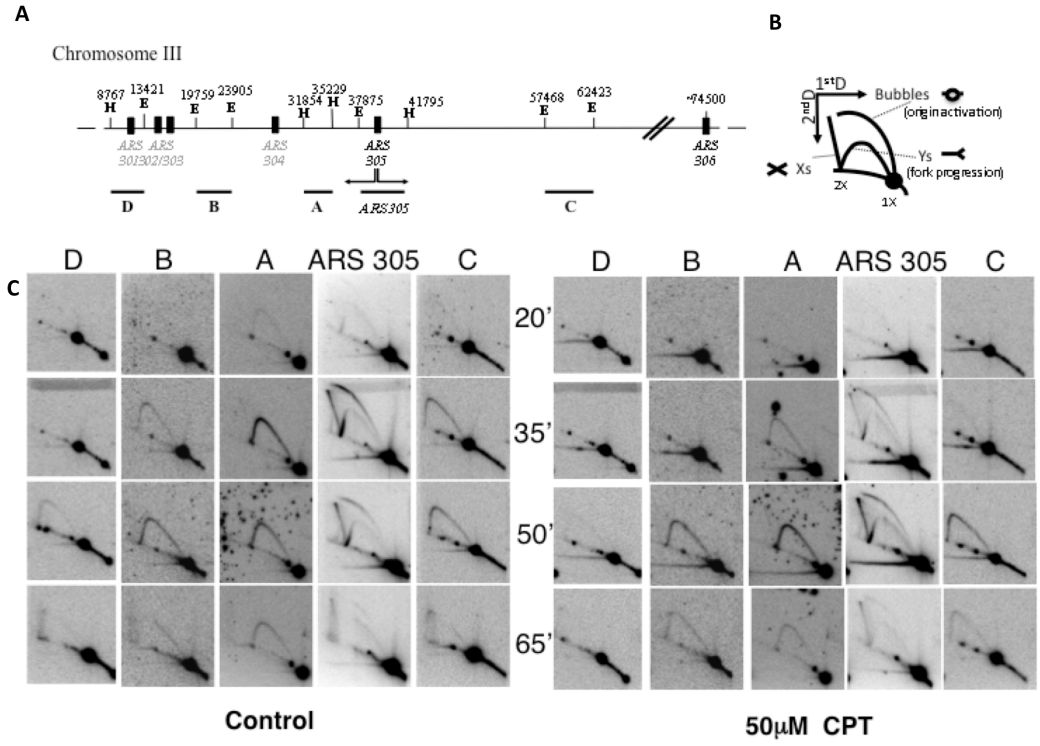

Fig.2.3. 2D-gel analysis of replication intermediates from wild type *S. cerevisiae* cells in presence or absence of CPT. (A) Chromosome III region adjacent to ARS305 with indication of the probes used for 2D-gel analysis . (B) Schematic representation of replication intermediates visualized by 2D-gels. (C) Time-course resolution of replication intermediates obtained from wild type cells released synchronously from G1 arrest at 25°C in presence or absence of 50μM CPT.

To further confirm the delay in fork progression in response to CPT, a bi-dimensional gel electrophoresis (2D-gels) was performed on wild yeast cells mock- or CPT-treated for the resolution of replication intermediates at different time points (Fig.2.3). Results showed a delayed detection of "large bubbles" at ARS305 (35 min). Since we

found (Fig.2.1) that CPT treatment does not affect the timing of origin firing (including ARS305), the delay seen in the detection of large bubbles is indicative of delayed progression of the forks emanating from the origin. Furthermore, replication fork progression monitored through the indicated adjacent fragments (A, B, C and D) appears significantly impaired by CPT treatment (35, 50 min): the forks emanating from ARS305 invade fragments A, B and C with approximately 15 min delay in the presence of CPT, although later resolution of replication intermediates (65 min) is comparable with and without CPT suggesting that the delay observed upon CPT treatment is transient. Together, results in Fig2.1-2.3 show significant proportions of yeast forks slowed down in response to CPT treatment.

2.2 Replication fork delay upon Top1 inhibition is not associated with detectable DSB in yeast.

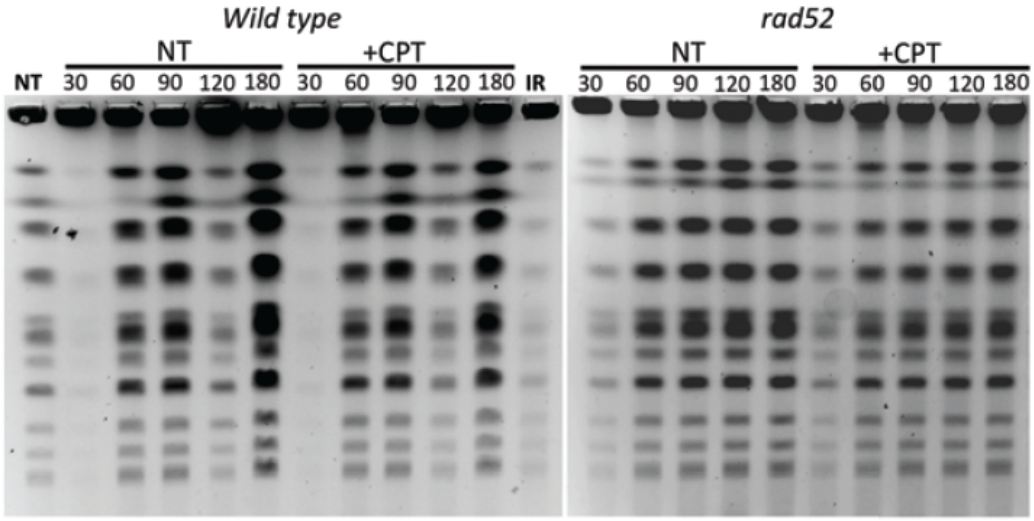

Fig.2.4. Detection of chromosomal breakage in synchronized, CPT-treated wt and DSB-repair defective (*rad52*) *S. cerevisiae* cells. Wt and *rad52*Δ cells were arrested in G1 with α-Factor and released in the presence or absence of 50μM CPT. Culture samples were processed for Pulse Field Gel Electrophoresis detection of DSB. The EtBr-stained gel is shown in reverse contrast. α-Factor arrested cells untreated (NT) or irradiated with 500 Gy (IR) were used as negative and positive control of chromosomal breakage, respectively.

Since fork stalling upon CPT treatment has been consistently linked to the formation of DSB, we expected the observed widespread fork delay in our experiments to be

associated with detectable DSB by fork collapse. Pulse Field Gel Electrophoresis (PFGE) was performed after treatment with CPT in wild type yeast cells, as well as *rad52Δ* cells which are defective for HR-dependent DSB repair (Fig.2.4).

Irradiation-induced DSB used as positive control led to markedly reduced signals for the chromosomal bands and appearance of a smear over the PFGE lane, particularly evident towards the smaller chromosomal bands (IR), suggesting chromosomal breakage. Upon release into S-phase of both wt and *rad52* cells, the chromosomal bands were, as expected, transiently retained within the plugs during replication (30 min) due to their highly branched structure. The bands promptly reappeared at later time points (≥60 min) despite the CPT treatment, correlating with completion of bulk DNA replication in all cases. Furthermore, we found no evidence for CPT-induced chromosomal breakage (band smearing) in either wt or *rad52* cells at any time point during the kinetic. The slight reduction in the intensity of the chromosomal bands in CPT treated compared to untreated *rad52* cells, in the absence of any detectable smear, may suggest partial chromosomal retention in the PFGE plugs, consistent with the possible requirement of HR for late steps of DNA replication/segregation upon CPT treatments.

Although ChIP-chip data showed a genome wide fork slowdown (Fig.2.2), it is still formally possible that Top1cc are too sparse under these experimental conditions and that the PFGE assay may not be sensitive enough to detect CPT-induced DSBs in yeast cells. We thus investigated the presence of DNA breaks by activation of the DNA damage checkpoint, as even a single, unrepaired DSB was shown to phosphorylate and activate the central yeast checkpoint kinase Rad53 (Pellicioli et al., 1999). CPT treatment did not lead to DNA damage checkpoint activation (Rad53 phosphorylation) in wild type cells (Fig.2.5A). On the contrary, DSB-repair defective *rad52* cells did show activation of the DNA damage checkpoint, but only after at least

90min from G1 release, a time point when bulk DNA replication is complete (Fig. 2.5A-B) and replication intermediates appear to be resolved (Fig.2.3C and Fig.2.4). Furthermore, *rad52* cells failed to progress into the next cell cycle after treatment (Fig.2.5B-C), but both wild type and *rad52* cells showed unaffected S phase progression upon CPT treatment and completed bulk DNA replication within 60 min after G1 release (Fig.2.5B). Altogether these results suggest that DSB, if any, can be temporally uncoupled from CPT-induced fork slowdown in yeast and that HR-repair is required only at the end of S-phase.

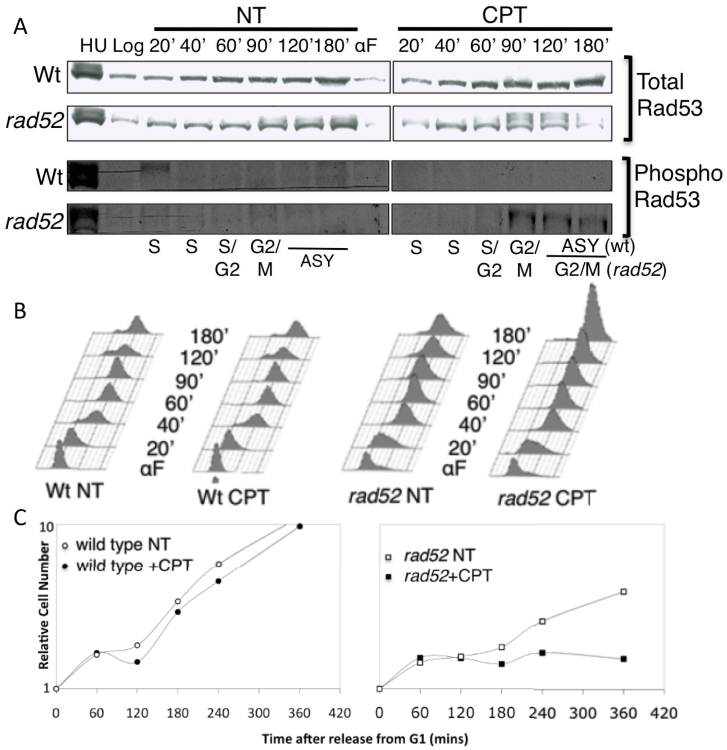

Fig.2.5. Checkpoint analysis, cell cycle progression and growth curve in synchronized, CPT-treated wt and DSB-repair defective (*rad52*) *S. cerevisiae* cells. (A) Western blot analysis for the activation of checkpoint protein Rad53 in CPT-treated yeast cells. Wild type and *rad52*Δ cells were arrested in G1 with α-Factor and released in the presence or absence of 50μM CPT. Total protein extracts at the indicated time points were probed for total-Rad53 and phospho-specific Rad53. (B) Analysis of cell cycle progression in response to CPT in wild type and *rad52*Δ cells. Wild type and *rad52*Δ cells were synchronized and treated as in (A). Cell cycle progression was monitored at the indicated time points by FACS analysis of DNA content (Propidium Iodide). (C) Growth curve analysis in response to CPT in wild type and *rad52*Δ cells. Wild type and *rad52*Δ cells were synchronized and treated as in (A). Cell number was counted at the indicated time points and used to build the growth curves.

2.3 CPT induces slow fork progression at low concentrations in mammalian cells.

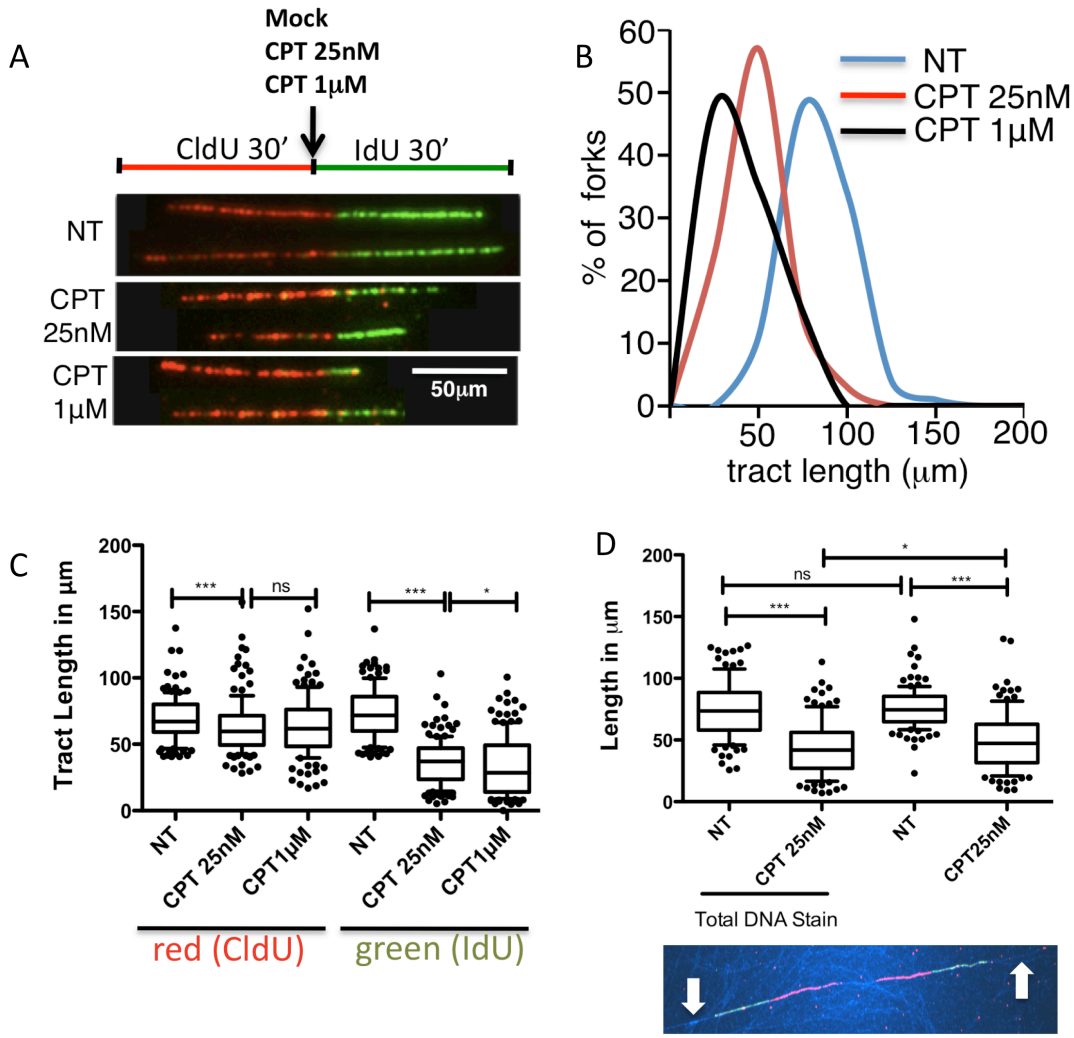

Fig.2.6. CPT induces slow fork progression in human cells. (A) *In vivo* analysis of replication fork progression by cell labelling with halogenated nulceotides (CldU and IdU), DNA fiber spreading and immunodetection of replicated tracts in Mock- or CPT-treated U2OS cells. CldU/IdU-containing tracts were immunostained in red and green respectively. Two representative fibers per experiment are shown. (B) The smoothened histogram distribution shows green (IdU) tract length in presence or absence of CPT. (C) The graph represents length in µm of DNA tracts synthesized before [CldU, red, left] and after mock (NT) or CPT treatment (25nM, 1µM) [IdU, green, right]. At least 100 tracts were scored for each dataset. Whiskers indicate 10-90 percentile. T test according to Mann-Whitney, results are *ns* not significant, * $p \leq 0.05$, *** $p \leq 0.0001$. (D) Identical experiment as in A), but DNA fibers have been counterstained with a "total DNA" (antiguanine) antibody (see the representative fiber below the graph). Fork progression in mock- or CPT 25nM-treated cells was scored by standard tract analysis as in A (two datasets on the right) or by restricting the analysis to intact forks ("total DNA stain"; red + green tracts flanked by continuous DNA stain, as in the inset).

As the poor permeability of standard *S. cerevisae* strains to CPT limits the number of Top1ccs induced at soluble CPT concentrations, we shifted our analysis in cultured human cells, where CPT-induced effects are already detectable in the nanomolar

range. S phase-checkpoint proficient U2OS cells were used for most experiments.

To analyze the effects of CPT on fork progression at single-molecule level, we took advantage of DNA chromosome spreads and immunofluorescent detection of replicated tracts, upon incorporation of halogenated nucleotides (CldU and IdU). CldU and IdU were added sequentially to the U2OS cells for 30 min each and CPT (0, 25nM or 1μM) was added during the IdU pulse. CldU- and IdU-incorporated tracts were identified on the fibers by specific antibodies and visualized in red and green respectively.

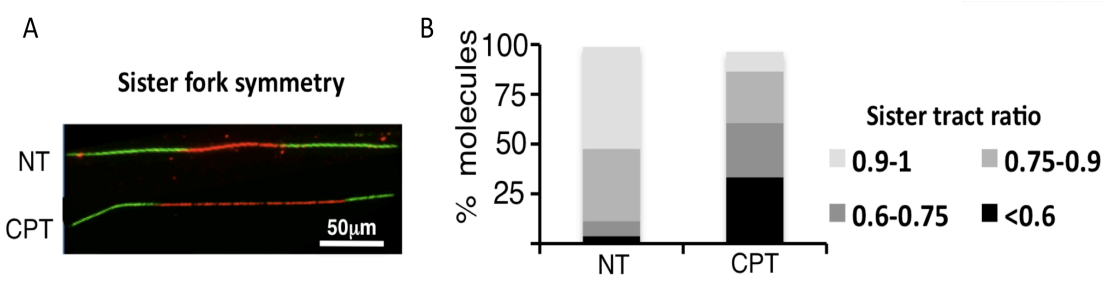

Fig.2.7. Cells treated with CPT show sister-fork asymmetry. DNA fibers from mock- and CPT-treated cells were scored for fork symmetry, comparing lengths (shorter over longer ratio) of green tracts departing from the same origin. (A) One representative picture of mock- and CPT 25nM-treated forks that were scored for sister fork symmetry. (B) Histogram analysis of sister tract ratio in the experiment in (A). At least 100 tracts were scored for each dataset.

We observed that treatment with 25nM CPT induced a global, marked delay in replication fork progression, while only marginal further decrease was induced by a 40-fold higher CPT dose (1μM) (Fig2.6A-C). The small, but significant difference in the length of red tracts between mock and 25nM CPT treated cells (Fig.2.6C) reflects CPT-induced fork slow-down, occurring immediately after addition of the drug, while residual CldU is still incorporated into the nascent DNA. The DNA fibers were also counterstained with a "total DNA" (antiguanine) antibody to focus our analysis on intact forks and address the possibility that the shorter tracts observed after CPT treatments were due to replication fork breakage (Fig.2.6D). The results revealed that the data sets obtained by both approaches were comparable indicating that the

replication fork slow down induced by 25nM CPT treatment is not accompanied by extensive fork breakage.

Furthermore, even the lowest concentration of CPT (25nM) used in the treatment of cells resulted in a significant degree of sister fork asymmetry (Fig2.7). Overall these data suggest that replication forks are frequently slowed down or stalled in response to even low (nM) CPT concentrations.

2.4 Slow fork progression at low CPT concentrations does not induce detectable DSB in mammalian cells.

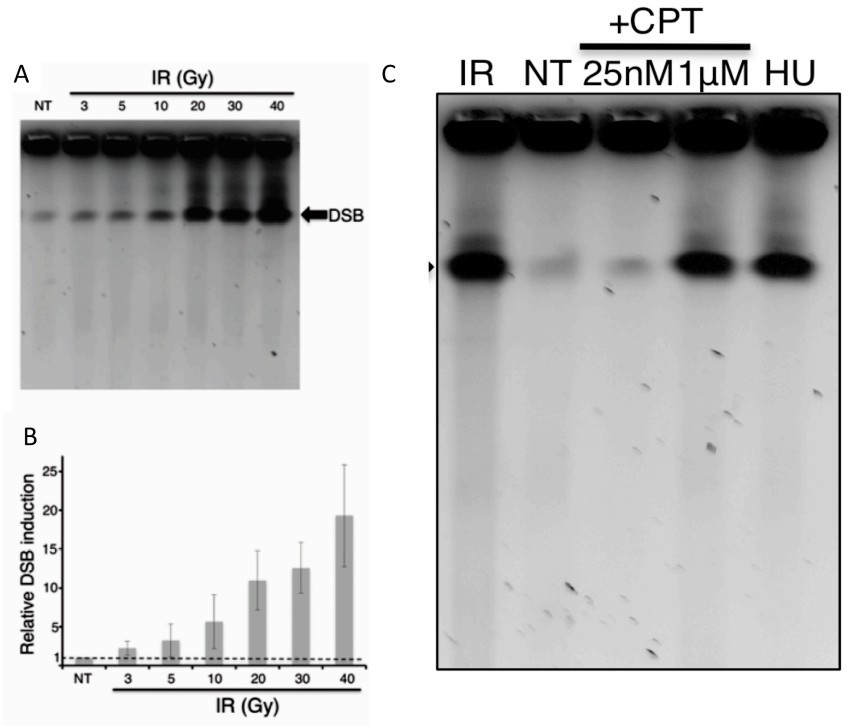

Fig.2.8. DSB Detection by PFGE in irradiated, HU-treated and CPT-treated U2OS cells. (A) PFGE analysis for DSB detection upon treatment of U2OS cells with different doses (3-40 Gy) of ionizing radiation. (B) DSB signals were quantified by ImageJ and normalized to unsaturated signals of DNA retained in the wells. The graph integrates results from three independent experiments and shows DSB levels relative to untreated conditions (NT, dashed line). (C) PFGE analysis for DSB detection upon 30 Gy ionizing radiation (IR, positive control), 24h treatment with HU 5mM (HU, positive control) and 4h treatment of U2OS cells with 0, 25nM or 1μM CPT.

To further investigate if the global fork slowdown observed upon CPT treatment is associated with formation of DSB by fork collapse, we performed PFGE analysis for the detection of DSBs. By this optimized PFGE procedure, broken DNA fragments ranging from 300kb to 5MB can be compacted into one single band, which helps

quantification of broken chromosomal DNA (Hanada et al., 2007).

Testing the sensitivity of the PFGE assay was one of the requirements of the experiment, as earlier PFGE protocols were considered not sensitive enough to detect a low number of DSBs. Thus, to test the sensitivity of our assay, DNA from cells treated with different doses of IR (3-40 Gy) was analyzed by this PFGE approach. DSB were reproducibly detected above background levels already at the minimal irradiation dose (3 Gy) (Fig2.8A-B). Similar results were obtained using two different irradiation apparatuses. As one Gray has been reported to induce approximately 30 DSB/cell (Ward 1988), we could conclude that this assay - due to the compaction in a single band of broken fragments of various size - is sensitive enough to reproducibly detect less than 100 DSB/cell.

We thus treated U2OS cells with 25nM and 1μM CPT to assess chromosome breakage upon CPT doses. Although DSBs could be clearly detected by our PFGE assay in 1uM CPT, we could not detect breaks above the background level when treating U2OS cells with 25nM CPT. These results suggest that CPT induced fork slowing can be largely uncoupled from DSB formation (see Discussion).

2.5 Slow fork progression in response to CPT in human cells and Xenopus egg extracts is HR-independent.

One of the main implications of the "run-off theory" is that forks collapsed upon CPT treatments would require HR to restart. Furthermore, as CPT treatments slow down replication forks genome-wide (Fig.2.6), HR-repair should be required for S-phase completion. To test this hypothesis, we investigated the effects of CPT on bulk DNA replication of synchronized Mock transfected (siCtrl) and HR defective (siCtIP) cells.

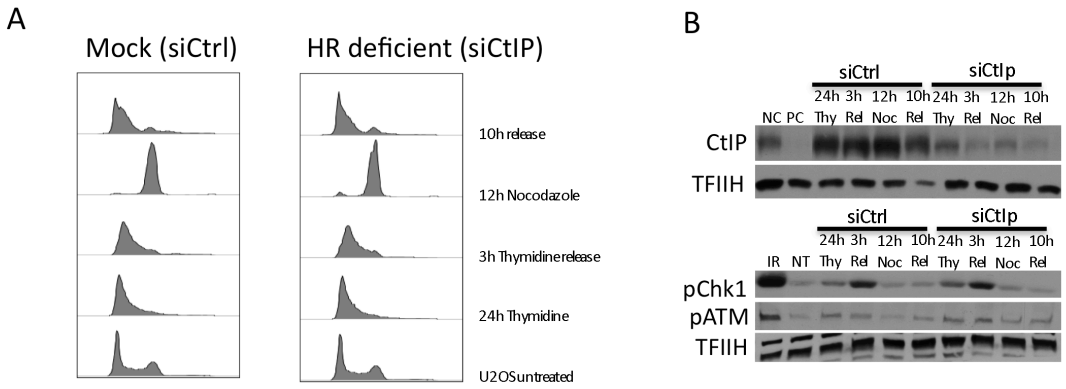

Fig.2.9. Synchronization of U2OS cells in S-phase. (A) Flow cytometric analysis (Propidium Iodide) of the synchronization procedure in mock-transfected (siCtrl) and HR defective (siCtIP) U2OS cells. (B) Western Blot analysis for the knockdown of CtIP and checkpoint status of SiCtrl and siCtIP cells during the synchronization procedure. Whole cell protein extracts from the indicated time points during the synchronization procedure were probed for CtIP, pChk1 and pATM. TFIIH was used as a loading control. 30Gy IR was used as positive control for Chk1 and ATM activation

Cells were synchronized by treating with 2mM thymidine (Thy) for 24h. The cells were then washed and released for 3h (Rel) before treating them with 75ng/ml nocodazole for 12h (Noc). The cells were finally released into the following cell cycle by washing and incubation in fresh medium. 10h after release (Rel) U2OS cells enter synchronously the next S phase (Fig.2.9A).

Analysis into the checkpoint status of the cells during the synchronization procedure showed that, despite some Chk1 activation during the thymidine treatment and following release procedure (Fig.2.9B), even the HR-defective cells showed no sign of checkpoint activation (pChk1, pATM) when entering the next S-phase after release (10h) (Fig.2.9B), suggesting that they are undergoing *bona fide* unperturbed DNA replication. Untreated cells traverse S phase in 6-8h (10-18h) (Fig.2.10A) and complete a full cell cycle in about 24h, which is consistent with the standard doubling time (24h) and with the detection of 25-35% S phase cells in asynchronously growing U2OS cells. On the other hand, treatment of mock transfected (siCtrl) cells with 25nM of CPT at the entry of S-phase (10h) resulted in a massive slowdown of cells in S-phase and delayed completion of bulk DNA replication by several hours. Furthermore, treating the cells with 1μM CPT at the entry of S-phase lead to a

persistent replication block which could not be overcome to finish bulk DNA replication (Fig.2.10A). Notably, effective downregulation of CtIP (Fig.2.10B) during the synchronization procedure, known to impair human HR and sensitize cells to CPT treatments (Sartori et al., 2007), did not induce any further delay in S-phase completion than that observed in CPT-treated, mock-transfected cells.

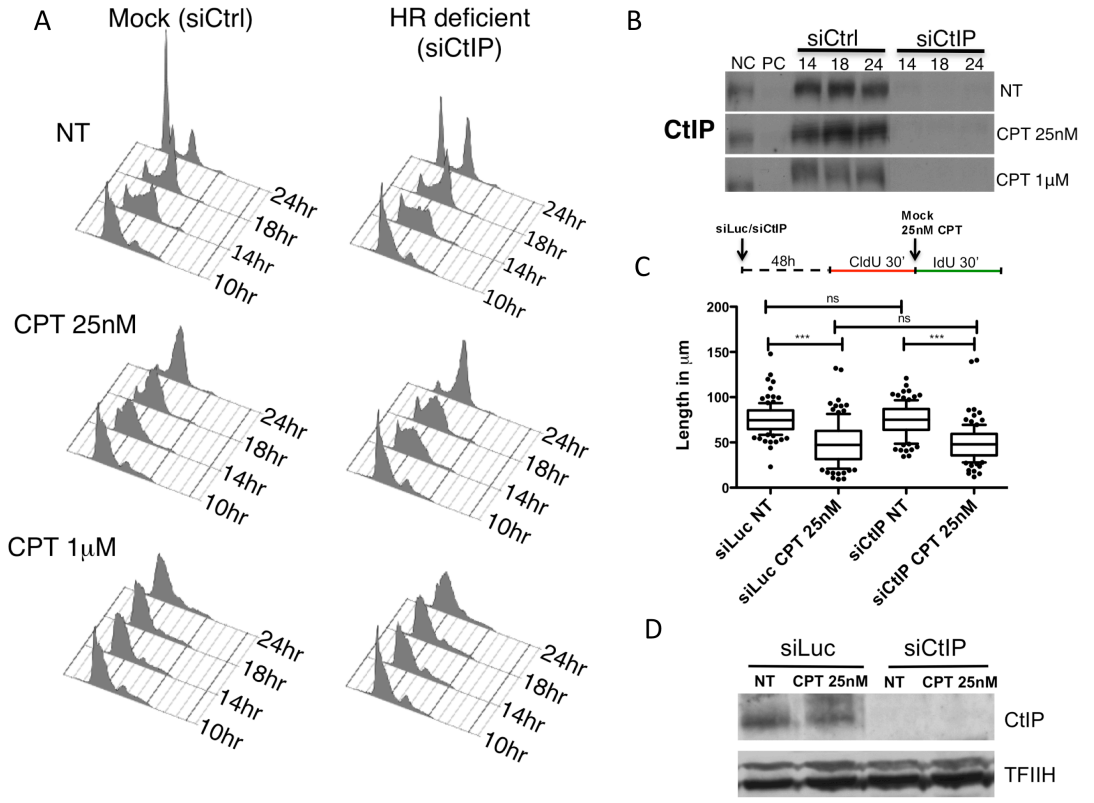

Fig.2.10. Upon mild CPT treatments, human cells can slowly, but successfully maintain fork progression and complete S phase, even in the absence of HR-mediated DSB repair. (A) Analysis of cell cycle progression by flow cytometric detection of DNA content upon synchronization of mock transfected (siCtrl) and HR-deficient (siCtIP) U2OS cells and CPT treatment. (B) Western blot analysis of CtIP depletion during the treatment of cells with CPT. (C) *In vivo* analysis of replication fork progression in Mock transfected (siLuc) and HR defective (siCtIP) cells by labelling with halogenated nulceotides (CldU and IdU), DNA fiber spreading and immunodetection of replicated tracts, as described in Fig.2.6. (D) Western blot for CtIP downregulation in the experiment in C. TFIIH, loading control.

To further confirm this observation, we performed a DNA fiber experiment to assess the role of HR in the progression of single forks (Fig.2.10C). Results confirmed that upon effective downregulation of CtIP (Fig.2.10D), single forks showed no further delay in their progression rate, than that observed upon CPT treatment in mock-

transfected cells.

Altogether, these data suggest that HR-mediated DSB repair is dispensable for slow fork progression and S-phase completion in CPT-treated human cells.

To also investigate the role of HR on bulk DNA replication in Xenopus egg extracts treated with Topotecan (TPT, a water soluble derivative of CPT more suitable for molecular investigations in this system), we depleted Rad51 from the extracts by the addition of GST-BRC4 peptide (Hashimoto et al., 2010). Sperm nuclei were incubated with egg extracts in the presence or absence of GST (mock) or GST-BRC4 and incubated with 50 or 100μM of TPT for different times (Fig.2.11).

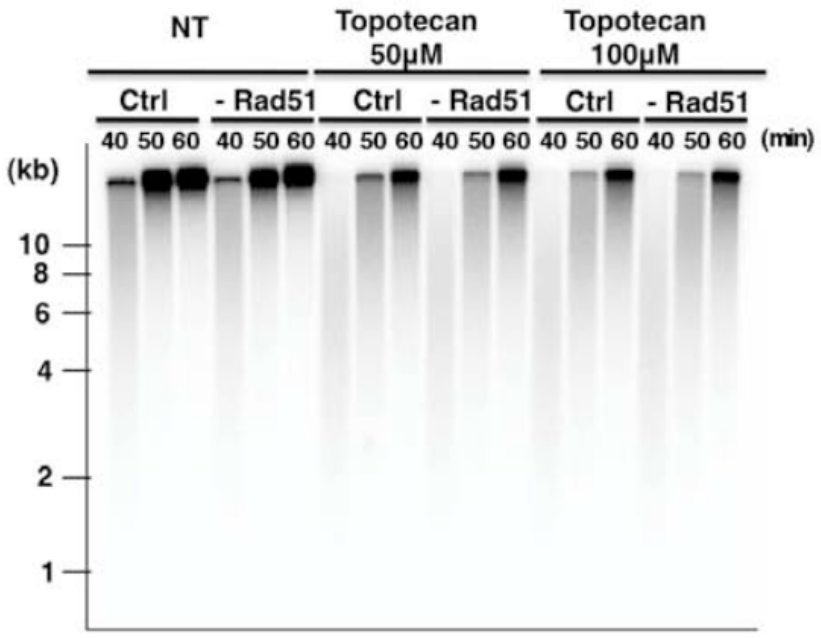

Fig2.11. **Homologous recombination-independent slow DNA synthesis in TPT-treated Xenopus egg extracts.** Sperm nuclei were incubated in 10 μl egg extract with α32P-dATP for the indicated times in the presence or absence of GST (mock) or GST-BRC4 HR deficient and topotecan (50 or 100μM). Replication products were resolved on 1% alkaline agarose gel and subjected to autoradiography.

TPT induced a marked slow down of incorporation rates in a concentration dependent manner (50min, Fig.2.11), but no further reduction in the rate of DNA synthesis was observed upon Rad51 depletion from the extracts. These data suggest that HR is also

dispensable for bulk DNA replication in Xenopus egg extracts upon treatment with Top1 poisons.

2.6. Slow DNA replication progression is not accompanied by detectable chromosomal breakage even upon prolonged treatment of S phase-synchronized human cells with low (nM) CPT doses.

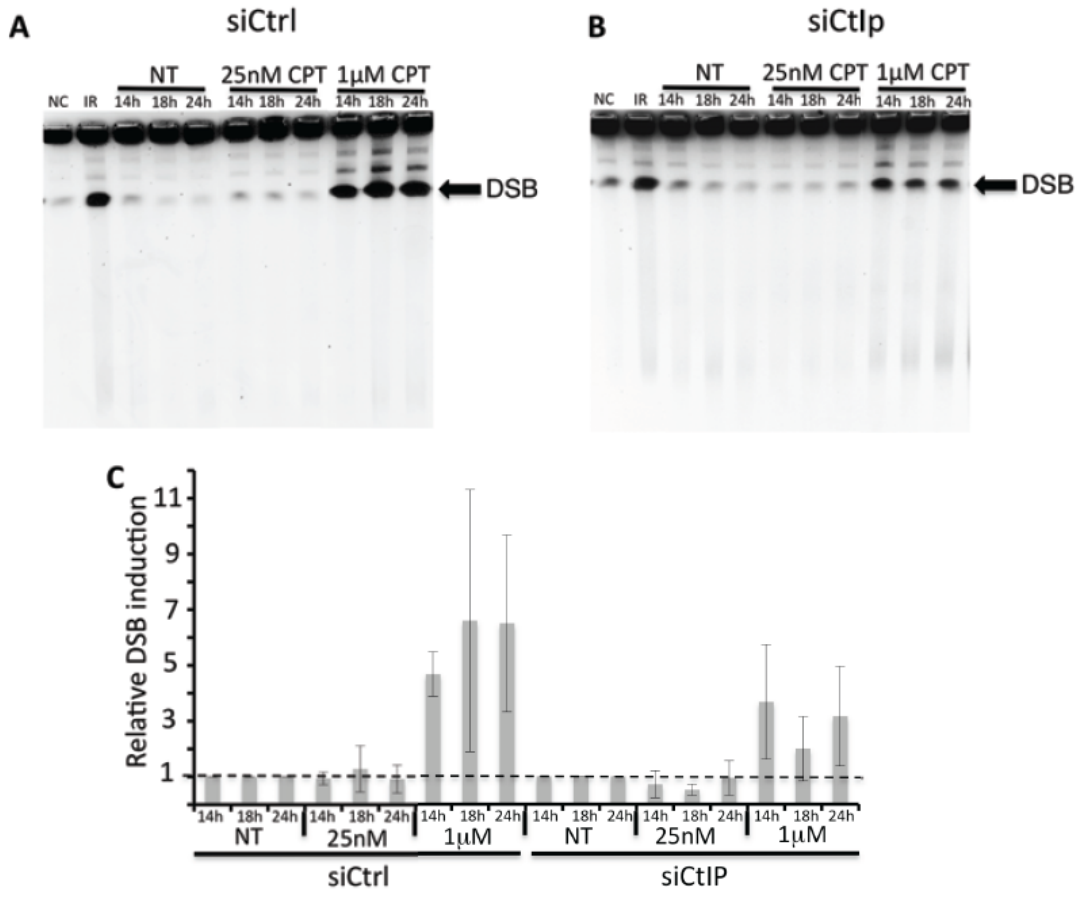

Fig.2.12. DSB Detection by PFGE in CPT-treated synchronized U2OS cells. U2OS cells were synchronized as in Fig. 9**,** transfected (siCtrl, A; siCtIP, B) and treated with CPT as described in Fig. 10A. Cell samples at the indicated time points were processed for PFGE to possibly detect DSB upon treatment with 25nM and 1μM CPT. NC (negative control): asynchronous U2OS cells; IR (positive control for DSB): U2OS cells 2 hours after 40Gy irradiation. C) DSB signals were quantified by ImageJ and normalized to unsaturated signals of DNA retained in the wells. The graph integrates results from two independent experiments and shows DSB levels relative to the same time point in untreated conditions (NT, dashed line).

To further investigate the mechanism of CPT action, we tested whether prolonged treatments with nM CPT doses would lead to detectable amounts of DSB in control or

HR-deficient cells. To do this, we used the same synchronization protocol as in Fig.2.10 - which allows to have S-phase synchronized cells CPT-treated for up to 14h (from 10h to 24h) - and assessed DSB induction by PFGE analysis (Fig.2.12).

The results confirmed our observation in Fig. 8 with asynchronous cells: even upon prolonged treatment of synchronous cells, DSB were clearly detected upon 1μM CPT treatments, but no DSB could be detected over background level in either mock-transfected (siCtrl) or DSB-repair defective (siCtIP) cells upon treatment with CPT 25nM (Fig.2.12A-C). Surprisingly, we reproducibly observed that treatment with high concentration of CPT (1μM) led to lower amounts of DNA breakage in HR-defective (siCtIP) cells than in mock treated cells (Fig.2.12B and C) (see Discussion).

Together, these data suggest that the slow DNA replication rate observed in mammalian cells upon treatment with low (nM) CPT concentrations is largely uncoupled from DSB accumulation.

2.7. nM CPT treatment results in checkpoint activation independently of detectable DSB and break processing.

As different kinds of damage have been shown to activate either or both the ATR/Chk1 and ATM/Chk1 pathway, we set out to investigate the kind of damage response elicited by the treatment with different CPT doses on mock-transfected (siCtrl) and HR-defective (siCtIP) cells synchronized in S-phase.

Our results showed that, although basal levels of checkpoint are detectable during unperturbed DNA replication (Fig.2.1A), both ATM/ Chk2 and ATR/Chk1 pathways get promptly activated by CPT treatments in synchronized cells (Fig.2.13A). Persistent activation of both the ATM/Chk2 and ATR/Chk1 pathways upon treatment with high doses of CPT (1μM) (Fig.2.13 A) should presumably be attributed to DSBs formation, as previously suggested (Fig.2.12). However, it was surprising to us that

ATM/Chk2 pathway gets clearly activated even upon mild CPT treatments (25nM), which do not lead to detectable DSB even upon prolonged exposure (Fig.2.13A and Fig.2.12), but already markedly affect replication fork rate (Fig.2.10). Furthermore, at these low CPT doses,Chk1 activation appears entirely independent of CtIP mediated DSB resection, differently from what reported at higher doses (Sartori et al., 2007).

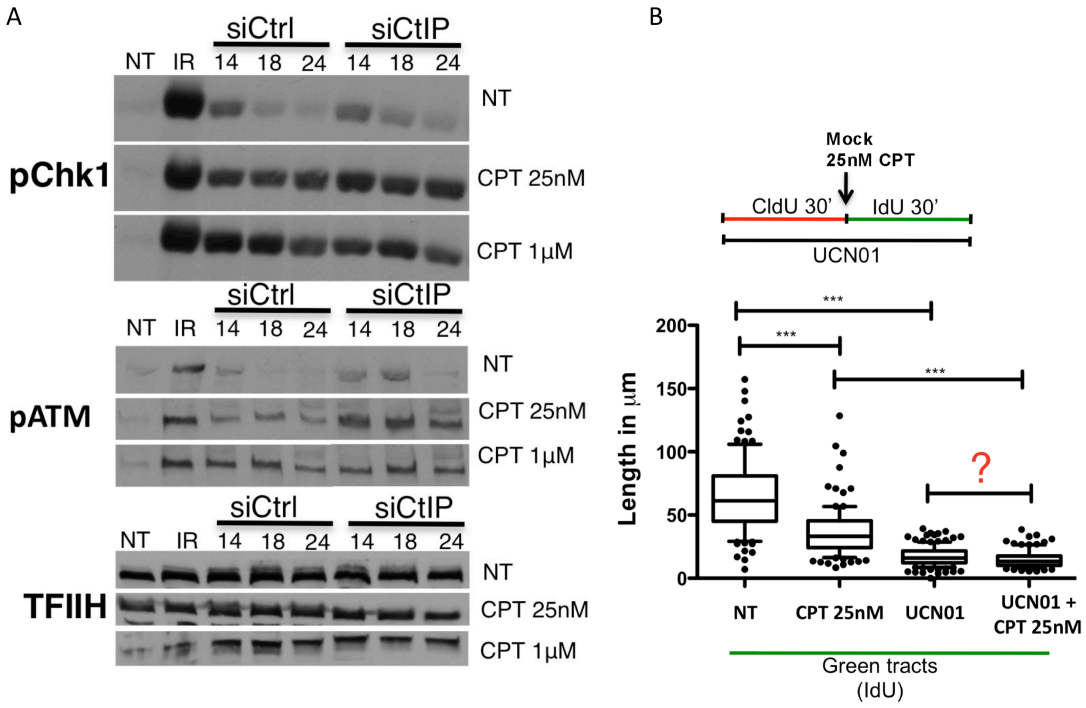

Fig.2.13. Checkpoint activation in CPT treated cells.(A) Western blot analysis of checkpoint activation (pATM and pChk1) on the same samples as in Fig.2.10. IR treatment with 30Gy was used as a positive control (IR) hasTFIIH, loading control. (B) Single-molecule analysis of replication fork progression in U2OS cells upon Top1 and/or Chk1 inhibition. Relative length of DNA tracts synthesized after mock (NT) or CPT treatment (25nM) [IdU, green]. At least 100 tracts were scored for each dataset. 300nM UCN01 (Chk1 inhibitor) was optionally added during the labellings. Whiskers indicate 10-90 percentile. T test according to Mann- Whitney, *** $p \leq 0.0001$.

As Chk1 is promptly activated in response to low CPT doses, we attempted to investigate a possible role of Chk1 activation on fork slowdown. For this purpose Chk1 was inhibited by UCN01 and fork progression rates were measured in the presence or absence of CPT. However our data, in agreement with earlier published data (Petermann et al., 2010) revealed that Chk1 inactivation, led "*per se*" to severe fork progression defects during unperturbed replication, thus precluding direct assessment of its role in CPT induced fork slowdown (Fig.2.13B).

2.8. Top1 poisoning results in replication fork reversal.

To gain insight on the possible DNA structures resulting from Top1 inhibition, we next visually inspected the fine architecture of *in vivo* replication intermediates (RIs), exploiting a combination of *in vivo* psoralen crosslinking and electron microscopy (EM) (Lopes, 2009), already extensively used in the past to characterize the molecular determinants of yeast and mammalian DNA replication stress.

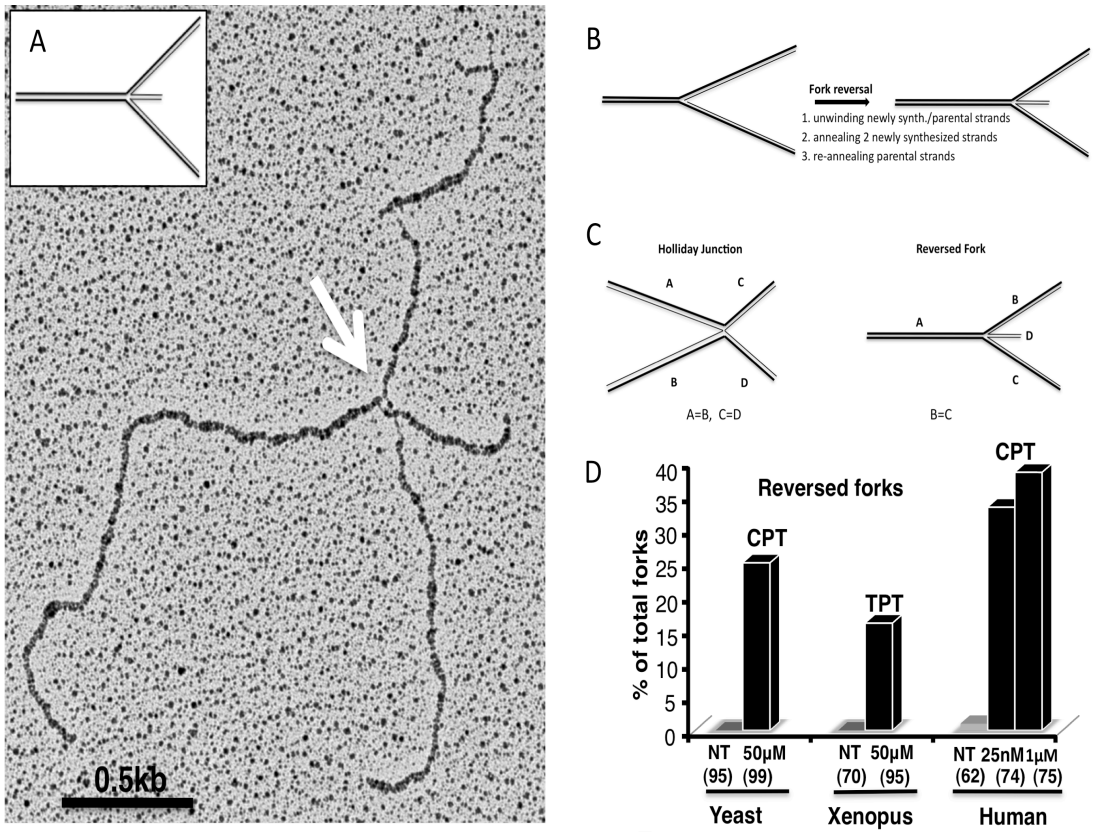

Fig.2.14.Top1 inhibition induces fork reversal (A) Representative electron micrograph and schematic drawing of a reversed fork observed on genomic DNA from CPT-treated U2OS cells. The white arrow points to the four-way junction at the replication fork. (B) Schematic representation of the process of fork reversal. (C) Schematic representation showing the distinction between Holliday Junctions and Fork reversal. (D)Frequency of fork reversal in *S. cerevisiae* cells (50μM CPT, 30min), *Xenopus* egg extracts (50μM TPT, 50 min) and U2OS cells (25nM or 1μM CPT, 1h). In brackets, the number of analyzed molecules.

This analysis revealed a significant fraction of replication forks with a fourth, regressed arm (reversed forks, RF) upon Top1 poisoning (Fig.2.14A). In order for a fork to be reversed, newly replicated strands need to be unwound from their parental counterparts and (when both are available) anneal with each other, forming a fourth

(regressed) arm at the replication fork. During this process, parental strands, previously unwound by the replicative helicase, are re-annealed (Fig.2.14B). Reversed forks can be identified by electron microscopy based on several parameters: 1) they are detected under DNA concentrations that minimize occasional crossing of DNA molecules; 2) in some cases a clear rhomboid Holliday Junctions (HJ)-like structure is detected where the two molecules overlap, assisting the interpretation. Furthermore, reversed forks can be distinguished from standard HJ based on length measurements: reversed forks should have only two of the four arms equal in length (due to the same distance of the replication fork from the restriction sites on the replicated duplexes), while standard HJ are symmetrically positioned in respect to all arms (Fig.2.14C).

A reproducible fraction of RF was observed on genomic DNA from CPT-treated yeast cells (25-30%) and on sperm DNA replicated in *Xenopus* egg extracts in presence of TPT (15-20%, Fig.2.14D). Remarkably, an even higher RF proportion (30-40%) was observed in U2OS cells replicating in 25nM CPT, while 40-times higher CPT doses (1μM) did not significantly increase RF frequency (Fig.2.14D). These data suggest that replication fork reversal is directly linked to fork slowing, while it is not necessarily associated with DSB formation (Fig.2.8C).

Although termination intermediates are rare in our EM samples - 33 among the total 689 CPT-treated RIs analyzed in this thesis - 17 of them (52%) showed one of the two forks reversed. Frequency of fork reversal at converging forks is thus higher than that observed in all systems at individual forks (Fig.2.14D), consistent with our yeast genomic data on fork progression (Fig.2.1C).

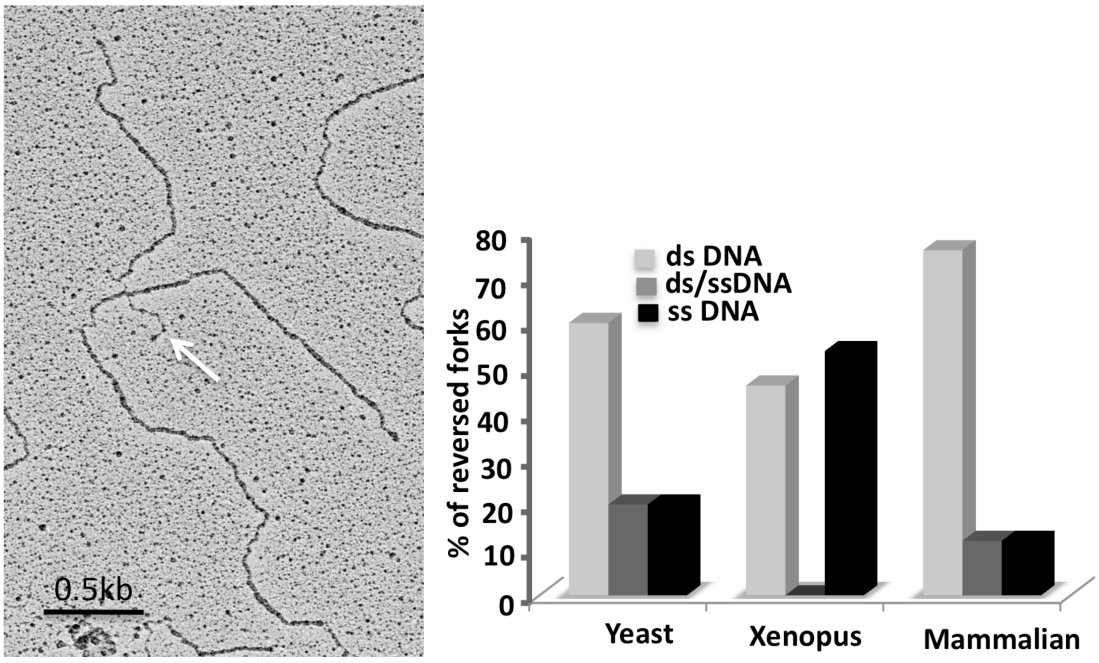

Fig.2.15. The regressed arm: analysis by electron microscopy. A) Representative electron micrograph of a reversed fork displaying a single sranded (ss-) regressed arm (white arrow). B) Statistical analysis of all identified regressed arms in the different experimental systems, in respect to their organization in double stranded (ds), single stranded (ss) or partially single stranded (ds/ss) DNA.

A further analysis on the nature of reversed arm formed upon CPT treatment revealed that approximately 20-50% of the regressed arm in all experimental systems used exposed ssDNA stretches (Fig2.15). These results may suggest that, reversal of forks with proper coupling of leading and lagging strand synthesis (normal forks) would result in ds ("blunt")-regressed arms, and that further processing (resection) of the ds-end may lead to the formation of ds-ss DNA stretches. Alternatively, fork reversal at a replication intermediate that is experiencing uncoupling of leading and lagging strand synthesis (uncoupled fork) may directly lead to ss-regressed arms (see Discussion).

2.9 *In vitro* resolution of topological stress upon Top1 inhibition results in better fork restart in Xenopus egg extracts.

Fork reversal has been shown to arise as a consequence of increased positive torsional strain on the DNA (Postow et al., 2001). Furthermore, Top1 poisons have been shown to induce torsional stress on the DNA by inhibition of the relaxation process (Koster et al 2007).

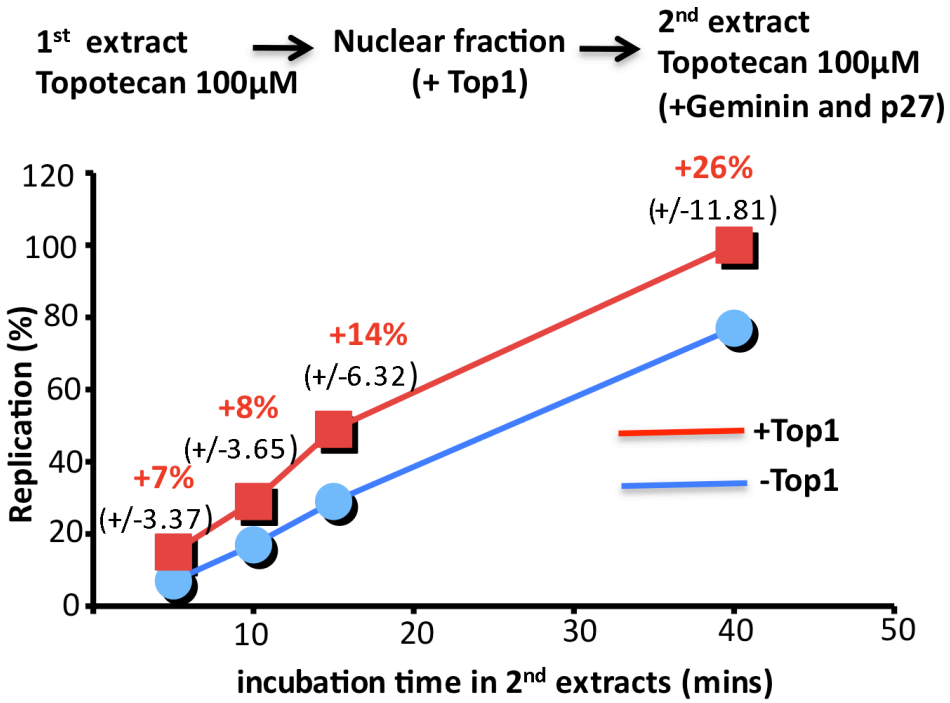

Fig.2.16. Effect of *in vitro*-resolution of topological stress on continued replication fork progression, upon TPT treatment of Xenopus egg extracts. In the 1st extract, sperm nuclei were incubated for 50 min in the presence of TPT (100µM). The nuclear fraction was isolated and divided equally into two aliquots, which were then incubated in the buffer with or without calf thymus Top1 (+Top1/ –Top1). The nuclear fractions were re-isolated and incubated for the indicated times in the 2nd extracts (containing alpha-^{32}P-dATP, His-Geminin, His-p27 and TPT), thus in conditions where only already active forks can contribute to DNA synthesis. Replication products were resolved on 0.8% TAE agarose gel and subjected to autoradiography. The obtained signal intensities were quantified by ImageQuant software. The same experiment was repeated three times. 100% incorporation was set to highest incorporation value observed (40min, +Top1 in all experiments). Relative incorporation was calculated at each time point and the average values from the three experiments were plotted in the graph. The difference in incorporation between +TopI and –TopI (Δ values) was calculated for each time point of each experiment. Average for Δ values and standard deviations (in brackets) are indicated at each time point, showing statistically significant increase of incorporation due to *in vitro* Top1 treatment. **This experiment was performed by Yoshi Hashimoto in the lab of Vincenzo Costanzo at Cancer Research UK**.

To assess whether accumulation of topological stress might contribute to impair fork progression upon CPT/TPT treatment, we took advantage of the biochemical versatility of the *Xenopus* egg extract system and of our ongoing collaboration with the group of Dr. Vincenzo Costanzo at Cancer Research UK. We initially let sperm nuclei replicate upon Top1 inhibition by TPT addition. After isolation, the nuclei were treated with calf thymus Topoisomerase I to partially release the accumulated topological tension and re-incubated in the presence of TPT, in conditions where

further DNA synthesis solely depends on elongation of already active forks. This was achieved by inhibition of further origin licensing. We observed that *in vitro* relaxation by purified Top1 could assist further fork progression in the presence of TPT, as detected by significant and reproducible increase of incorporation of radiolabeled nucleotides at all time points along the kinetic (Fig.2.16).

2.10 PARP inhibition prevents fork slowdown upon Top1 poisoning.

The poly (ADP-ribose) polymerase (PARP) family has been previously involved in the cellular response to Top1 inhibitors assisting Top1cc repair by largely elusive mechanisms (Curtin, 2005). PARP1 was previously shown to prevent fork slowdown upon CPT treatment (Sugimura et al., 2008), although it does not affect the number of primary lesions induced by Top1 poisons (Top1ccs) (Zhang et al., 2011). Due to the implications of PARP in Top1 poisoning, we set out to investigate a possible role for PARP in the observed molecular responses to Top1 poisons. We started by reproducing in U2OS cells the effects on fork progression observed upon CPT treatment in Hela and DT40 cells (Sugimura et al., 2008).

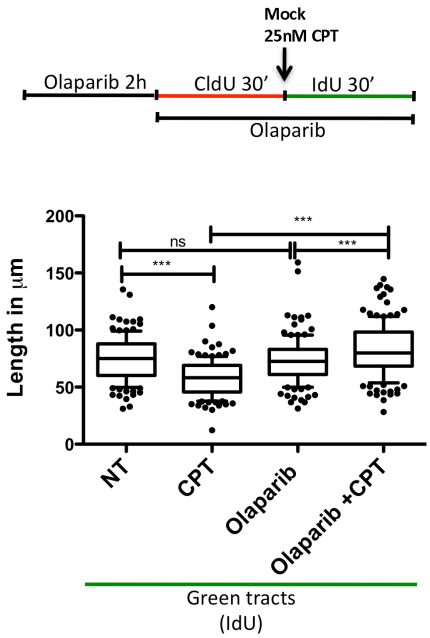

Fig.2.17. Single-molecule analysis of replication fork progression in U2OS cells upon Top1 and/or PARP inhibition. Relative length of DNA tracts synthesized after mock (NT) or CPT treatment (25nM) [IdU, green]. At least 100 tracts were scored for each dataset. 10µM Olaparib was optionally added 2h before CldU labelling and maintained during labellings. Whiskers indicate 10-90 percentile. T test according to Mann-Whitney, results are *ns* not significant, *** $p \leq 0.0001$.

In agreement with that publication, we also found that fork slowdown mediated by Top1 poisoning is completely abolished upon PARP inhibition by Olaparib (Fig.2.17). These data suggest that PARP plays a role in controlling fork progression in response to CPT treatments and its inhibition leads to unrestrained fork progression upon Top1 poisoning.

2.11 PARP inhibition reduces the frequency of fork reversal upon Top1 poisoning.

Since our data confirmed that fork slowdown upon Top1 inhibition is mediated by PARP, we investigated whether fork reversal upon Top1 inhibition was also dependent on PARP activity. PARP inhibition by NU1025 markedly reduced (9-fold) RF frequency in TPT-treated sperm DNA replicating in Xenopus egg extracts (Fig.2.18). Similarly, PARP inactivation by Olaparib reduced RF frequency by 7-fold in CPT-treated U2OS cells (Fig.2.18). To exclude unspecific effects of PARP inhibitors we also analyzed RF frequency upon CPT treatment of MEFs derived from $PARP1^{+/+}$ and $PARP1^{-/-}$ mice. We observed a significant (2-3 fold) reduction in CPT-induced reversed forks in absence of PARP1. The milder effect observed in PARP1 knock-out cells compared to PARP inhibitors could be due to the partially redundant role of other PARPs in the $PARP1^{-/-}$ background, whereas all PARPs are co-targeted by the inhibitors. These results show that, in *Xenopus*, human and mouse cells, effective fork slowing and reversal upon Top1 inhibition require PARP activity.

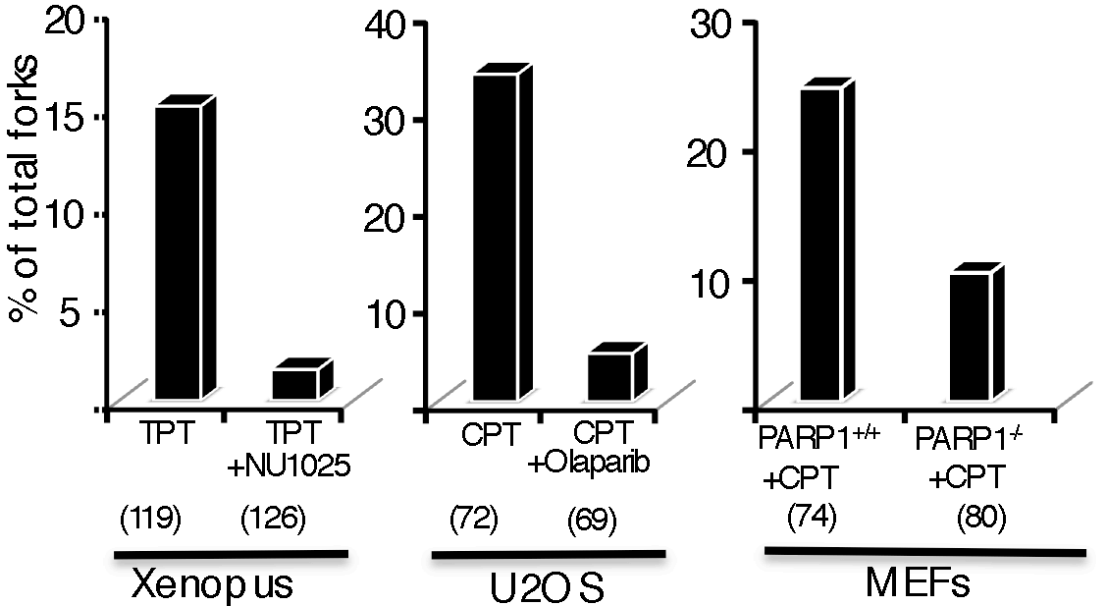

Fig.2.18. Top1 inhibition induces PARP-mediated replication fork reversal. Frequency of fork reversal in *Xenopus* egg extracts (50μM TPT ± 200μM NU1025), U2OS cells (25nMCPT ± 10μM Olaparib) and CPT-treated (25nM) PARP1+/+ and PARP1-/- MEFs by EM. In brackets, the number of analyzed molecules. Similar results were obtained in at least one independent experiment.

3.12 PARP inhibition leads to defective bulk DNA synthesis and increased DSB formation upon Top1 poisoning.

Since PARP activity is required for fork slowdown upon CPT treatments, we next investigated its role in bulk DNA synthesis and checkpoint activation. To address this, a cell cycle analysis was performed in asynchronous cells treated with CPT and/or Olaparib. While Olaparib treatment lead *per se* to modest checkpoint activation and transient delay of cell cycle progression (Fig.2.19A), CPT 25nM treatment markedly delayed S phase progression and strongly activated the DNA damage checkpoint (Fig.2.19A-B), confirming our results in the synchronization setting (Figs.2.10 and Fig.2.13). Simultaneous Top1 and PARP inhibition (CPT + Olaparib) further delays S phase completion, retaining a strong activation of the DNA damage checkpoint (both pChk1 and pATM) (Fig2.19A-B). Considering that PARP inactivation prevents fork slowdown by CPT treatment (Fig.2.17 and Sugimura et al., 2008), these data suggest that slower bulk DNA synthesis rates and consistent checkpoint activation could result from unrestrained fork progression resulting in DSB.

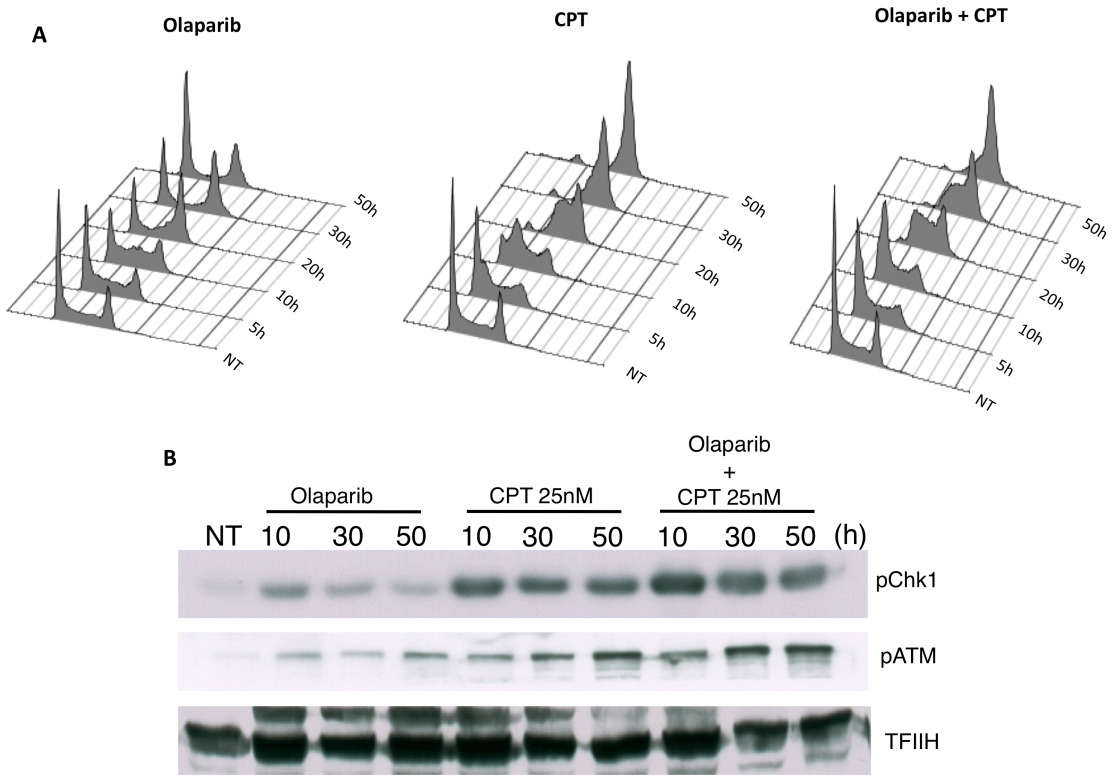

Fig.2.19. **Combined effects of Top1 and PARP inhibition on cell cycle progression and checkpoint activation.** Asynchronously growing U2OS cells were treated with 10μM Olaparib, 25nM CPT or both for the indicated time points. A) Analysis of cell cycle progression by flow cytometric detection of DNA content (Propidium Iodide). B) Western blot analysis of checkpoint activation (pATM and pChk1). TFIIH, loading control.

We thus tested the hypothesis that, upon PARP inhibition, DSB could be detected also upon CPT treatment at low (nM) concentrations. Indeed, PFGE analysis revealed that PARP inhibition by Olaparib in U2OS lead to detectable amounts of DSB upon CPT treatments that showed no detectable (25nM) or only barely detectable (100nM) DSB in control conditions (Fig.2.20). As we did for our EM analysis (Fig.2.18), to rule out possible aspecific effects of PARP inhibitors, similar PFGE experiments were done in PARP1 deficient MEFs. Again, similarly to what we found for fork reversal (Fig.2.18), genetic PARP1 inactivation ($PARP1^{-/-}$ MEFs) led to a mild, but significant DSB accumulation upon 100nM CPT treatment (Fig.2.20).

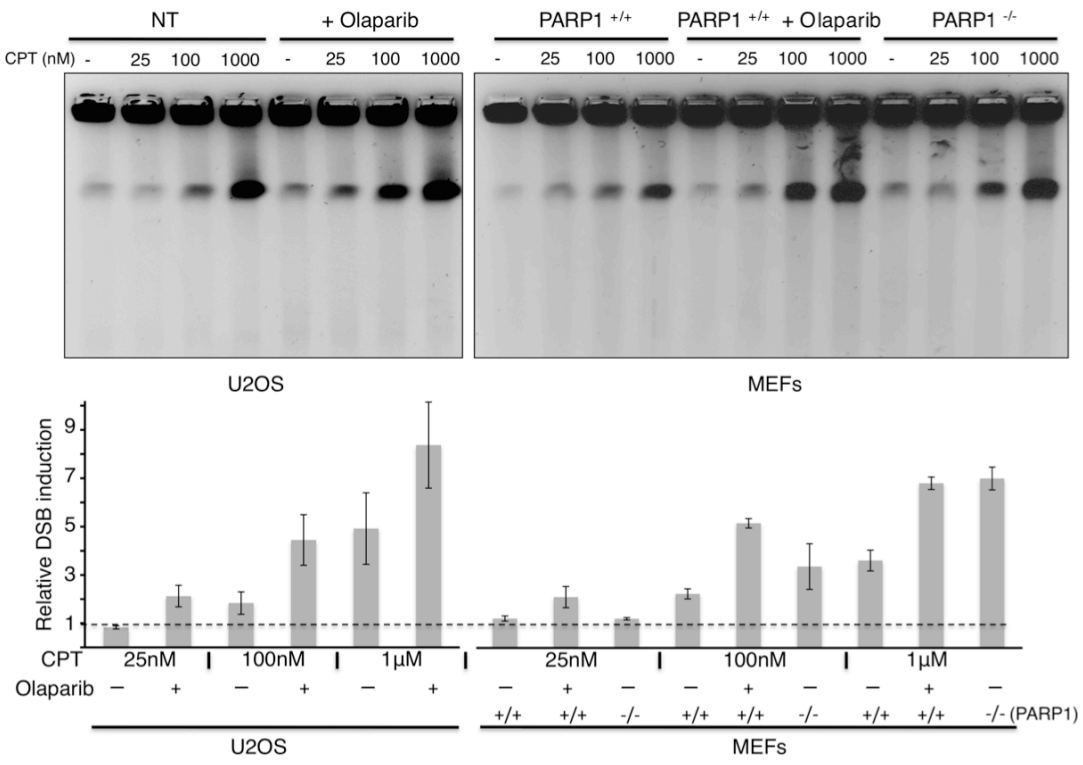

Fig.2.20. PARP inactivation in U2OS and MEFs leads to DSB formation at minimal CPT doses. (A) PFGE analysis for DSB detection upon 4h CPT treatments of U2OS cells, PARP1$^{+/+}$and PARP1$^{-/-}$ MEFs ± 10µM Olaparib. The graph integrates results from three independent experiments and shows DSB levels relative to untreated conditions (dashed line).

To further confirm this observation, we also followed DSB formation by colocalization of the DSB repair factors γH2AX and 53BP1 in nuclear foci. As expected, Olaparib treatment per se had no detectable effect on the detection of the two markers, while γH2AX and 53BP1 showed a high degree of colocalization in IR-induced foci (Fig.2.21A). A high number of γH2AX foci were already detectable in S phase cells at minimal (25nM) CPT doses, but only a minor fraction of them colocalized with 53BP1 (Fig.2.21B). Notably, PARP inhibition in CPT-treated cells did not significantly change the number of γH2AX-positive cells or the total number of γH2AX foci, but led to a higher degree of colocalization of γH2AX and 53BP1 foci upon nM CPT treatments (Fig.2.21B-C). Lethal CPT treatments (≥1µM) lead to more heterogeneous patterns, most probably resulting from replication independent effects (Fig.2.21C). These data suggest that PARP activity limits DSB formation upon Top1 poisoning and that most γH2AX foci formed upon sublethal CPT treatments

identify structures different from DSB.

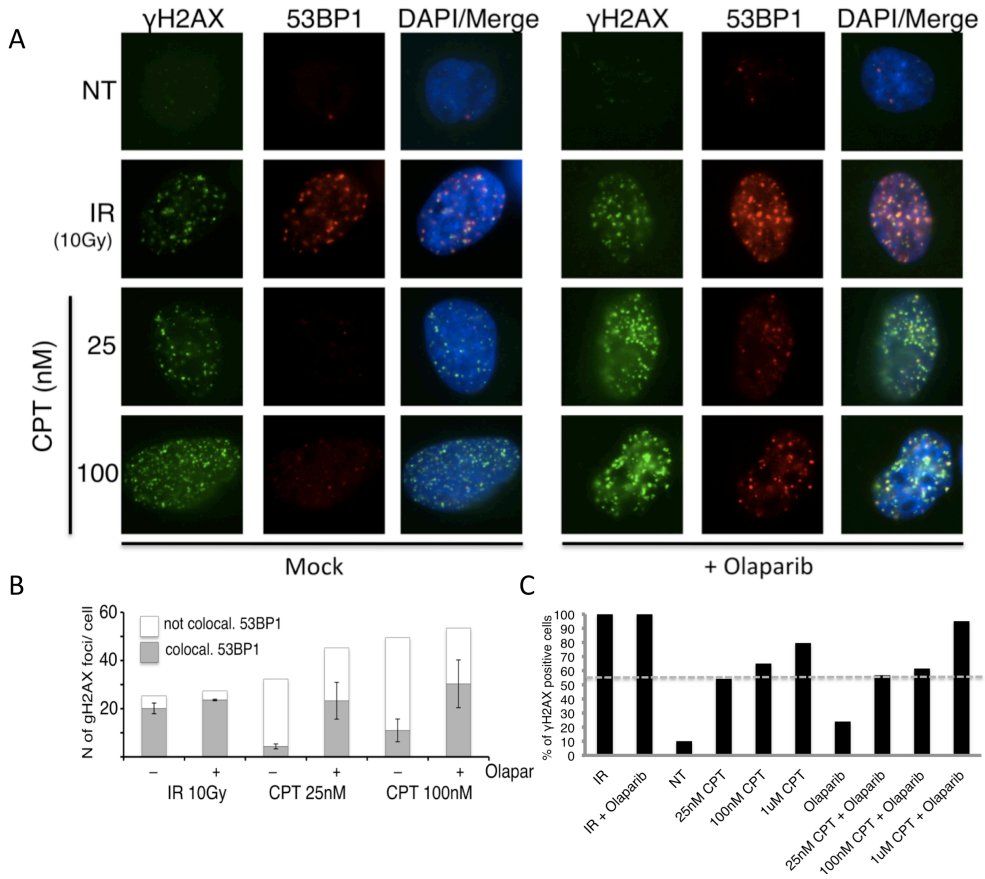

Fig.2.21. IF analysis of DSB markers (γH2AX and 53BP1) upon PARP inactivation at minimal CPT doses. (A) Representative pictures of U2OS cells treated for 1h with CPT, as indicated, ±10μM Olaparib, and co-stained for γH2AX and 53BP1. (B) The graph shows the average number of γH2AX foci per cell and the average fraction (and standard deviations) of γH2AX foci colocalizing with 53BP1. (C) Cells were treated as in (A) and scored for the DNA damage marker γH2AX. The gray dotted line indicates the percentage of cells in S-phase, as determined by an independent EdU incorporation experiment. At least 100nuclei were analyzed in all conditions; positive cells had >5 foci per nucleus. IR (positive control for γH2AX) : U2OS cells 1h after 10Gy irradiation.

Table2.1. List of chromosomal regions showing CPT-induced fork delay by BrdUChIP-chip analysis and their association with centromeres and termination sites. Chromosome numbers, extent (kb) of CPT-induced fork delay, corresponding origin of replication and CPT-delayed fork positions are shown. "+" indicates the presence of a specific genomic element, such as centromeres (CEN) or replication termination regions

Chr	CPT-delay (Kb)	emanating from ARS	Location delayed fork	Termination Fachinetti et al., 2010	CEN database
I	3.2	107	122		
	1.6	108	144		
	1.2	109	155	+	
	2.0	110	168	+	
II	1.5	202	57		
	2.6	208	242	+	
	1.6	209	248	+	
	1.0	209	268		
	2.1	211	328		
	1.0	216	482		
	1.0	new	639		
III	1.1	305	33		
	2.0	305	46		
	1.7	307	103		
	1.5	310	161		
	1.6	315	221		
	2.3	315	228		
IV	1.5	406	122		
	1.7	413	325		
	3.2	414	404		
	1.9	new	428		
	1.7	new	448	+	+
	1.2	416	468	+	
	4.0	417	477		
	1.5	450	507		
	1.4	418	548		
	1.7	418	561		
	2.3	428	918		
	1.5	430	1016		
	1.0	440	1409		

Chr	CPT-delay (Kb)	emanating from ARS	Location delayed fork	Termination Fachinetti et al., 2010	CEN database
V	1.8	507	54		
	1.6	507	64		
	1.0	508	87		
	3.7	511	167		
	1.1	514	292		
	1.1	516	360		
	1.0	517	404		
	1.5	518	436		
	2.0	520	504		
VI	1.4	603.5	123	+	
	1.1	606	173		
	2.0	607	189		
	1.7	608	217		
VII	2.6	707	166		
	1.2	710	208		
	1.6	714	281		
	1.8	718	427		
	1.6	719	479		
	1.4	719	492	+	
	1.2	720	503		
	1.6	722	578		
	1.2	727	662		
	1.0	729	784		
	1.2	731	828		
VIII	1.8	805	59		
	1.0	813	246		
	1.4	820	457		
IX	1.1	913	220		
	1.8	new	319		
	1.4	919	348	+	
	3.5	920	353	+	+

Chr	CPT-delay (Kb)	emanating from ARS	Location delayed fork	Termination Fachinetti et al., 2010	CEN database
X	1.4	1006	96		
	2.1	1009	226		
	1.5	1009	233		
	1.4	1012	368		
	1.1	1012	381		
	1.6	1014	412		
	1.2	1014	423		
	1.4	1015	448	+	
	1.2	1017	455	+	
	1.2	1021	677		
	1.0	1021	686		
XI	2.0	1103	52		
	1.6	1127	212		
	1.0	new	296		
	1.6	new	308		
	1.6	1109	325		
	1.6	1109	327		
	1.9	1112	388		
	2.6	1113	421		
	1.1	1114	442		+
	1.4	new	464		
XII	2.1	new	145	+	
	1.8	1209	149	+	+
	1.8	1211	225		
	1.1	1211	237		
	1.0	1215	417		
	1.1	1217	518		

Chr	CPT-delay (Kb)	emanating from ARS	Location delayed fork	Termination Fachinetti et al., 2010	CEN database
XIII	1.7	1303	37		
	1.5	1305	92		
	1.2	1305	97		
	1.8	1308	177		
	1.0	1312	364		
	1.0	1320	543		
	1.7	1323	614		
	2.0	1325	645		
	1.8	1330	809		
	1.4	1330	822		
	1.6	1332	894		
XIV	2.6	1407	93		
	1.2	1415	316		
	1.5	1421	550	+	
	1.1	1422	552	+	
	2.5	1426	632	+	+
	1.4	1426	641		
XV	1.4	1531	40		
	1.1	1509	111		
	1.4	new	233		
	3.4	1513	353		
	1.4	new	487		
XVI	2.5	1619	413		
	1.2	1633	457		
	1.0	new	548		
	1.6	1622	571		
	1.0	new	586		
	1.1	1625	685		
	1.8	1635	777		
	1.0	1627	816		
	1.8	1628	837		

Additional collaborative results (Steve Fosters and John Petrini; Memorial Sloan Kettering Cancer Center, New York, USA)

It was earlier shown that Ku deficiency mitigates the IR sensitivity of mre11Δ strains, and that the suppressive effect was outside of G1 cells (Bressan et al., 1999). Loss of yKu70 has a similar effect on MMS sensitivity of rad50Δ mutants(Wasko et al., 2009). Based on these observations, and the observation that the Mre11 complex deficiency primarily affects DNA repair by HR (Krogh and Symington, 2004), it was hypothesized that Ku complex had an inhibitory effect on HR. Given its role in DSB end resection (Mimitou and Symington, 2008; Zhu et al., 2008), we examined effects of yKu70 deficiency in mutants with impaired Mre11 nuclease activity (*mre11-3*) upon treatment with CPT.

2.13 yKu70 deficiency rescues the CPT sensitivity of mre11-3 mutants, by an Exo1-mediated mechanism.

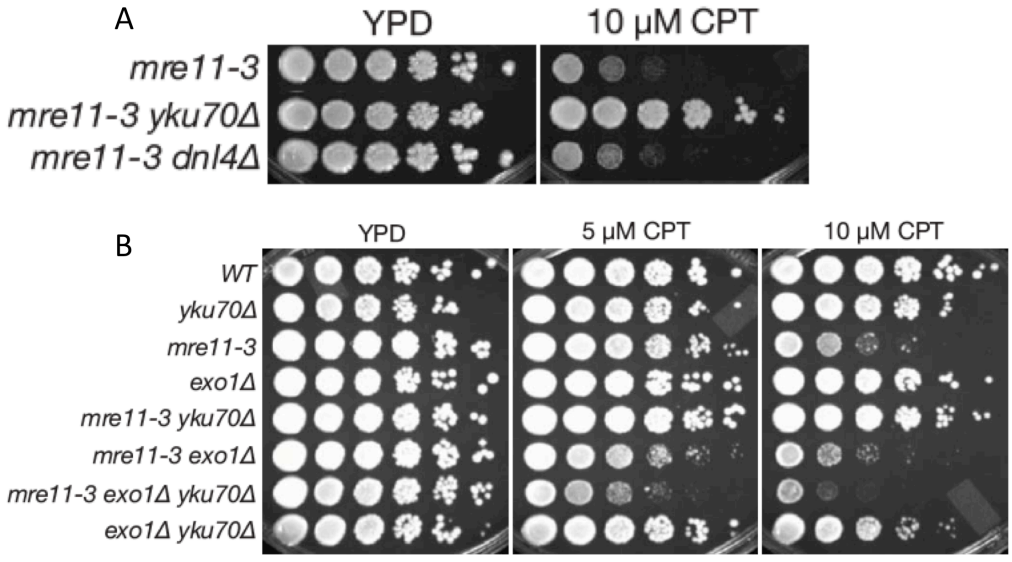

Fig.2.22 yKu70 deficiency rescues the sensitivity of *mre11* nuclease mutants to CPT, by an Exo1-mediated mechanism (Experiments performed by Steve Fosters, MSKCC, NY). Cultures were serially diluted 5-fold, spotted onto YPD containing the indicated doses of CPT and grown at 30°C for 2.5 days. (A) yKu70 deficiency rescues the CPT sensitivity of *mre11-3* mutants. *DNL4* deletion does not rescue the CPT sensitivity of *mre11-3* mutants. (B) Exo1 deficiency abolishes the *yku70Δ*-dependent rescue of *mre11-3* CPT sensitivity.

To investigate how CPT treatment affects survival of different yeast strains, serial dilutions of yeast cultures were spotted on YPD plates containing different CPT doses (Fig.2.22A). 10μM CPT treatments led to high degree of sensitivity in *mre11-3* cells. *mre11-3 yku70Δ* double mutants, on the other hand exhibited reduced sensitivity to CPT (Fig2.22A). The rescue of CPT sensitivity was not attributable to *yku70Δ* -associated defects in NHEJ, as DNA ligase IV deficiency in *mre11-3* mutants did not alter CPT sensitivity at any dose tested (Fig.2.22A). These data indicate that yKu70 has an NHEJ independent function that increases the toxicity of CPT-induced DNA lesions.

Furthermore, it was found that Exo1 deficiency abolished *yku70Δ*-dependent suppression of *mre11-3* CPT sensitivity (Fig.2.22B), as shown by higher CPT sensitivity of *mre11-3 exo1Δ yku70Δ* triple mutants compared to either *mre11-3 yku70Δ* or *mre11-3* cells. In addition, Exo1 deficiency partially increased the CPT sensitivity of both *mre11-3* and *yku70Δ* single mutants, supporting the view that DNA end resection by Exo1 is the basis of the *yku70Δ* rescue (Fig.2.22B). These data suggest that Ku inhibits the ability of Exo1 to act at DNA ends and that this Exo1 activity becomes crucial for CPT resistance in the absence of Mre11 nuclease activity.

2.14. EXO1 mediated *yku70Δ*-dependent suppression does not alter the frequency of fork reversal but leads to aberrant DNA structures.

Since treatment with CPT induces rapid fork reversal in yeast, we hypothesized that Mre11 could be responsible for mediating resection of the regressed arm, to promote fork restart. According to this model, in the absence of Mre11-resection, , Ku70 would bind to the regressed arm and stabilize the structure, aborting replication intermediates and leading to increased CPT cytotoxicity. In the absence of both

Mre11 nuclease activity and Ku, Exo1 may gain access to the fork and provide an alternative nuclease activity to promote reversed fork restart. To test this hypothesis, we treated wt, *mre11-3*, *yku70Δ, mre11-3 yku70Δ* and *mre11-3 yku70Δexo1Δ* cells with CPT and analyzed their RIs by EM.

Analysis of RIs revealed no significant difference in the frequency of reversed

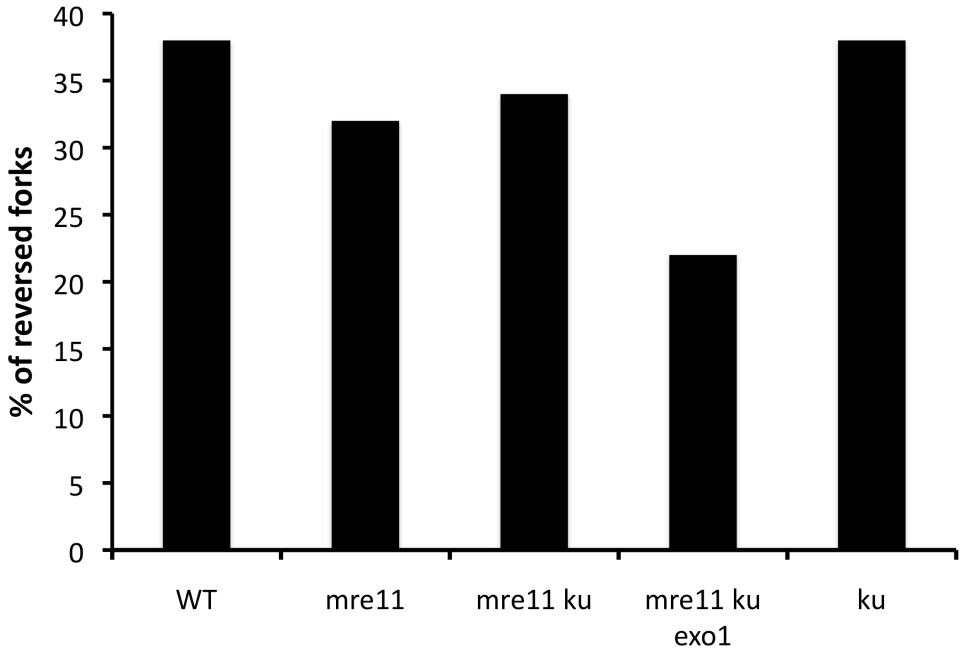

Fig.2.23 Similar frequency of CPT-mediated fork reversal in wt, *mre11-3*, *yku70Δ, mre11-3 yku70Δ* and *mre11-3 yku70Δexo1Δ* cells. Preliminary data for frequency of fork reversal in Wt, *mre11-3*, *yku70Δ, mre11-3 yku70Δ* and *mre11-3 yku70Δexo1Δ* cells treated with CPT 50μM. At least 50 molecules were analyzed for each strain.

fork formation in all the strains with the exception of *mre11-3 yku70Δexo1Δ* (Fig.2.23). *mre11-3 yku70Δexo1Δ* showed a lower frequency of reversed fork formation than the other strains, but this analysis needs to be completed by increasing the total number of RIs analyzed in order to assess whether this difference may be statistically significant.

Furthermore, all strains bearing the mre11-3 mutation showed frequent aberrant DNA structures characterized by increased numbers of "ramifications" on the DNA, that

cannot be attributed to any recognizable molecular pattern typically observed at RIs (Fig.2.24A-B). This pathological phenotype was never previously observed at RIs in response to different kinds of replication stress and is a relatively rare event also in CPT-treated wt and *yku70Δ* cells (Fig.2.24B). Therefore, these unusual intermediates may contribute to explain the strong CPT-sensitivity associated with the *mre11-3* mutation (Fig.2.24A). The frequency of these unusual ramified molecules reaches approximately 50% of the total number of analyzed molecules in *mre11-3* and *mre11-3 yku70Δ exo1Δ*, the two CPT-hypersensitive strains. Interestingly, although *mre11-3 yku70Δ* cells also showed these molecules, their overall frequency (approximately 30%) was reduced compared to *mre11-3* and *mre11-3 yku70Δexo1Δ* mutants (Fig.2.24B).. A similar trend was also observed considering the number of ramifications in individual DNA molecules, with the *mre11-3* and *mre11-3 yku70Δexo1Δ* strains showing the highest number of ramifications/molecule, compared to *mre11-3 yku70Δ.*

It is currently unclear how these aberrant molecules are formed and what is their relationship with the observed, CPT-induced reversed forks. One interesting hypothesis to pursue in the future is that these molecules result from restart of forks that had been previously, transiently reversed. In this scenario, the observed reversed forks may mark transiently stalling at the specific time chosen for DNA extraction, which is not necessarily expected to change in the different genetic backgrounds. On the other hand, the aberrant "ramified" molecules may reflect failing attempts to restart forks that had been stalled and reversed at an earlier time point. In this respect, the lower penetrance of this phenotype in *mre11-3 yku70Δ* cells may result from more effective, Exo1-mediated processing of these structures, which could eventually result in restored genome integrity and contribute to the CPT-resistance observed in

this genetic background. Additional work will be required to test this hypothesis and fully understand the surprising molecular phenotypes observed in these strains upon Top1 inhibition.

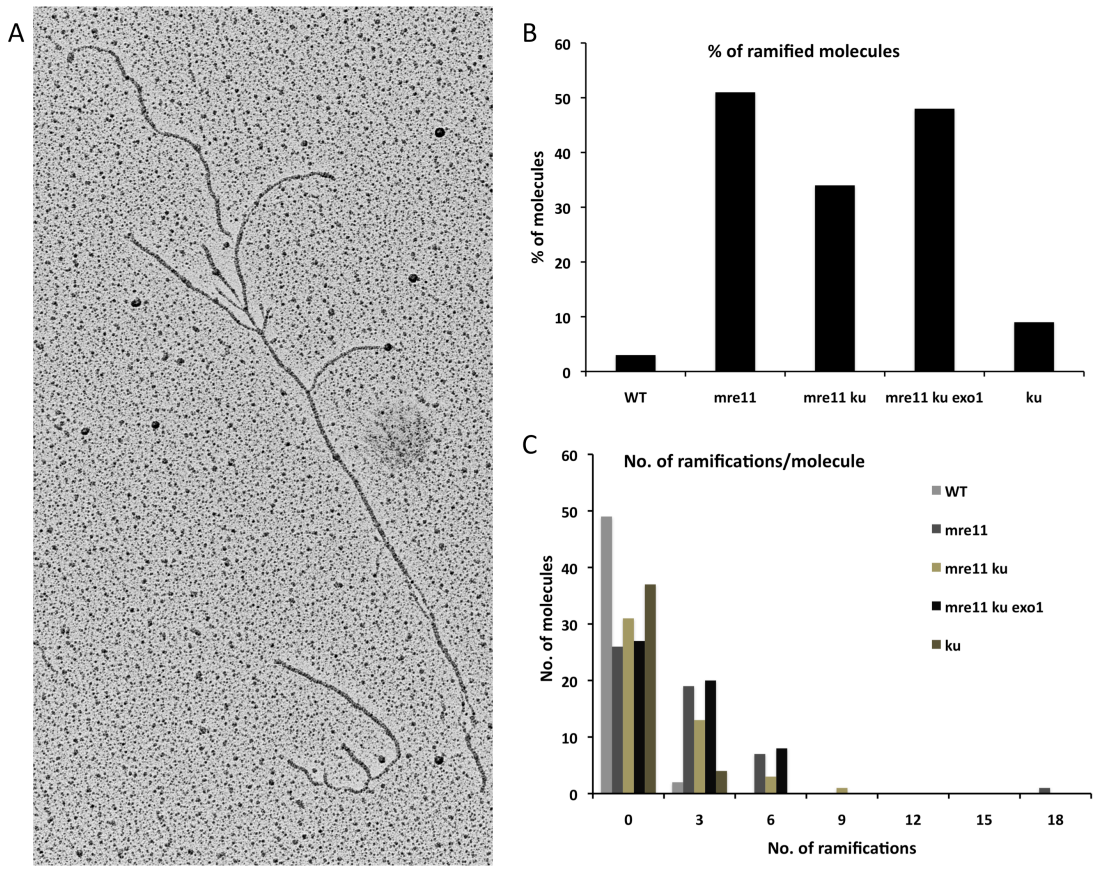

Fig.2.24 Top1 inhibition results in aberrant DNA structures in *mre11-3*, *mre11-3 yku70Δ* and *mre11-3 yku70Δexo1Δ* cells. A) Representative electron micrograph of an aberrant RI observerd in CPT-treated *mre11-3* cells. (B) Statistical analysis of the percentage of "ramified" molecules in Wt, *mre11-3*, *yku70Δ, mre11-3 yku70Δ* and *mre11-3 yku70Δexo1Δ* cells treated with CPT 50μM. At least 50 molecules were analyzed for each strain. (C) Statistical analysis of the number of ramifications/molecule in the strains as in (B)

nature structural & molecular biology

Rad51 protects nascent DNA from Mre11-dependent degradation and promotes continuous DNA synthesis

Yoshitami Hashimoto[1], Arnab Ray Chaudhuri[2], Massimo Lopes[2] & Vincenzo Costanzo[1]

The role of Rad51 in an unperturbed cell cycle has been difficult to distinguish from its DNA repair function. Here, using EM to visualize replication intermediates assembled in *Xenopus laevis* egg extract, we show that Rad51 is required to prevent the accumulation of single-stranded DNA (ssDNA) gaps at replication forks and behind them. ssDNA gaps at forks arise from extended uncoupling of leading- and lagging-strand DNA synthesis. In contrast, ssDNA gaps behind forks, which are prevalent on damaged templates, result from Mre11-dependent degradation of newly synthesized DNA strands and are suppressed by inhibition of Mre11 nuclease activity. These findings reveal direct roles for Rad51 at replication forks, demonstrating that Rad51 protects newly synthesized DNA from Mre11-dependent degradation and promotes continuous DNA synthesis.

Genomic DNA is highly vulnerable to mutagenesis during DNA replication as replication fork progression is frequently impaired by DNA lesions caused by exogenous or endogenous factors such as ultraviolet light and reactive oxygen species. Many redundant pathways preserve fork integrity in the presence of DNA damage[1,2]. This prevents the lethal effects caused by the complete collapse of replication forks leading to double-strand breaks (DSBs). DNA lesions can be bypassed by error-prone translesion synthesis polymerases such as Pol η or Pol ζ[3]. This polymerase switching requires monoubiquitination of proliferating cell nuclear antigen (PCNA) at Lys164 mediated by the Rad6–Rad18 complex[4].

Another pathway called template switching ensures continuous, error-free replication across DNA lesions by using newly synthesized, undamaged daughter strand as a template, instead of the damaged parental strand, so as to bypass the lesion. Template switching has been proposed to involve fork regression by annealing of nascent strands at the fork[1,2].

Strand invasion of the paused nascent strand into the sister chromatid to continue replication is also possible. This pathway requires homologous recombination proteins such as Rad51, the eukaryotic ortholog of RecA in *Escherichia coli*, which has a central role in homologous recombination during meiosis as well as during DSB repair[5].

Rad51 is not essential in yeast, but it is required for cell proliferation in vertebrates[6,7]. This suggests that in vertebrates Rad51 has indispensable roles not only in meiotic chromosomal recombination and segregation but also in the normal cell cycle. A role for Rad51 in S phase has been postulated[8–10]. However, it is unclear whether Rad51 is solely required to repair DSBs that spontaneously arise during the normal cell cycle, or whether it has an additional replicative role beyond DSB repair.

The pathways described above (translesion synthesis, template switching and homologous recombination), which are involved in postreplication repair, could operate at the fork to ensure its progression through DNA damage. However, these pathways might not be necessary for the fork progression itself and could instead be deployed to repair gaps behind the fork[11]. This issue is only poorly understood because there is not enough structural information available about replication forks and their surrounding regions. A few studies have highlighted DNA gaps behind forks in the presence of obstacles to replication fork progression[12,13]. Rad51 has been suggested to mediate two distinctive pathways: one promotes replication restart after short exposure to hydroxyurea, whereas the other promotes repair of forks completely collapsed by prolonged exposure to hydroxyurea[14]. The former pathway is also supported by evidence showing that nucleotide excision repair (NER) mutant cells irradiated with ultraviolet light accumulate collapsed forks, which are mainly rescued by a Rad51-dependent pathway to enable restart[15]. These results suggest that Rad51 functions both at forks and behind them.

In this study, we established a cell-free system based on *X. laevis* egg extract to study the role of Rad51 during DNA replication. Using EM-based analysis to directly observe replication fork structures and a biochemical assay to detect DNA gaps, we have discovered that Rad51 is required to prevent formation of DNA gaps at forks and behind them. DNA gaps behind forks are suppressed by inhibition of Mre11 nuclease activity, indicating that Rad51 protects nascent DNA from nuclease-mediated degradation.

RESULTS

Rad51 associates with replicating chromatin

Xenopus laevis egg extracts can be used to biochemically characterize essential DNA repair proteins involved in DNA replication[16–19].

[1]London Research Institute, South Mimms, Hertfordshire, UK. [2]Institute of Molecular Cancer Research, University of Zürich, Zürich, Switzerland. Correspondence should be addressed to V.C. (vincenzo.costanzo@cancer.org.uk) or M.L. (lopes@imcr.uzh.ch).

Received 29 April; accepted 8 September; published online 10 October 2010; doi:10.1038/nsmb.1927

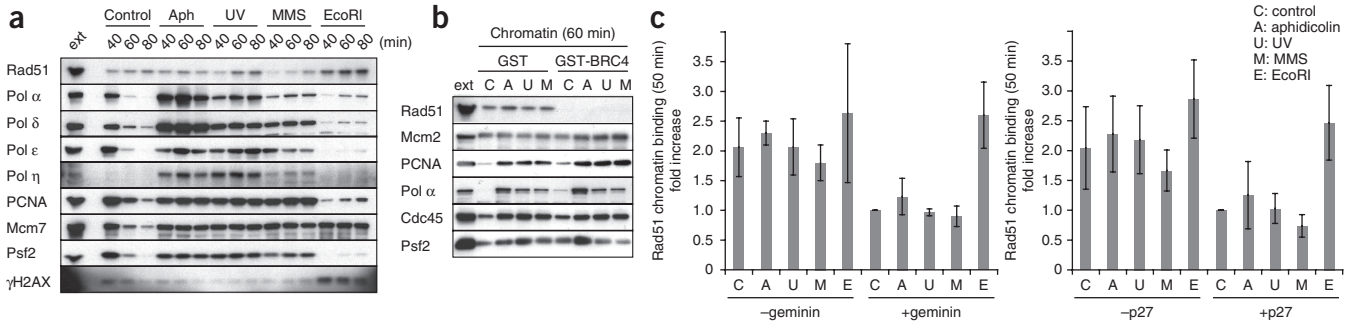

Figure 1 Rad51 binding to undamaged and damaged chromatin during DNA replication. (**a**) Time course of chromatin association of Rad51 and the indicated replication proteins. Immunoblotting was carried out for chromatin fractions incubated in 30 μl egg extract for indicated times in presence or absence of aphidicolin (Aph, 10 μg ml^{-1}) or EcoRI (0.1 unit μl^{-1}). Where indicated, sperm nuclei were treated with 1,000 J m^{-2} ultraviolet (UV) light and 1% (v/v) MMS, respectively. 0.5 μl egg extract (ext) was used as control. (**b**) Effect of BRC4 on chromatin association of Rad51 and replication fork proteins. Immunoblotting was carried out for chromatin fractions incubated in 25 μl of egg extract for 60 min in the presence of 0.5 mg ml^{-1} GST or 0.5 mg ml^{-1} GST-BRC4. Sperm nuclei were incubated in extracts that were untreated (–) or incubated with 50 μg ml^{-1} aphidicolin. Where indicated sperm nuclei were irradiated with ultraviolet light at 1,000 J m^{-2} or treated with 1% (w/v) MMS before the incubation in egg extract. 1 μl extract (ext) was used as control. (**c**) Quantification of Rad51 bound to damaged and undamaged chromatin in the presence (+geminin) or in the absence (–geminin) of 160 nM geminin, and in the presence (+p27) or absence (–p27) of 40 μg ml^{-1} p27 recombinant protein. Graph, average relative values of several repeated experiments taking as reference the amount of Rad51 bound to undamaged chromatin in the presence of geminin or p27 (C, control). Error bars, ± s.d. Representative immunoblots are shown in **Supplementary Figure 1a–b**.

To verify whether Rad51 has a role in DNA replication, we monitored chromatin binding of *X. laevis* Rad51, which is highly conserved among vertebrates and is present at 20 nM in *X. laevis* egg extract (data not shown). We also monitored the binding of other replication factors during DNA replication on undamaged and damaged templates. We found that Rad51 binds to chromatin during DNA replication (**Fig. 1a**). Its binding is impaired by inhibition of replication origin assembly, induced by supplementing extract with geminin, which prevents minichromosome maintenance (MCM) helicase loading[20] (**Fig. 1** and **Supplementary Fig. 1a**), and by inhibition of origin firing, achieved by treating extracts with cyclin-dependent kinase inhibitor p27 (ref. 21; **Fig. 1** and **Supplementary Fig. 1b**). Rad51 binding in the presence of agents that stall replication forks, such as aphidicolin, ultraviolet light and methylmethanesulfonate (MMS), was also sensitive to geminin and p27 (**Fig. 1** and **Supplementary Fig. 1b**). In contrast, the induction of DSBs mediated by EcoRI endonuclease, revealed by the presence of γH2AX, was resistant to geminin and p27 treatments (**Fig. 1** and **Supplementary Fig. 1a,b**). These data indicate that a fraction of Rad51 binding to chromatin takes place after replication forks have been established and depends partly on the number of active replication forks. Consistent with this, the amount of Rad51 bound to chromatin was linearly correlated with the levels of Psf2 and therefore with the number of active forks (**Fig. 1a**). Accordingly, the relative amount of Rad51 per fork, calculated by

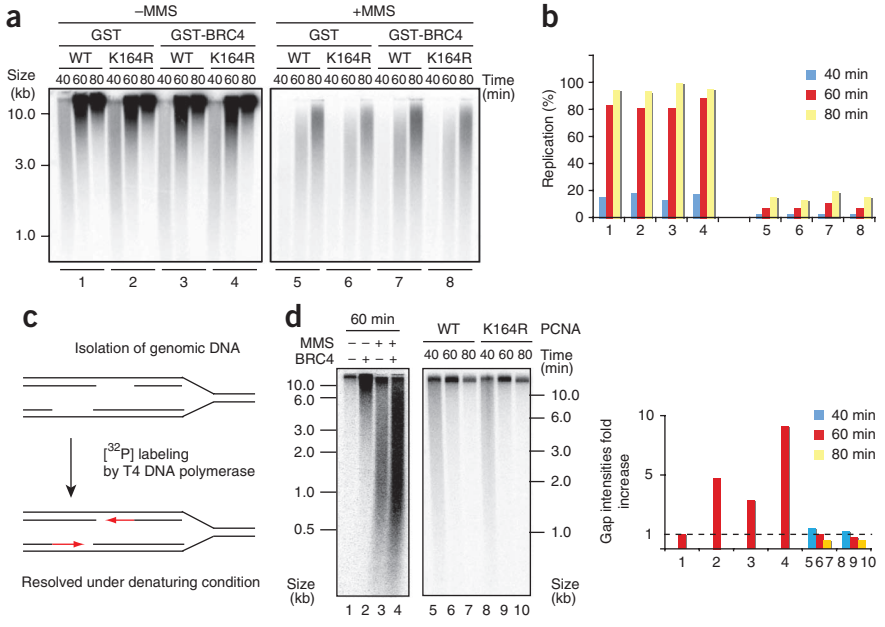

Figure 2 Rad51 and PCNA modifications in DNA replication and ssDNA gap accumulation. (**a**) Rad51 and PCNA requirement for replication of untreated and MMS-treated DNA. Replication products resolved on 1% (w/v) alkaline gels obtained by incubating sperm nuclei in 10 μl egg extract with [α-^{32}P]dATP for the indicated times in presence or absence of 0.7 mg ml^{-1} GST or GST-BRC4 and MMS (– or +), and 0.2 mg ml^{-1} of recombinant wild-type (WT) or mutated (K164R) PCNA. (**b**) Quantification of signal intensities in **a**. Experiments shown represent a typical result. (**c**) Gap-labeling procedure using T4 DNA polymerase. Replicating genomic DNA was isolated and used as a template for gap-filling assay using T4 DNA polymerase. The labeled nascent molecules extended by T4 were then resolved on alkaline agarose gel. (**d**) Untreated (–MMS) and MMS-treated (+MMS) sperm nuclei were incubated in 10 μl of egg extract in the presence of GST or GST-BRC4 for 60 min (lanes 1–4). Untreated sperm nuclei were incubated for 40, 60 or 80 min in the presence of wild-type (WT) PCNA or PCNA K164R (lanes 5–10). Genomic DNA was isolated and subjected to the gap-labeling reaction followed by autoradiography. Exposure times are equivalent for the two gels, although kinetic profile starts at 40 min in lanes 5–10. Graph, relative fold increase in optical density for each lane taking as reference untreated chromatin recovered at 60 min. Experiment shows a typical result.

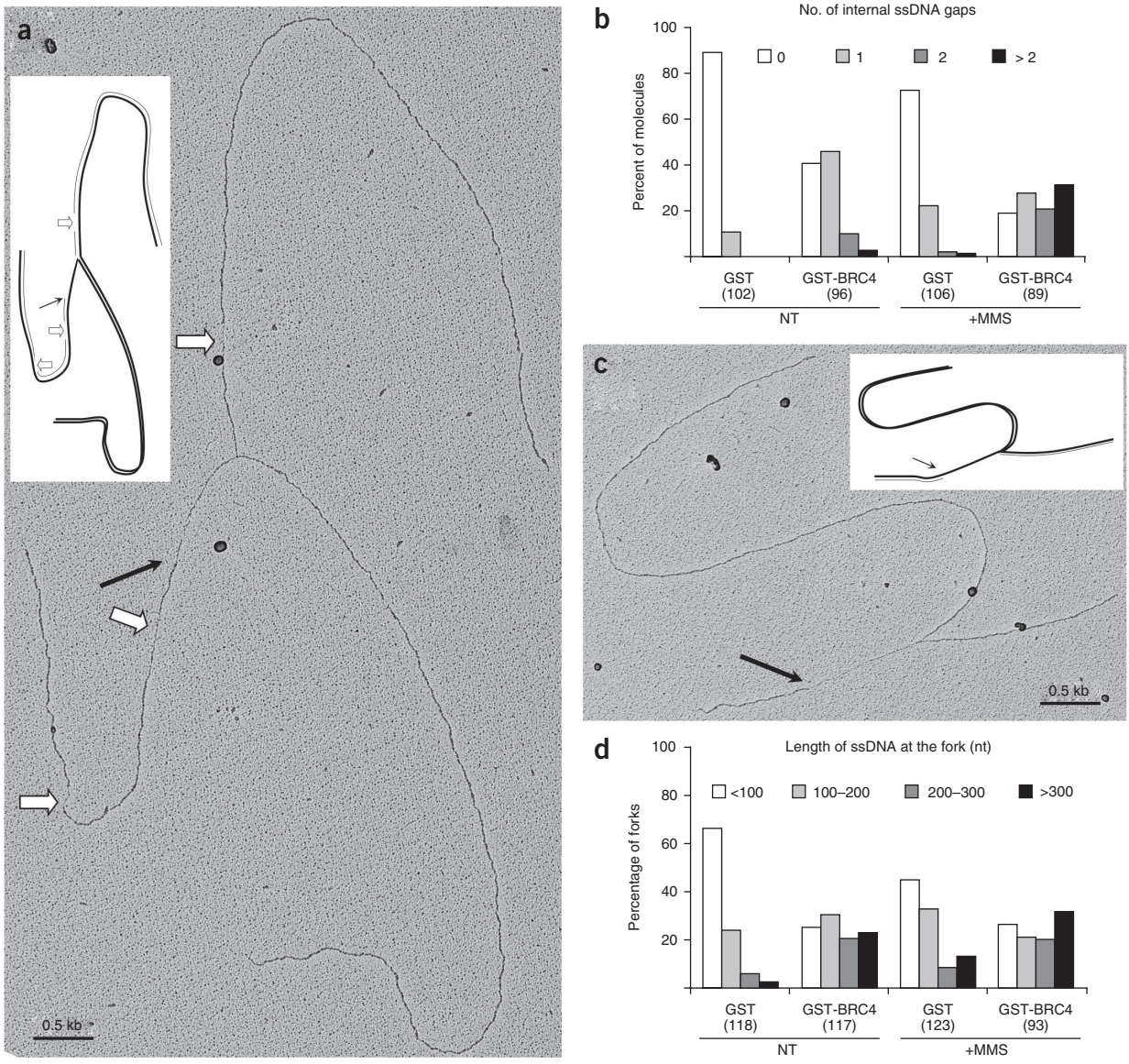

Figure 3 Rad51 is required to prevent replication fork uncoupling and ssDNA accumulation on damaged and undamaged templates. (**a**) Electron micrograph (and schematic drawing) of a representative replication intermediate isolated from sperm nuclei incubated in GST-BRC4 treated extracts. Black arrows, ssDNA regions at the replication fork. White arrows, ssDNA gaps along the replicated duplexes (internal gaps). (**b**) Statistical distribution of internal gaps in the analyzed population of molecules. Number of molecules analyzed is in parentheses. (**c**) Electron micrograph of a representative replication intermediate showing an extended ssDNA region at the fork (arrow). (**d**) Statistical distribution of ssDNA length at replication forks isolated in the indicated conditions. Number of forks analyzed is in parentheses.

determining the ratio between Rad51 and Psf2 signal intensities at 40 min, was 0.35 for untreated extracts and 0.57, 0.55 and 0.51 for extracts treated with aphidicolin, ultraviolet light and MMS, respectively. Overall, these data suggest that in addition to its role in DSB repair, Rad51 is involved in DNA replication.

Effects of impaired Rad51 chromatin binding

To study the replication function of Rad51, we inhibited Rad51 binding to chromatin using recombinant human BRC4 (one of eight BRC motifs of BRCA2 that has a strong affinity for Rad51; ref. 22) fused to glutathione S-transferase (GST), GST-BRC4, which efficiently binds *X. laevis* Rad51 even at high salt concentrations (**Supplementary Fig. 1c**). GST-BRC4 completely suppressed Rad51 chromatin binding but did not impair the binding of replication proteins such as Mcm2, PCNA, Pol α, Cdc45 and Psf2 of the GINS complex (**Fig. 1b**). This indicates that Rad51 is not required for the assembly of replication proteins onto chromatin. Unlike the BRC4 peptide used by Carreira *et al.*[23], the peptide used here (residues 1511–1579 of BRCA2) does not promote Rad51 binding to ssDNA *in vitro*. We used the minimal GST-BRC4 concentration required to effectively suppress Rad51 binding to chromatin (data not shown). As at this concentration GST-BRC4 suppressed both ssDNA and double-stranded DNA (dsDNA) binding of Rad51 (**Supplementary Fig. 1d**), we could not determine whether the effects we observed on chromatin derive mainly from the inhibition of Rad51 binding to ssDNA or to dsDNA.

To determine the role of Rad51 in DNA synthesis, we analyzed nascent ssDNA molecules recovered from *X. laevis* egg extracts in which Rad51 chromatin binding was inhibited by GST-BRC4. As redundant

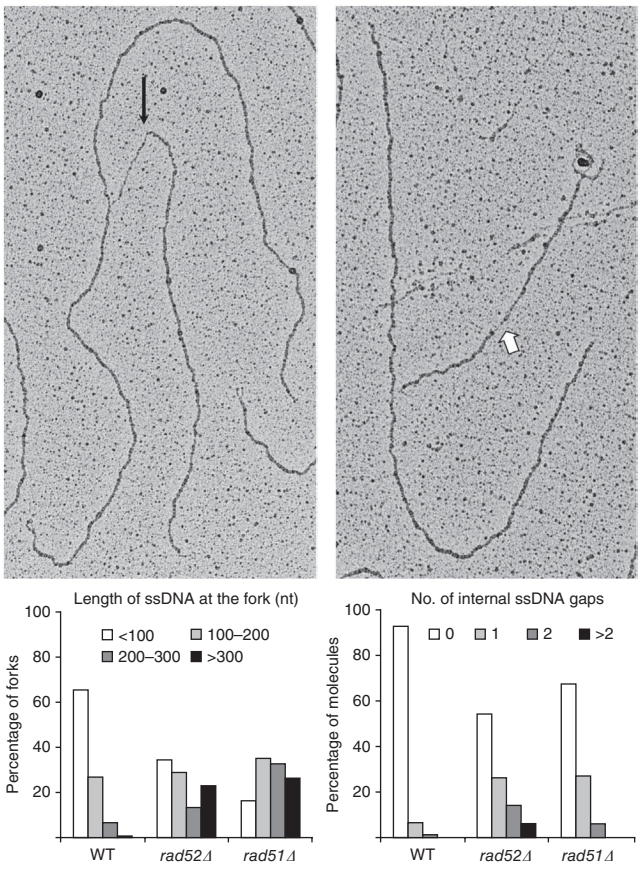

Figure 4 Accumulation of ssDNA gaps in the absence of Rad52 and Rad51 in *S. cerevisiae*. Top, electron micrographs of representative replication intermediates isolated from *rad52* mutant *S. cerevisiae* growing cells. Black arrow, extended ssDNA regions at the replication fork. White arrow, ssDNA gap behind the fork. Bottom, statistical distribution of ssDNA length at replication forks (left) and of the number of ssDNA gaps (right) observed on replication intermediates isolated from wild-type (WT), *rad52Δ* and *rad51Δ* mutant *S. cerevisiae* growing cells.

postreplication repair pathways such as translesion synthesis could mask the role of homologous recombination in replication fork progression, we also attenuated translesion synthesis using a recombinant mutant PCNA (PCNA K164R) that cannot be ubiquitinated[24] and therefore does not fully support binding of translesion Pol η to chromatin (**Supplementary Fig. 1e**). DNA replication efficiency was not affected by inhibition of Rad51 chromatin binding and/or impairment of translesion synthesis (**Fig. 2a**,**b**, lanes 1–4). Furthermore, after DNA damage induced by MMS, the efficiency of DNA replication decreased (**Fig. 2a**,**b**, lanes 5–8) owing to hindrance of fork progression and checkpoint-mediated inhibition of further origin firing[25]. However, residual DNA replication was not affected, and nascent DNA strands matured with similar kinetics in the absence of Rad51 and/or PCNA ubiquitination (**Fig. 2a**, lanes 5–8). Collectively, these data show that Rad51 is dispensable for fork progression even with impaired translesion synthesis.

Accumulation of ssDNA gaps in the absence of Rad51

Having ruled out a role in replication fork progression for Rad51, we investigated subtler genomic defects to elucidate the function of Rad51 in DNA replication. Chicken DT40 cells deficient in Rad51 accumulate ssDNA gaps[26] and DSBs[7] after one or a few cell cycles, respectively. However, it is unclear whether such lesions arise directly from defects in the DNA replication process or in DNA repair. We did not detect formation of DSBs after one round of DNA replication in the absence of Rad51 bound to chromatin (data not shown). However, using a gap-filling assay[27] based on T4 DNA polymerase, which has primer extension and translesion synthesis[28] but not strand displacement activities (**Fig. 2c**,**d**), we observed a five-fold increase of labeled ssDNA molecules on undamaged (>10 kilobases (kb)) and MMS-damaged templates (0.5–10 kb) in extracts treated with GST-BRC4, confirming that although DNA replication is not inhibited, ssDNA gaps accumulate in the absence of Rad51 bound to chromatin (**Fig. 2d**, lanes 1–4).

We also monitored the accumulation of ssDNA gaps in extracts deficient in translesion synthesis, which helps prevent the accumulation of ssDNA gaps after damage by ultraviolet light. As we expected, we observed increased ssDNA gaps on damaged templates in the absence of translesion synthesis (**Supplementary Fig. 2**), and we observed no additive effects in the presence of both GST-BRC4 and PCNA K164R, suggesting that Rad51 and translesion synthesis operate in the same gapped regions. These observations are consistent with the postreplication repair model, in which replication forks proceed past DNA damage, leaving unreplicated ssDNA gaps that are subsequently sealed by translesion synthesis and/or homologous recombination[11,29].

However, in contrast to our findings for Rad51, translesion synthesis impairment alone did not induce noticeable accumulation of ssDNA gaps on undamaged templates (**Fig. 2d**, lanes 5–10). This indicates that Rad51 but not translesion synthesis prevents the accumulation of such lesions on undamaged templates and suggests that Rad51 has a specific role in preventing replication-associated DNA lesions in addition to its role in DNA repair.

Notably, an excess of recombinant *X. laevis* Rad51 added back to egg extract containing GST-BRC4 suppressed the accumulation of ssDNA gaps (**Supplementary Fig. 3**). We obtained similar results by adding recombinant human Rad51, but not by adding an irrelevant protein such as GST (data not shown). These control experiments confirm the specificity of GST-BRC4 effects on Rad51.

Replication intermediate structure in the absence of Rad51

To investigate Rad51 function during DNA replication, we carried out *in vivo* EM analyses of genomic replication intermediates coupled to psoralen cross-linking, according to established methods and procedures[30] that we adapted to sperm nuclei replicated in *X. laevis* egg extracts, with and without DNA damage (see Online Methods). Under standard enrichment procedures used for analogous analysis in yeast and mammalian cells[12,30,31], EM samples showed a high frequency of replication intermediates. After we identified replication intermediates (see Online Methods), we assessed the frequency and length of ssDNA regions by detecting local differences in filament thickness. Although ssDNA stretches can also be detected by EM using single strand–binding proteins, short ssDNA stretches do not consistently assemble nucleoprotein complexes and may escape EM detection[12]. Instead, we assessed DNA thickness along replicating molecules to score the number and size of ssDNA gaps, focusing on relative differences from control samples under the same experimental conditions[12]. We found that, during DNA replication, 60% of replication intermediates isolated from extracts in which Rad51 chromatin binding was inhibited showed at least one ssDNA gap behind the replication fork (internal gaps, **Fig. 3a**,**b**), a rare event in control extracts. Whereas control extracts treated with MMS accumulated relatively few internal gaps, Rad51-depleted extracts treated

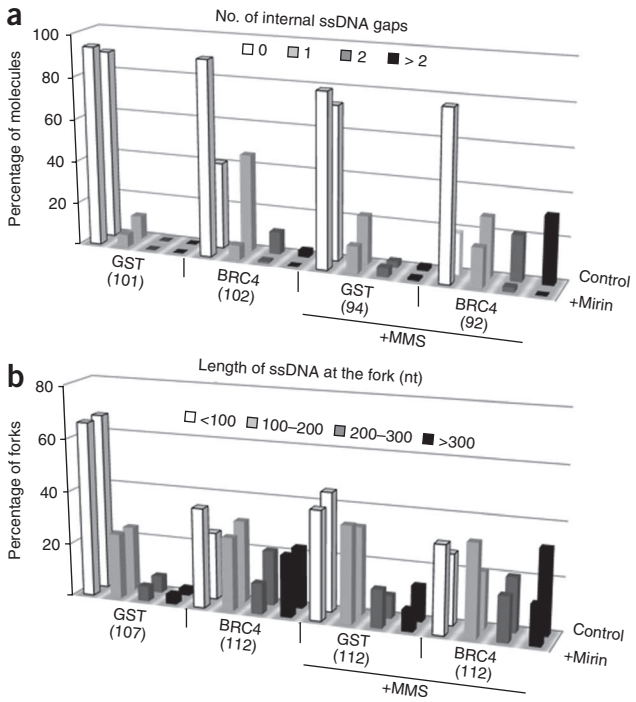

Figure 5 Rad51 protects nascent strand DNA from Mre11-dependent degradation. (**a**) Statistical distribution of internal gaps in the analyzed population of molecules isolated from extracts supplemented with buffer (control) or 100 μM mirin and treated as indicated. Number of molecules analyzed is in parentheses. (**b**) Statistical distribution of ssDNA length at replication forks isolated from extracts supplemented with buffer (control) or 100 μM mirin and treated as indicated. Number of molecules analyzed is in parentheses.

with MMS had gaps in 80% of replication intermediates, and more than two gaps on the same fork in 30% of replication intermediates (**Fig. 3b**). The size of the internal gaps is rather heterogeneous, but in most cases <300 nucleotides (nt). Even though Rad51-depleted extracts had more gaps than the control extracts, the size distribution of the gaps was similar (**Supplementary Fig. 4**). Such ssDNA gaps behind replication forks have been observed and related to repriming events downstream of lesions on the template[12]. Consistently, their persistence in cells deficient in homologous recombination and translesion synthesis has been attributed to defects in postreplication repair.

As repriming was shown to result from extended uncoupling of leading- and lagging-strand synthesis[12], we analyzed replication intermediates for the presence of ssDNA regions directly at the fork. Small ssDNA regions (<200 nt) are often detectable by this assay at unperturbed replication forks, marking discontinuous lagging strand synthesis[12]. Notably, even without exogenous DNA damage, ~50% of replication intermediates in Rad51-depleted extracts had a markedly long (>200 nt) ssDNA region at the fork (**Fig. 3c**,**d**), suggesting frequent uncoupling of leading- and lagging-strand synthesis. In many cases, we detected ssDNA regions of up to 800 nt (**Fig. 3c**). As has been shown for yeast[12], MMS treatment, even at concentrations that markedly affect fork progression (**Fig. 2**), had limited effects on leading- and lagging-strand uncoupling, as 80% of control replication intermediates had ssDNA regions at the fork of <200 nt in the presence of MMS (**Fig. 3d**). This suggests that the mechanism producing ssDNA at forks is distinct from the one responsible for ssDNA-gap formation behind them in the presence of MMS-induced DNA damage. Notably, we also observed that ssDNA tracts accumulated during DNA replication at forks and behind them in yeast *rad52Δ* mutants (**Fig. 4**) in which Rad51 chromatin loading is impaired[32,33]. We obtained similar results with yeast *rad51Δ* mutants, although the accumulation of post-replicative ssDNA gaps was less pronounced than in *rad52* cells. This probably reflects the contribution of *S. cerevisiae* Rad59, a Rad52 paralog that mediates Rad51-independent recombination mechanisms[34]. Overall, these data indicate that the function of Rad51 to prevent the accumulation of ssDNA gaps is conserved across different species.

Mre11-dependent formation of ssDNA gaps behind forks

We then tested whether ssDNA accumulation arises from nuclease-dependent degradation of newly synthesized DNA. To this end, we treated extracts with mirin, which specifically inhibits the activity of Mre11 (ref. 35), a major nuclease present at replication forks[17,36]. Notably, mirin prevented accumulation of detectable ssDNA gaps behind forks formed upon suppression of Rad51 binding to DNA (**Fig. 5a**). In contrast, Mre11 inhibition by mirin did not suppress accumulation of ssDNA at forks (**Fig. 5b**). EM analysis was more useful in assessing the effects of mirin and Rad51 inhibition than the gap-filling assay, as this could not discriminate between ssDNA

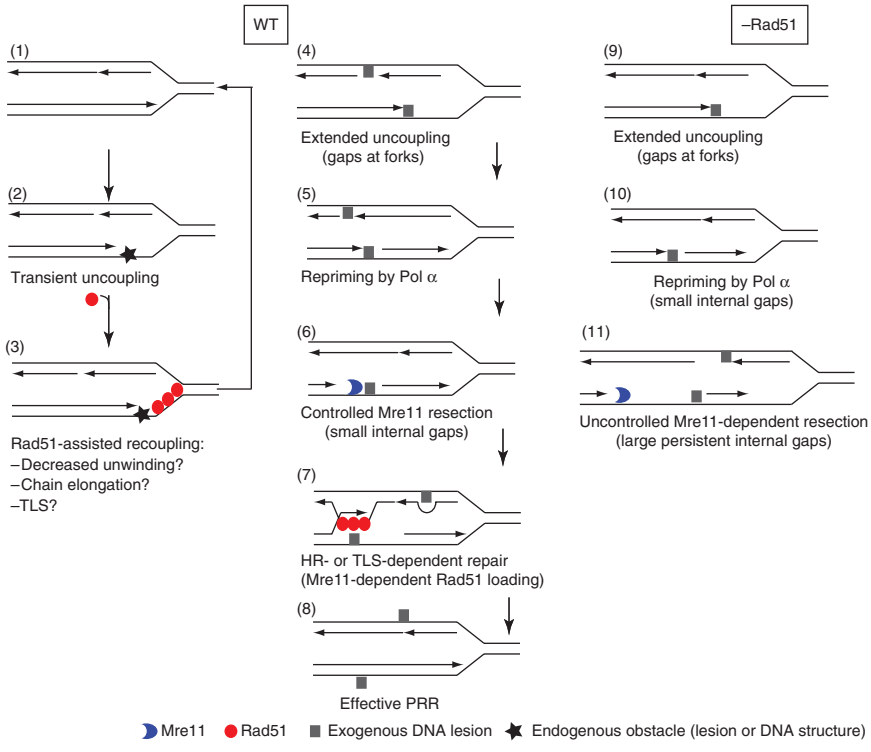

Figure 6 A model for possible roles of Rad51 during DNA replication. See text for explanation. HR, homologous recombination; TLS, translesion synthesis; PRR, postreplication repair.

at forks and behind them. However, consistent with the EM analysis, mirin substantially lowered the number of gaps detected with the gap-filling assay (**Supplementary Fig. 5**). In this assay, the effect is more noticeable with MMS treatment, in which the majority of the labeled fragments result from ssDNA gaps behind the fork. These observations indicate that ssDNA gaps behind forks are due to Mre11-dependent degradation of nascent DNA in the absence of Rad51. ssDNA gaps at forks, instead, arise independently from Mre11, either through processing by a different nuclease or solely from a defect in DNA synthesis.

DISCUSSION

The role of recombination factors in DNA replication has been postulated in the past. However, direct demonstration of this function has been impeded by the lack of an experimental system to directly address the function of recombination proteins during DNA replication. A possible direct role for Rad51 in the replication process has been inferred from recent investigations of Rad51 inactivation in DT40 cells[26]. Consistent with this, we also observed ssDNA gap accumulation at forks and behind them in yeast cells lacking Rad51 and in Rad52-deficient cells in which Rad51 function is impaired[32,33]. Rad51 foci can be observed during unperturbed S-phase progression in cultured mammalian cells[37,38]. Rad51 also mediates restart of transiently stalled forks, but this function is not linked to foci formation or to its standard role in DSB repair[34].

Although all these observations suggest that a replicative function of recombination factors could be well conserved among eukaryotes, they cannot effectively distinguish between a replicative and DNA repair function of Rad51. The accumulation of DNA lesions in Rad51-defective cells may depend on defective repair of DNA lesions accumulated after one or few cell cycles, or upon short genotoxic treatments. However, our results on *X. laevis* egg extracts now discriminate Rad51 function during DNA synthesis in the presence and absence of exogenous DNA lesions, combining selective Rad51 depletion just before one round of DNA replication and direct visualization of replication intermediates.

Our data suggest a dual role for the recombination factor Rad51 during DNA replication: restoring coupling of uncoupled leading- and lagging-strand synthesis and protecting nascent DNA from nucleolytic degradation (**Fig. 6**). Our observations indicate that Rad51 binding to chromatin during DNA replication might be required to limit the size of ssDNA stretches at replication forks (**Fig. 6**, (1)–(3)). We propose that Rad51 is recruited to replication forks upon transient uncoupling of the fork at natural impediments and consequent accumulation of longer stretches of ssDNA, similarly to DSB end resection[5]. Presumably, Rad51 could be recruited to forks undergoing problematic progression. Indeed, transient replication fork stalling and uncoupling (**Fig. 6**, (2)) may be frequent even in the absence of exogenous DNA damage and may result from endogenous lesions, multiprotein complexes obstructing fork progression or sequences prone to form secondary structures. This is reflected in the high frequency of pathological ssDNA regions at forks when Rad51 binding to chromatin is suppressed during unperturbed DNA replication. We envision three possible, non–mutually exclusive scenarios for the function of Rad51 in this context (**Fig. 6**, (3)): (i) Rad51 may bind extended ssDNA on the blocked leading strand and use its strand annealing activity to favor re-annealing with the unwound lagging strand, thus counteracting helicase activity and limiting further fork uncoupling; (ii) Rad51 binding to the transiently uncoupled fork may assist the processivity of the stalled polymerases that encounter obstacles to DNA synthesis, such as ssDNA secondary structures; and (iii) Rad51 binding may facilitate local recruitment of translesion polymerases to promote continuous synthesis across endogenous lesions. Notably, translesion polymerases assist DNA synthesis on Rad51-dependent recombination intermediates[39]. In addition, RecA, a Rad51-related protein in *E. coli*, promotes recruitment of translesion polymerases[40,41].

At the same time, if persistent uncoupling at bulky lesions leads to DNA synthesis repriming, which is especially frequent in the presence of exogenous DNA damage (**Fig. 6**, (4)–(5)), Rad51 binding to the resulting ssDNA gaps behind the forks may effectively engage them in postreplication repair (**Fig. 6**, (7)–(8)). According to this model, Rad51 binding to replication forks should be transient and selective for temporary uncoupled forks, whereas it is probably more stable in the presence of permanent DNA lesions. Notably, mammalian Rad51 paralogs that regulate Rad51 recruitment bind fork structures with high affinity and specificity[42]. Analogously, it is tempting to speculate that anti-recombinase helicases such as Srs2, Bloom or R-TEL[43,44] may prevent unscheduled homologous recombination events by counteracting inappropriate or permanent Rad51 fork association.

Although a general role for Rad51 in postreplication repair is well established, our data show that post-replicative ssDNA gaps not bound to Rad51 are prone to extensive Mre11-dependent degradation (**Fig. 6**, (9)–(11)). Rad51 may directly counteract Mre11 on these ssDNA substrates. We propose that Mre11 and Rad51 are in a dynamic equilibrium at ssDNA and counteract each other's activity through a feedback mechanism. On one hand, Mre11-dependent controlled resection could be required for Rad51 binding to ssDNA (**Fig. 6**, (6)), similarly to the mechanisms of DSB repair and RecA ssDNA-binding in *E. coli*[45]. On the other hand, the engagement of these gaps in Rad51-dependent repair could prevent excessive nucleolytic degradation, sequestering the substrates once optimal Mre11-dependent resection is achieved (**Fig. 6**, (7)). In this view, the accumulation of Mre11-dependent ssDNA gaps behind forks in absence of Rad51 may reflect the accumulation of ssDNA intermediates unproductive for strand invasion, which may in turn become susceptible to the resection apparatus. The absence of detectable post-replicative ssDNA gaps upon mirin treatment and Rad51 depletion may suggest that, in the absence of Mre11 activity, nonresected postreplicative ssDNA gaps may be below the resolution limit of EM (50–100 nt) and escape detection even in the absence of Rad51.

Notably, mutations in SbcD, the putative ortholog of Mre11 in *E. coli*, suppress lethality of RecBCD recombination-defective cells in the presence of repetitive palindromic sequences[46]. The suppression is due to the inability of SbcD mutant cells to degrade secondary structures formed at or behind replication forks[47]. However, whereas SbcD processes secondary structures formed on the template strands, the gaps we observe are caused by Mre11-dependent degradation of nascent DNA strands. The nuclease activity of Mre11 probably does not target parental DNA in eukaryotes. In any case, these observations suggest that Mre11's role in processing replication structures undergoing recombination events is conserved across species.

METHODS

Methods and any associated references are available in the online version of the paper at http://www.nature.com/nsmb/.

Note: Supplementary information is available on the Nature Structural & Molecular Biology website.

ACKNOWLEDGMENTS

We thank S. West, S. Boulton and members of the genome stability lab for their insightful comments, H. Mahbubani, J. Kirk for technical support with *X. laevis*

and the Center for Microscopy and Image Analysis of the University of Zurich for technical assistance with electron microscopy. This work was funded by Cancer Research UK. V.C. is also supported by the European Research Council start-up grant (206281), the Lister Institute of Preventive Medicine and the European Molecular Biology Organization (EMBO) Young Investigator Program. M.L. and A.R.C. are supported by the Swiss National Science Foundation grant (PP00A-114922). A.R.C. was also supported by an EMBO short-term fellowship. Recombinant human Rad51 proteins and the cDNA fragment encoding human BRC4 (residues 1511–1579 of BRCA2) cloned into pDONR221 were provided by F. Esashi (Oxford University). The pET28-based expression vectors of wild-type and mutant (K164R) *X. laevis* PCNA and the pET21-based expression vector of human p27 were provided by H. Ulrich (Cancer Research UK) and T. Hunt (Cancer Research UK), respectively. Mirin was provided by J. Gautier (Columbia University). Antibodies to Mcm2, Cdc45, Psf2 and Pol ε p60 subunit were provided by H. Takisawa (Osaka University); antibodies to Pol δ p125 subunit and Pol η were provided by S. Waga (Japan Women's University) and M. Akiyama (Nara Institute of Technology).

AUTHOR CONTRIBUTIONS

Y.H. and A.R.C. carried out experiments; M.L. and V.C. conceived experiments and wrote the manuscript.

COMPETING FINANCIAL INTERESTS

The authors declare no competing financial interests.

Published online at http://www.nature.com/nsmb/.
Reprints and permissions information is available online at http://npg.nature.com/reprintsandpermissions/.

1. Branzei, D. & Foiani, M. Maintaining genome stability at the replication fork. *Nat. Rev. Mol. Cell Biol.* **11**, 208–219 (2010).
2. Lambert, S., Froget, B. & Carr, A.M. Arrested replication fork processing: interplay between checkpoints and recombination. *DNA Repair (Amst.)* **6**, 1042–1061 (2007).
3. Prakash, S., Johnson, R.E. & Prakash, L. Eukaryotic translesion synthesis DNA polymerases: specificity of structure and function. *Annu. Rev. Biochem.* **74**, 317–353 (2005).
4. Moldovan, G.L., Pfander, B. & Jentsch, S. PCNA, the maestro of the replication fork. *Cell* **129**, 665–679 (2007).
5. West, S.C. Molecular views of recombination proteins and their control. *Nat. Rev. Mol. Cell Biol.* **4**, 435–445 (2003).
6. Tsuzuki, T. *et al.* Targeted disruption of the Rad51 gene leads to lethality in embryonic mice. *Proc. Natl. Acad. Sci. USA* **93**, 6236–6240 (1996).
7. Sonoda, E. *et al.* Rad51-deficient vertebrate cells accumulate chromosomal breaks prior to cell death. *EMBO J.* **17**, 598–608 (1998).
8. Aguilera, A. & Gomez-Gonzalez, B. Genome instability: a mechanistic view of its causes and consequences. *Nat. Rev. Genet.* **9**, 204–217 (2008).
9. Lambert, S., Watson, A., Sheedy, D.M., Martin, B. & Carr, A.M. Gross chromosomal rearrangements and elevated recombination at an inducible site-specific replication fork barrier. *Cell* **121**, 689–702 (2005).
10. Alabert, C., Bianco, J.N. & Pasero, P. Differential regulation of homologous recombination at DNA breaks and replication forks by the Mrc1 branch of the S-phase checkpoint. *EMBO J.* **28**, 1131–1141 (2009).
11. Lehmann, A.R. & Fuchs, R.P. Gaps and forks in DNA replication: Rediscovering old models. *DNA Repair (Amst.)* **5**, 1495–1498 (2006).
12. Lopes, M., Foiani, M. & Sogo, J.M. Multiple mechanisms control chromosome integrity after replication fork uncoupling and restart at irreparable UV lesions. *Mol. Cell* **21**, 15–27 (2006).
13. Heller, R.C. & Marians, K.J. Replisome assembly and the direct restart of stalled replication forks. *Nat. Rev. Mol. Cell Biol.* **7**, 932–943 (2006).
14. Petermann, E. & Caldecott, K.W. Evidence that the ATR/Chk1 pathway maintains normal replication fork progression during unperturbed S phase. *Cell Cycle* **5**, 2203–2209 (2006).
15. Moriel-Carretero, M. & Aguilera, A. A postincision-deficient TFIIH causes replication fork breakage and uncovers alternative Rad51- or Pol32-mediated restart mechanisms. *Mol. Cell* **37**, 690–701 (2010).
16. Hekmat-Nejad, M., You, Z., Yee, M.C., Newport, J.W. & Cimprich, K.A. *X. laevis* ATR is a replication-dependent chromatin-binding protein required for the DNA replication checkpoint. *Curr. Biol.* **10**, 1565–1573 (2000).
17. Trenz, K., Smith, E., Smith, S. & Costanzo, V. ATM and ATR promote Mre11 dependent restart of collapsed replication forks and prevent accumulation of DNA breaks. *EMBO J.* **25**, 1764–1774 (2006).
18. Costanzo, V. *et al.* Mre11 protein complex prevents double-strand break accumulation during chromosomal DNA replication. *Mol. Cell* **8**, 137–147 (2001).
19. Trenz, K., Errico, A. & Costanzo, V. Plx1 is required for chromosomal DNA replication under stressful conditions. *EMBO J.* **27**, 876–885 (2008).
20. McGarry, T.J. & Kirschner, M.W. Geminin, an inhibitor of DNA replication, is degraded during mitosis. *Cell* **93**, 1043–1053 (1998).
21. Hashimoto, Y. & Takisawa, H. *X. laevis*Cut5 is essential for a CDK-dependent process in the initiation of DNA replication. *EMBO J.* **22**, 2526–2535 (2003).
22. Thorslund, T. & West, S.C. BRCA2: a universal recombinase regulator. *Oncogene* **26**, 7720–7730 (2007).
23. Carreira, A. *et al.* The BRC repeats of BRCA2 modulate the DNA-binding selectivity of RAD51. *Cell* **136**, 1032–1043 (2009).
24. Leach, C.A. & Michael, W.M. Ubiquitin/SUMO modification of PCNA promotes replication fork progression in *X. laevis* egg extracts. *J. Cell Biol.* **171**, 947–954 (2005).
25. Stokes, M.P. & Michael, W.M. DNA damage-induced replication arrest in *X. laevis* egg extracts. *J. Cell Biol.* **163**, 245–255 (2003).
26. Su, X., Bernal, J.A. & Venkitaraman, A.R. Cell-cycle coordination between DNA replication and recombination revealed by a vertebrate N-end rule degron-Rad51. *Nat. Struct. Mol. Biol.* **15**, 1049–1058 (2008).
27. Fukui, T. *et al.* Distinct roles of DNA polymerases delta and epsilon at the replication fork in *X. laevis* egg extracts. *Genes Cells* **9**, 179–191 (2004).
28. Tsujikawa, L., Weinfield, M. & Reha-Krantz, L.J. Differences in replication of a DNA template containing an ethyl phosphotriester by T4 DNA polymerase and *Escherichia coli* DNA polymerase I. *Nucleic Acids Res.* **31**, 4965–4972 (2003).
29. Nagaraju, G. & Scully, R. Minding the gap: the underground functions of BRCA1 and BRCA2 at stalled replication forks. *DNA Repair (Amst.)* **6**, 1018–1031 (2007).
30. Lopes, M. Electron microscopy methods for studying in vivo DNA replication intermediates. *Methods Mol. Biol.* **521**, 605–631 (2009).
31. Sogo, J.M., Lopes, M. & Foiani, M. Fork reversal and ssDNA accumulation at stalled replication forks owing to checkpoint defects. *Science* **297**, 599–602 (2002).
32. Symington, L.S. Role of RAD52 epistasis group genes in homologous recombination and double-strand break repair. *Microbiol. Mol. Biol. Rev.* **66**, 630–670 (2002).
33. Petrini, J.H., Bressan, D.A. & Yao, M.S. The RAD52 epistasis group in mammalian double strand break repair. *Semin. Immunol.* **9**, 181–188 (1997).
34. Krogh, B.O. & Symington, L.S. Recombination proteins in yeast. *Annu. Rev. Genet.* **38**, 233–271 (2004).
35. Dupré, A. *et al.* A forward chemical genetic screen reveals an inhibitor of the Mre11–Rad50–Nbs1 complex. *Nat. Chem. Biol.* **4**, 119–125 (2008).
36. Petrini, J.H. S-phase functions of the Mre11 complex. *Cold Spring Harb. Symp. Quant. Biol.* **65**, 405–411 (2000).
37. Tashiro, S. *et al.* S phase specific formation of the human Rad51 protein nuclear foci in lymphocytes. *Oncogene* **12**, 2165–2170 (1996).
38. Tarsounas, M., Davies, D. & West, S.C. BRCA2-dependent and independent formation of RAD51 nuclear foci. *Oncogene* **22**, 1115–1123 (2003).
39. McIlwraith, M.J. *et al.* Human DNA polymerase eta promotes DNA synthesis from strand invasion intermediates of homologous recombination. *Mol. Cell* **20**, 783–792 (2005).
40. Schlacher, K., Cox, M.M., Woodgate, R. & Goodman, M.F. RecA acts in trans to allow replication of damaged DNA by DNA polymerase V. *Nature* **442**, 883–887 (2006).
41. Reuven, N.B., Arad, G., Stasiak, A.Z., Stasiak, A. & Livneh, Z. Lesion bypass by the *Escherichia coli* DNA polymerase V requires assembly of a RecA nucleoprotein filament. *J. Biol. Chem.* **276**, 5511–5517 (2001).
42. Compton, S.A., Ozgur, S. & Griffith, J.D. Ring-shaped Rad51 paralog protein complexes bind Holliday junctions and replication forks as visualized by electron microscopy. *J. Biol. Chem.* **285**, 13349–13356 (2010).
43. Sung, P. & Klein, H. Mechanism of homologous recombination: mediators and helicases take on regulatory functions. *Nat. Rev. Mol. Cell Biol.* **7**, 739–750 (2006).
44. Barber, L.J. *et al.* RTEL1 maintains genomic stability by suppressing homologous recombination. *Cell* **135**, 261–271 (2008).
45. Lisby, M. & Rothstein, R. Choreography of recombination proteins during the DNA damage response. *DNA Repair (Amst.)* **8**, 1068–1076 (2009).
46. Gibson, F.P., Leach, D.R. & Lloyd, R.G. Identification of sbcD mutations as cosuppressors of recBC that allow propagation of DNA palindromes in *Escherichia coli* K-12. *J. Bacteriol.* **174**, 1222–1228 (1992).
47. Eykelenboom, J.K., Blackwood, J.K., Okely, E. & Leach, D.R. SbcCD causes a double-strand break at a DNA palindrome in the *Escherichia coli* chromosome. *Mol. Cell* **29**, 644–651 (2008).

ONLINE METHODS

Recombinant proteins and antibodies. Recombinant human Rad51 proteins and the cDNA fragment encoding human BRC4 (residues 1511–1579 of BRCA2) cloned into pDONR221 (Invitrogen) were provided by F. Esashi (Oxford University). The fragment was then cloned into DEST15, an expression vector for GST-tagged recombinant proteins, using the Gateway system (Invitrogen). The BRC4-DEST15 plasmid was transformed to BL21-Al cells, and recombinant GST-BRC4 protein production was induced by 0.2% (w/v) L-arabinose and purified with glutathione–Sepharose 4B according to standard procedures (GE Healthcare). Control GST protein was prepared using pGEX 6P-1 empty vector (GE Healthcare). The cDNA encoding full-length *X. laevis* Rad51 was amplified by PCR using as 5′ primer (5′-ATGGATCCATGGCCATGCAAGCTCACTATC-3′) and 3′ primer (5′-AGAATTCTCAGTCCTTGGCATCTCCCAC-3′) using a *X. laevis* oocyte cDNA library and cloned into pGEX 6P-1. The GST-tagged recombinant protein was expressed and purified with glutathione–Sepharose 4B, and the GST tag was removed by Prescission Protease (GE Healthcare) treatment to obtain an untagged version of Rad51. The pET28-based expression vectors of wild-type and mutant (K164R) *X. laevis* PCNA and the pET21-based expression vector of human p27 were provided by H. Ulrich (Cancer Research UK) and T. Hunt (Cancer Research UK), respectively, and the recombinant His_6-tagged proteins were purified with Ni-NTA agarose (QIAGEN). His_6-tagged geminin was prepared as described[19].

Antibodies to Rad51 (14B4, Abcam), Pol α p180 subunit (ab31777, Abcam), PCNA (MCA1558, Serotec), Mcm7 (sc-9966, Santa Cruz), γ-H2AX (JW301, Upstate) and RPA32 (ab10359, Abcam) were obtained from the indicated providers. Antibodies to Mcm2, Cdc45, Psf2 and Pol ε p60 subunit were provided by H. Takisawa (Osaka University); antibodies to Pol δ p125 subunit and Pol η were provided by S. Waga (Japan Women's University) and M. Akiyama (Nara Institute of Technology).

***Xenopus laevis* egg extracts, chromatin fractions, replication assay and gap-filling assay.** Interphase egg extracts were prepared as described[19]. To isolate chromatin fractions, usually 4,000 demembranated sperm nuclei per μl were incubated in egg extract and diluted with 20 volumes of EB buffer (100 mM KCl, 50 mM HEPES-KOH, pH 7.5, 2.5 mM $MgCl_2$) containing 0.2% (v/v) Triton X-100 and layered onto 200 μl of a 30% (w/v) sucrose cushion made with the same buffer. The chromatin was centrifuged at 10,000*g* for 5 min at 4 °C, washed with 300 μl of EB buffer and centrifuged again at 16,100*g* for 1 min. The pellet was suspended with SDS-PAGE sample buffer and analyzed by immunoblotting. DNA replication assay with neutral[19] and alkaline agarose gel[27] and gap-labeling assay[27] were carried out as described. Mirin was provided by J. Gautier (Columbia University). ssDNA and dsDNA celluloses were obtained from Worthington.

Electron microscopy. Demembranated sperm nuclei (5,000 μl^{-1}) were incubated in 1.2–1.5 ml of egg extracts for 45 min (untreated sperm) or for 60 min (0.2% (v/v) MMS-treated sperm), diluted with 5 ml of EB buffer, layered onto 2 ml of EB buffer plus 30% (w/v) sucrose and centrifuged at 3,000*g* for 10 min at 4 °C. The pellets were resuspended in 600 μl of EB buffer and transferred to a 96-well plate (100 μl per well). 4,5′,8-Trimethylpsoralen (TMP) was added at 10 $\mu g\ ml^{-1}$ to each well. Samples were incubated on ice for 5 min in the dark and irradiated with 366-nm ultraviolet light for 7 min on a precooled metal block. The procedure from TMP addition to irradiation with ultraviolet light was repeated three more times. Then, the genomic DNA was purified through proteinase K (1 $mg\ ml^{-1}$) and RNase A (167 $\mu g\ ml^{-1}$) treatment, phenol-chloroform extraction and isopropanol precipitation. The purified DNA (20 μg) was digested with NdeI endonuclease (100 units) for 5 h, and the replication intermediates were further purified on a BND cellulose column[30] and were processed for the observation with EM as described[30]. Upon length measurements (ImageJ) of the resulting micrographs, DNA replication intermediates were identified by two parameters: (i) the presence of at least one fork (three-way junction) and (ii) the presence of at least two 'legs' of equal length, as expected after restriction digestion of a genomic fragment containing a replication fork. The analysis of replication forks derived from *rad52* mutant cells was carried out as described[12]. *Rad52* and *rad51* strains have been described[12].

See also **Supplementary Methods** for further details.

doi:10.1038/nsmb.1927

3. DISCUSSION

Topoisomerase1 is an essential mammalian enzyme. It is also the only known target of the alkaloid camptothecin, from which potent, FDA-approved anticancer agents irinotecan and topotecan are derived. Furthermore, camptothecin has been regularly used in basic research to study replication associated DNA damage. The currently accepted mode of action for this class of drugs suggests that the cytotoxicity induced by Top1 poisons is due to the formation of replication-dependent DSB. These DSB have been proposed to be central, upstream intermediates produced by unavoidable collision of replication forks with discontinuities left on the template by Top1 trapping on the nicked DNA (Top1cc and "run-off" theory, see Introduction). This model has been popular for more than 20 years, but has two important implications that have not been thoroughly tested experimentally, namely i) that replication fork stalling in response to Top1 poisons should be a direct consequence of, and thus strictly coupled to, DSB formation; ii) that HR-dependent DSB repair should be required for replication fork restart and, if a sufficiently high number of forks is affected by Top1cc, even contribute to S phase completion. This long-standing model has recently been challenged (Koster et al., 2007), wherein it was shown that Top1 poisons not only inhibit the religation step of the Top1 "cycle", but also its DNA relaxation activity, exerted by controlled rotation of the nicked DNA strand (Koster et al., 2005). This leads to the formation of positive supercoils on the DNA, which by yet unknown mechanisms would lead to fork stalling and collapse.

The main objective of this thesis was to address experimentally the implications of the "run-off theory" and to search for possible evidence of topological stress on DNA replicating *in vivo* upon Top1 poisoning.

Our BrdU ChIP-chip analysis in yeast suggests that Top1 inhibition does not affect origin timing and distribution (Fig.2.1), but leads genome-wide to transient replication fork slowdown, observable at any time point at about one third of the active replication forks (Fig.2.2). This phenomenon is even more dramatic in human cells, where the whole population of active forks is persistently slowed down already at the lowest tested CPT dose (Fig.2.6), as also supported by the high degree of sister fork asymmetry revealed by our DNA fiber analysis (Fig.2.7). Higher CPT doses, however, led to only marginal further decrease in fork progression rates, suggesting that maximal effects of Top1 poisoning are already visible at nM CPT concentrations, which are the only relevant doses to consider for clinical applications (Teicher, 2008) and to study physiological cellular responses to Top1 inhibition in basic research (O'Connell et al., 2010). Although we did detect the formation of DSB at higher CPT doses (≥1uM) in mammalian cells, DSBs could never be detected above background levels in cells treated with nM CPT doses (Fig.2.8), that are sufficient to induce a marked and global decrease in replication fork progression. Even prolonged treatments in pre-synchronized S-phase cells failed to generate detectable DSBs at nM CPT concentrations (Fig.2.12). Thus, although we cannot exclude that few breaks may escape detection in our PFGE assay, these few DSB (<100/cell; Fig2.8A-B and Ward, 1988) could not account for the marked slowdown observed upon 25nM CPT treatment on the entire population of forks [3000-12000/cell; (Ge and Blow, 2010)]. Overall, these data strongly suggest that fork slowdown can be largely uncoupled from DSB formation upon mild (nM) CPT treatments in human cells. Similarly, in yeast cells, although a general DNA damage marker (H2A phosphorylation; Redon et al., 2003) and delayed progression of a subset of replication forks are promptly detected in S-phase cells upon CPT treatment, the same experimental conditions do

not lead to levels of DSBs detectable by PFGE (Fig.2.4), nor to the activation of a sensitive DSB marker (Rad53 phosphorylation) in S phase (Redon et al., 2003 and Fig.2.5A). These data taken together strongly suggest that Top1 inhibition challenges DNA replication forks upstream of DSB formation. Consistent with this hypothesis, inactivation of HR-dependent DSB repair in three different eukaryotic systems (*S.cerevisiae*, human cell cultures and Xenopus egg extracts) did not further affect bulk DNA replication, nor the rate of fork progression upon Top1 inhibition (Fig.2.5B, Fig.2.10A, Fig.2.10C and Fig.2.11). HR seems instead to be required for later functions in the cell cycle, as HR defective yeast cells fail to progress to the next cell cycle and activate a CPT-induced checkpoint response after completion of bulk DNA synthesis (Fig.2.5). Furthermore, HR defects in both yeast and mammalian cells (Fig.2.4 and Fig.2.12.) did not lead to increased amounts of breaks even upon continuous CPT treatments. On the contrary, our PFGE experiments with CtIP-depleted mammalian cells even showed reduced amounts of DSBs when compared with the Mock treated upon treatment with high doses of CPT (Fig.2.12). Since CtIP acts at the very upstream steps of DSB repair (DNA resection), it will be important to test whether other HR mutants would show a similar phenotype. It is possible that - in the absence of resection - an alternative, faster repair pathway (NHEJ) takes over the repair process, reducing the number of detectable DNA breaks upon μM CPT treatment. An alternative hypothesis is that CtIP could directly contribute to break formation upon CPT treatments by assisting resection of the stalled/reversed forks and finally favoring fork collision with Top1ccs. Overall, these data exclude that HR-dependent DNA repair is strictly required for fork progression and S phase completion upon Top1 inhibition, thus contradicting one of the main implications of the "run-off theory".

If not collision with Top1ccs and DSB formation, what is then slowing down the replication forks upon Top1 inhibition? CPT treatments in all eukaryotic model systems resulted in rapid accumulation of reversed forks. Several lines of evidence suggest that this could result from accumulation of topological stress ahead of the forks upon CPT treatments: 1) Fork reversal was shown as an intermediate formed upon accumulation of positive supercoils ahead of the replication fork (Postow et al., 2001); 2) Top1 poisons impair the relaxation of torsional stress resulting in the increase of positive supercoiling on the DNA (Koster et al., 2007); 3) CPT induced fork slowing and reversal are frequent at chromosomal locations particularly susceptible to topological stress (i.e. termination zones and centromeres)(Fig.2.2C); 4) A significant proportion of slow moving forks due to Top1 inhibition in Xenopus egg extracts can be assisted in further progression by *in vitro* resolution of associated topological stress (Fig.2.16).

Although increased supercoiling can *per se* lead to fork reversal (Postow et al., 2001), we show here that PARP activity is required for effective fork reversal in higher eukaryotes (Fig.2.18). We envision several types of mechanism by which PARP activity could mediate fork reversal. First, in agreement with early findings (Durkacz et al., 1981), PARP could play a direct role in fork reversal by maintaining or restoring DNA supercoiling during DNA repair through PARylation of yet unknown substrates. Alternatively, PARP could have an indirect role in the process of fork reversal by regulating chromatin modifications and structure around replication forks (Hassa and Hottiger, 2008). It has been recently shown that PARP is involved in the modification of histone tails (Messner et al., 2010) thus implicating its role in nucleosome dynamics. Another indirect role of PARP in fork reversal would be imply the recruitment of other factors to the replication forks, which could in turn mediate

fork reversal upon Top1 inhibition and possibly other types of replication stress. Recent collaborative work with the group of Alessandro Vindigni (ICGEB, Trieste, Italy) suggests that PARP could be involved in the recruitment of proteins of the RecQ helicase family (particularly RecQ1), which in turn could possibly mediate fork reversal upon treatment with CPT. We are actively working on this exciting hypothesis, although the data are at this stage too preliminary to be included in this thesis. Further work will be required to identify additional cellular factors (possibly PARP targets) involved in this process and to clarify the molecular mechanism by which PARP mediates for reversal (see Perspectives). Besides impairing fork reversal, PARP inhibition also prevents CPT-induced fork slowdown (Sugimura et al, 2008, Fig.2.17) and lead to increased amounts of DSBs at low (nM) CPT concentrations (Fig.2.20 and Fig.2.21) suggesting that PARP mediated fork reversal could prevent the formation of DSBs by limiting the impact of replication forks with unrepaired Top1cc.

The CPT-induced slowdown and reversal of replication forks seem largely independent from checkpoint activation. Two lines of evidence supporting this conclusion are: 1) Fork slowdown is observed both in the presence (Fig.2.13) and absence (Fig.2.2A and Fig.2.5A) of checkpoint activation; 2) PARP inactivation abolishes CPT-induced fork slowdown (Fig.2.17) and reversal (Fig.2.18) while retaining an active checkpoint response (Fig2.19). Our attempts to study directly the role of the checkpoint response in slowing fork progression upon Top1 inhibition were overall inconclusive, as, in agreement with published results (Peterman et al., 2010), Chk1 inactivation resulted *per se* in severe fork progression defects, thus precluding to directly assess its contribution to CPT induced fork slowdown. Intriguingly, both ATR/Chk1 and ATM/Chk2 checkpoint pathways are promptly

activated at low CPT doses (25nM), associated with no detectable DNA breakage (Fig. 2.12A and Fig.2.13A). Moreover, in our experimental conditions, Chk1 activation was also found to be independent of DNA end resection mediated by CtIP, further suggesting that structures different from DSB may contribute to the checkpoint response observed upon Top1 inhibition. An interesting hypothesis is that the regressed arm may itself represent a new "DNA end", presumably indistinguishable from a DSB for the checkpoint apparatus, but generated in the absence of chromosomal breakage and/or classical DSB processing. While such a double stranded end may *per se* be recognized by the ATM checkpoint machinery, further resection of the double stranded end or partial uncoupling of leading and lagging strand at the time of fork reversal may lead to single stranded overhangs capable of activating also the ATR checkpoint response (Fig.3.1). The cellular response elicited by these alternative structures may well vary in different systems, reflecting different thresholds and mechanisms of checkpoint activation: similar DNA intermediates (reversed forks) may indeed be signaling structures in mammalian cells, but be unable to activate a DNA damage checkpoint in yeast cells (Redon et al., 2003, Fig.2.5 and Fig.2.14D). Importantly, under the same conditions, a general DNA damage marker, like H2A phosphorylation, is promptly activated in yeast cells (Redon et al., 2003). Furthermore, even in mammalian cells, treatment with low concentrations of CPT induces γH2AX foci, but these do not colocalize with the DSB marker 53BP1 (Fig.2.21). Overall these data suggest that several markers previously used to diagnose CPT-induced DSB may in fact identify different structures (e.g. the regressed arms).

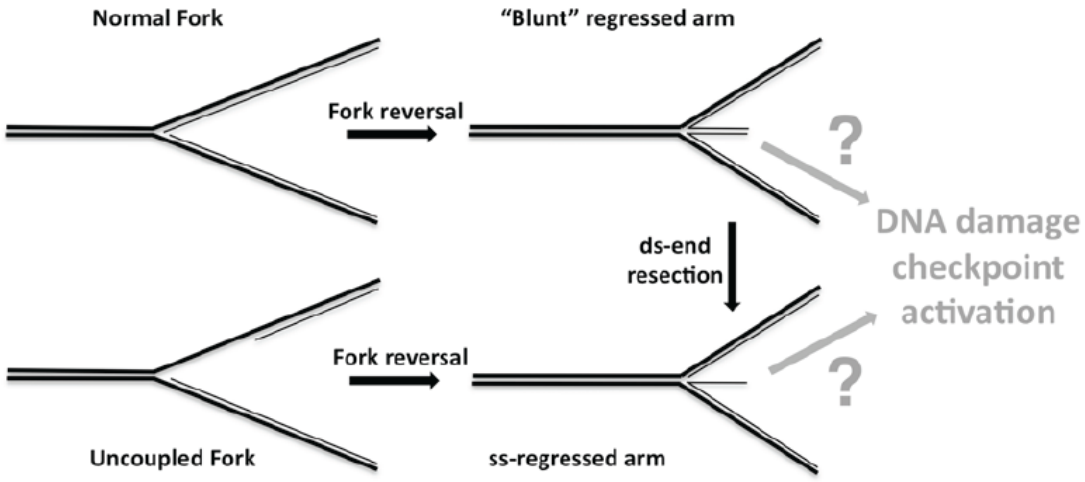

Fig.3.1 Hypothetical model for the contribution of regressed arms to checkpoint activation upon Top1 inhibition. Reversal of forks with proper coupling of leading and lagging strand synthesis (normal forks) results in ds ("blunt")-regressed arms; these could be recognized as DSB and activate *per se* the DNA damage checkpoint, even in the absence of chromosomal breakage. Further processing (resection) of the ds-end may also contribute to checkpoint activation. Fork reversal at a replication intermediate that is experiencing uncoupling of leading and lagging strand synthesis (uncoupled fork) may directly lead to ss-regressed arms and further contribute to checkpoint activation upon Top1 inhibition.

Replication forks were recently reported to slow down before impacting a DSB on the template (Doksani et al., 2009) or in short proximity to an inter-strand crosslink (Raschle et al., 2008). In both cases, active control of fork progression is proposed to assist effective repair and fork fusion at the lesion. Analogously, PARP1 could participate directly in the removal of trapped Top1 (Malanga and Althaus, 2004) and simultaneously provide more time for this reaction, by slowing/reversing active forks and preventing Top1cc conversion into DSB (Fig.3.2). It will be important to investigate whether fork reversal reflects a general strategy to protect the integrity of replicating chromosomes in face of different sources of replication stress and whether reversed forks can be reactivated for continued replication (see Perspectives).

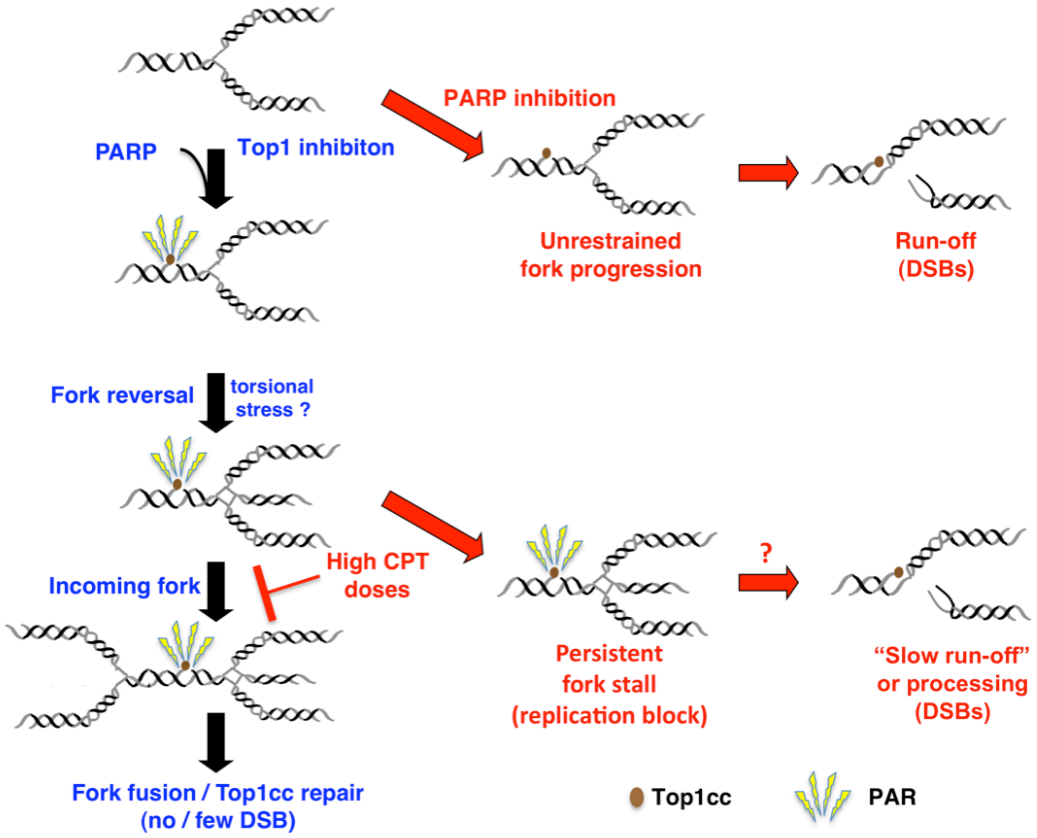

Fig.3.2. Model for the mechanism of Top1 inhibition. Upon Top1 inhibition replication forks rapidly experience reduced progression and reversal, mediated by PARP activity in higher eukaryotes, assisting Top1cc repair and replication completion. PARP inactivation leads to increased DSB, due to unrestrained fork run-off at Top1cc. High CPT doses lead to incomplete replication and persistent fork stalling, causing DSB by eventual fork run-off and/or processing.

In higher eukaryotes, checkpoint activation upon replication stress further assists replication completion by promoting local initiation events (Ge and Blow, 2010). Nonetheless, the extreme number of Top1cc upon acute (≥1μM) CPT treatments will continually stall all active replication forks (Fig.2.10A) and lead to DSB by eventual fork impact with unrepaired Top1cc by run off and/or stalled fork processing by endonucleases (Fig.3.2). However, these high CPT doses are lethal also to normal, untransformed cells (Teicher, 2008) and are not suitable for clinical use. Accordingly, genetic contributions to CPT resistance are consistently revealed in the low nanomolar range (O'Connell et al., 2010). While DSB are not detectable in these experimental conditions, a significant fraction of active replication forks (25-40%) is reversed in human and mouse cells, suggesting that reversed fork formation, remodeling and/or resolution may be more crucial determinants than DSB repair for

CPT resistance (see Perspectives).

Overall, the data in this thesis provide a mechanistic rationale for the combination of PARP and Top1 inhibitors in cancer therapy, currently in promising clinical development. Indeed, minimal doses of Top1 inhibitors - insufficient *per se* to induce significant numbers of DSB - could result in more extensive chromosomal breakage when combined with PARP inhibitors. This synergistic effect could be particularly toxic in cancer cells, often defective in DNA repair and genome integrity pathways.

4. PERSPECTIVES

In this thesis, it was shown that Top1 poisons rapidly induce replication fork slowing and reversal, which can be uncoupled from DSB formation at sub-lethal doses. Poly (ADP-ribose) polymerase (PARP) activity is required for effective fork reversal and limits DSB formation, making DSB processing dispensable for bulk DNA replication and checkpoint activation. These data have shown - for the first time in eukaryotic cells - that fork reversal could be used as cellular strategy to prevent chromosome breakage upon CPT induced replication stress and provide a mechanistic basis for the synergistic effects of PARP- and Top1 inhibitors.

The identification of fork reversal as a strategy to prevent DSBs upon CPT treatment has opened new important biological questions and corresponding avenues of research. Some of the directions that will be investigated in the future are listed below.

It would be important to analyze whether fork reversal represents a general strategy to protect replicating chromosomes in the face of both exogenous and endogenous lesions. Specific experiments will be designed to look at replication intermediates upon treatment with different kinds of DNA damages like interstrand crosslinking (induced by agents like mitomycin C and cisplatin), DNA polymerase inhibitor aphidicolin, etc. These experiments would initially be performed in Xenopus egg extracts as this provides an excellent platform for EM analysis due to the high frequency of replication intermediates, which speeds up this kind of analysis. Any encouraging result would then be further investigated in the mammalian cell culture system. It would also be important to investigate if fork reversal is also a mechanism to deal with endogenous lesions faced during replication, although this kind of analysis is potentially hampered by paucity of these events on the large eukaryotic genomes. PARP is activated after different kinds of DNA damage, but gets rapidly degraded after activation, which is mediated by PAR glycohydrolase (PARG). Since PARP is essential for fork reversal upon CPT treatment (this thesis), we hypothesize

that, if fork reversal is a general mechanism used to face endogenous lesions, inhibition/depletion of PARG might stabilize PAR polymers and leading to accumulation of reversed forks even in the absence of exogenous damage. Experiments will be designed to test this hypothesis by the inhibition/depletion of PARG and analysis of replication intermediates by EM. Similarly, PARG inhibition may hamper restart of reversed forks once DNA damaging agents (Top1 inhibitors and/or others) are removed from the culture media.

It will also be important to elucidate the role of different factors that contribute to form/revert/process reversed forks in response to CPT treatment. Genetic defects in several members of the RecQ helicase family (WRN, BLM and RecQ1) are associated with increased sensitivity to CPT, suggesting a possible role in the fork reversal process. Furthermore, recent collaborative work with the group of Alessandro Vindigni (ICGEB, Trieste, Italy) has identified RecQ1 as an interacting partner and target of PARP1. Intriguingly, our preliminary collaborative data suggest that RecQ1 depletion phenocopies PARP inhibition upon CPT treatment in terms of DSB formation and replication fork progression. EM experiments are thus being performed to test whether, upon CPT treatment, RecQ1 could be required for PARP-mediated fork reversal. Similar experiments will also be performed with WRN and BLM depleted cells to test their contributions to fork reversal, fork slowing and DSB formation upon CPT treatments. Another important candidate to test is the Fanconi Anemia group M protein (FANCM), a translocase of the FA family. It has been shown to promote reversal of replication fork structures *in vitro* (Gari et al., 2008)and has been proposed to sense and remodel stalled replication forks(Luke-Glaser et al., 2010). Collaborative efforts have been planned to address this open question with the groups of Angelos Constantinou (CNRS, Montpellier, France) and Johan de Winter (Amsterdam, NL), focused on FANCM and other related replication stress factors. We will test the role of FANCM, analyzing MEFs from FANCM defective mice upon treatment with CPT and other DNA damaging drugs.

Finally, we are obviously interested in investigating the mechanism by which PARP could directly mediate fork reversal. As discussed earlier, PARP activation could restore DNA supercoiling and has also been shown to modify histone tails. We will start our investigations in this direction by testing whether any of the PARP-dependent chromatin modifications is required for fork reversal upon CPT treatments.

5. MATERIALS AND METHODS

Materials

The antibodies used in this study were goat polyclonal anti-CtIP (Santa Cruz), rabbit monoclonal pATM-Ser1981 (Epitomics), rabbit monoclonal pChk1-Ser345 (Cell signalling), rabbit polyclonal TFIIH (Santa Cruz), mouse monoclonal anti-BrdU antibody 2B1 (MBL) and anti-PK SV5-Pk1 antibody (AbD Serotec), EL7 for total Rad53 and F9 for pRad53 (Bermejo et al., 2007), mouse monoclonal γH2AX (Millipore), rabbit polyclonal 53BP1 (Santa Cruz). The chemicals and peptides used in this study were: Camptothecin (Sigma); Topotecan Hydrochloride (Molekula); α1-Mating Factor (Sigma); Nocodazole (Sigma); Thymidine (Sigma), Olaparib (Selleck Chemicals), NU1025 (Sigma), UCN-01 (Sigma).

Cell growth, labeling and synchronization

The *S. cerevisiae* strains used in this study are W303-1A and its isogenic derivative *rad52D* (CY2272). Strains were grown in YPD, presynchronized in G1 by adding 3μg/ml α factor and released from the G1 arrest by addition of Pronase 200μg/ml in presence or absence of 50μM CPT at 25°C. For BrdU ChIP-chip experiments, strains and conditions were described (Bermejo et al., 2007; Katou et al., 2003). For these experiments, cells were released from α factor at 16°C, by media replacement with pre-cooled YPD in the presence of Pronase 200μg/ml. Rpc25 and Rpb3 subunit binding were analyzed by ChIP-chip 60min after release in presence of CPT or during unperturbed S-phase respectively.

U2OS-derived cells were cultured in Dulbecco's modified Eagle's medium (DMEM) supplemented with 10% fetal bovine serum (FBS) and standard antibiotics. For

synchronization, 50% confluent U2OS cells were treated with 2mM Thymidine for 24h. The cells were then washed 3 times with PBS and released into fresh medium for 3h. This was followed by nocodazole treatment for 12h (75ng/ml). The cells were again washed three times with PBS and incubated in fresh medium. At the indicated times, cells were trypsinized and processed for cell cycle analysis, western blots and PFGE.

Primary MEFs PARP-$1^{+/+}$ (F20) and PARP-$1^{-/-}$ (A1) (Wang et al., 1995) were maintained in Dulbecco's modified Eagle's medium (DMEM) supplemented with 10% fetal bovine serum, 100 U/ml penicillin, and 100 μg/ml streptomycin in an atmosphere containing 10% CO_2 at 37 °C.

siRNA depletions in mammalian cells

U2OS cells were transfected with relevant siRNA using Oligofectamine (Invitrogen) according to the manufacturer's instructions. The cells were then incubated for 48-72 hrs. The mRNA target sequences used for siRNAs were the following: siLuciferase (CGUACGCGGAAUACUUCGA), siCtIP (GCUAAAACAGGAACGAAUCUUTT)

ChIP-chip analysis

S.cerevisiae oligonucleotide microarrays were provided by Affymetrix (*S.cerevisiae* Tiling 1.0R, P/N 900645). BrdU ChIP-chip analyses were carried out as described (Katou et al., 2003), using similar statistical parameters for peak identification. Orange (untreated, NT) and blue (CPT) histogram bars in the Y-axis show the average signal ratio of loci significantly enriched in the BrdU-immunoprecipitated fraction (IP) along the indicated regions in log2 scale (detection p-value and change p-value are <0.001). Merging of the BrdU peaks +/- CPT is also shown in green. The

X-axis shows chromosomal coordinates. *ARS* elements are indicated, green lines indicate centromeres and the blue horizontal bars mark the position of the ORFs.

CPT-induced replication fork delay and association with specific chromosomal features (CEN, TERs) were scored as described in the legends of Fig.2.1, Fig.2.2and Table 2.1.

Cell Cycle Analysis, Protein Extraction and Western Blotting

The procedures for yeast protein extraction, Western blotting, and FACS analysis were already described (Pellicioli et al., 1999). U2OS cells were processed for FACS analysis as described (Stojic et al., 2004). Mammalian cell extracts were prepared in Laemmli buffer (4% SDS, 20% glycerol, 120 mM Tris-HCl pH 6.8), proteins were resolved by SDS-PAGE and transferred to nitrocellulose. Immunoblots were performed using the appropriate antibodies.

Mammalian fork progression by DNA fibre analysis

Asynchronously growing U2OS cells were labelled with 30μM CldU, washed with PBS and exposed to 250μM IdU. Cells were lysed and DNA fibres were stretched onto glass slides as reported earlier (Jackson and Pombo, 1998) The DNA fibres were denatured with 2.5M HCl for 1 h, washed with PBS and blocked with 2% BSA in PBST for 30 min. The newly replicated CldU and IdU tracks were revealed with anti-BrdU antibodies recognizing CldU (Abcam, rat) and IdU (Becton Dickinson, mouse), respectively. The following secondary antibodies were used: anti-mouse Alexa 488 (Molecular Probes), anti-rat Cy3 (Jackson Immunoresearch). Microscopy was carried out with an Olympus IX81 fluorescence microscope and acquired with a CCD camera (Orca AG, Hamamatsu). The images were processed with CellR software (Olympus).

Statistical analysis of tract length was performed using GraphPad Prism.

DSB detection by PFGE

DSB detection by PFGE was performed as described (Hanada et al., 2007), with minor modifications. Synchronous or asynchronous subconfluent cultures of U2OS cells were harvested by trypsinization, and agarose plugs of $5x10^5$ cells were prepared in a disposable plug mold (BioRad). Plugs were then incubated in lysis buffer (100mM EDTA, 1% (w/v) sodium lauryl sarcosyl, 0.2% (w/v) sodium deoxycholate, 1mg/ml proteinase K) at 37°C for 72h. Plugs were then washed four times in 20mM Tris-HCl pH 8.0, 50mM EDTA before loading onto an agarose gel. Electrophoresis was performed for 23h at 14°C in 0.9% (w/v) Pulse Field Certified Agarose (BioRad) containing Tris-borate/EDTA 1X buffer in a BioRad CHEF DR III apparatus, according to the following protocol (Block I: 9h, 120° included angle, 5.5 V/cm, 30-18s switch; Block II: 6h, 117° included angle, 4.5 V/cm, 18-9s switch; Block III: 6h, 112° included angle, 4.0 V/cm, 9-5s switch). The gel was then stained with ethidium bromide and analyzed using an Alpha Innotech Imaging system. DSB quantification was performed by the ImageJ software, normalizing DSB signals to unsaturated signals of DNA trapped in the well (loading control). For each treatment, relative DSB levels were obtained comparing each treatment to the background DSB signals observed in untreated (NT) conditions. Average values and standard deviations were obtained from three biological replicates of the same experiment.

***Xenopus* egg extracts and replication assays**

Interphase egg extracts were prepared as described (Trenz et al., 2006). DNA replication assay with neutral (Trenz et al., 2006) and alkaline agarose gels (Fukui et

al., 2004) were previously described. The fork restart assay (Fig2.16) was performed as follows. After the first incubation of sperm nuclei in the presence of 100μM TPT, the extract sample (40μl) was first diluted with 10 vol. of EB-buffer (100mM KCl, 50mM Hepes-KOH [pH 7.5], 2.5mM MgCl2) + 0.005 % Triton X-100, layered onto 200μl of EB-buffer + 30% Sucrose, and spun at 10,000g for 5 min at 4°C. The pellet was resuspended with 20μl of the buffer (50mM Tris-HCl [pH 7.5], 50mM KCl, 10mM MgCl2, 0.5mM DTT, 0.1mM EDTA, 30μg/ml BSA) in the presence or absence of 6 units of purified calf thymus Topoisomerase I (Invitrogen). After 30 min incubation at 37°C, 300μl of the EB-buffer was added to the reaction, which was subsequently spun at 10,000g for 2 min at 4°C. The pellet was resuspended with 40μl of the 2nd extract - containing a-32P-dATP, His-geminin (320nM), His-p27 (40μg/ml) and TPT (100μM) - incubated for the indicated times and subjected to DNA replication assay.

EM analysis of genomic DNA in yeast, mammalian cells and *Xenopus* egg extracts

In vivo psoralen cross-linking, isolation of total genomic DNA, and enrichment of the RIs from yeast and mammalian cells were performed as described (Lopes, 2009). For Xenopus egg extracts demembranated sperm nuclei (5,000/μl) were incubated in 1.2-1.5 ml of egg extracts for 50 min in presence or absence of 50μM TPT, diluted with 5ml of EB-buffer, layered onto 2ml of EB-buffer + 30% Sucrose and spun at 3,000g for 10 min at 4°C. The pellets were re-suspended in 600μl of EB-buffer and transferred to a 96 well plate (each 100μl/well). Trimethylpsoralen (TMP) was added at 10μg/ml to each well. Samples were incubated on ice for 5 min in the dark, irradiated with 366nm UV light for 7 min on a pre-cooled metal block. The procedure

from TMP addition to UV irradiation was repeated three more times. Then, the genomic DNA was purified by proteinase K (1mg/ml) and RNase A (167µg/ml) treatment, phenol/chloroform extraction, and isopropanol precipitation. The purified DNA (20µg) was digested with NdeI endonuclease (100 units) for 5 hr, and the replication intermediates were further purified on BND cellulose column and processed for EM observation as previously described (Lopes 2009).

Agarose bi-dimensional gel electrophoresis (2D gel)

Total genomic DNA was extracted by the CTAB method (Lopes et al., 2003) and used for 2D gel electrophoresis, as originally described (Brewer and Fangman, 1987). First dimensions were run at RT for 16 hr at 50 V in 0.4% agarose gels in 1X TBE. Second dimensions were run at 4°C for 9 hr at 140 V in 1.0% gels in 1X TBE + 0.3µg/ml EtBr recirculating buffer. Restriction fragments, probes, and hybridization conditions were as described (Lopes et al., 2003), except that DNA was here blotted onto BIORAD Zeta-Probe GT membranes prior to hybridization.

Immunofluorescence staining and analyses

For immunostaining, cells were fixed in methanol, stained with 53BP1 (sc-22760, Santa Cruz 1/500) and γH2AX (05-636, Upstate; 1/500), detected by appropriate secondary antibodies (Molecular Probes) and mounted with vectashield (Vector Laboratories). Cells were imaged in a Leica DM RB microscope equipped with a Leica DFC 360 FX camera. Images were taken at 60x magnification using the Leica Application Suite 3.3.0 software.

Foci counting was performed by ImageJ, using the "Analyze particle" function. Average values for foci number and γH2AX/53BP1 colocalization were obtained

from at least 50 cells per sample. Very similar numbers to those shown in Figure 2.21 have been obtained by an independent experiment.

6. REFERENCES

Akbari, M., and Krokan, H.E. (2008). Cytotoxicity and mutagenicity of endogenous DNA base lesions as potential cause of human aging. Mech Ageing Dev *129*, 353-365.

Bartek, J., and Lukas, J. (2003). Chk1 and Chk2 kinases in checkpoint control and cancer. Cancer Cell *3*, 421-429.

Bartek, J., and Lukas, J. (2007). DNA damage checkpoints: from initiation to recovery or adaptation. Curr Opin Cell Biol *19*, 238-245.

Baxter, J., and Diffley, J.F. (2008). Topoisomerase II inactivation prevents the completion of DNA replication in budding yeast. Mol Cell *30*, 790-802.

Bell, S.P., and Stillman, B. (1992). ATP-dependent recognition of eukaryotic origins of DNA replication by a multiprotein complex. Nature *357*, 128-134.

Bermejo, R., Doksani, Y., Capra, T., Katou, Y.M., Tanaka, H., Shirahige, K., and Foiani, M. (2007). Top1- and Top2-mediated topological transitions at replication forks ensure fork progression and stability and prevent DNA damage checkpoint activation. Genes & Development *21*, 1921-1936.

Branzei, D. (2010). Ubiquitin family modifications and template switching. FEBS Lett *2011*.

Bressan, D.A., Baxter, B.K., and Petrini, J.H. (1999). The Mre11-Rad50-Xrs2 protein complex facilitates homologous recombination-based double-strand break repair in Saccharomyces cerevisiae. Mol Cell Biol *19*, 7681-7687.

Brewer, B.J., and Fangman, W.L. (1987). The localization of replication origins on ARS plasmids in S. cerevisiae. Cell *51*, 463-471.

Bromberg, K.D., Burgin, A.B., and Osheroff, N. (2003). A two-drug model for etoposide action against human topoisomerase IIalpha. J Biol Chem *278*, 7406-7412.

Bryant, H.E., Petermann, E., Schultz, N., Jemth, A.S., Loseva, O., Issaeva, N., Johansson, F., Fernandez, S., McGlynn, P., and Helleday, T. (2009). PARP is activated at stalled forks to mediate Mre11-dependent replication restart and recombination. EMBO J *28*, 2601-2615.

Buschta-Hedayat, N., Buterin, T., Hess, M.T., Missura, M., and Naegeli, H. (1999). Recognition of nonhybridizing base pairs during nucleotide excision repair of DNA. Proc Natl Acad Sci U S A *96*, 6090-6095.

Bzymek, M., Thayer, N.H., Oh, S.D., Kleckner, N., and Hunter, N. Double Holliday junctions are intermediates of DNA break repair. Nature *464*, 937-941.

Caiafa, P., and Zlatanova, J. (2009). CCCTC-binding factor meets poly(ADP-ribose) polymerase-1. J Cell Physiol *219*, 265-270.

Calzada, A., Hodgson, B., Kanemaki, M., Bueno, A., and Labib, K. (2005). Molecular anatomy and regulation of a stable replisome at a paused eukaryotic DNA replication fork. Genes Dev *19*, 1905-1919.

Costa, R.M., Chigancas, V., Galhardo Rda, S., Carvalho, H., and Menck, C.F. (2003). The eukaryotic nucleotide excision repair pathway. Biochimie *85*, 1083-1099.

De Bont R, v.L.N. (2004). Endogenous DNA damage in humans: a review of quantitative data. Mutagenesis *19(3):169-85.*

Desai, S.D., Liu, L.F., Vazquez-Abad, D., and D'Arpa, P. (1997). Ubiquitin-dependent destruction of topoisomerase I is stimulated by the antitumor drug camptothecin. J Biol Chem *272*, 24159-24164.

Doksani, Y., Bermejo, R., Fiorani, S., Haber, J.E., and Foiani, M. (2009). Replicon dynamics, dormant origin firing, and terminal fork integrity after double-strand break formation. Cell *137*, 247-258.

Durkacz, B.W., Shall, S., and Irwin, J. (1981). The effect of inhibition of (ADP-ribose)n biosynthesis on DNA repair assayed by the nucleoid technique. Eur J Biochem *121*, 65-69.

Esteller, M. (2007). Epigenetic gene silencing in cancer: the DNA hypermethylome. Hum Mol Genet *16 Spec No 1*, R50-59.

Fien, K., Cho, Y.S., Lee, J.K., Raychaudhuri, S., Tappin, I., and Hurwitz, J. (2004). Primer utilization by DNA polymerase alpha-primase is influenced by its interaction with Mcm10p. J Biol Chem *279*, 16144-16153.

Friedman, K.L., Raghuraman, M.K., Fangman, W.L., and Brewer, B.J. (1995). Analysis of the temporal program of replication initiation in yeast chromosomes. J Cell Sci Suppl *19*, 51-58.

Frosina, G., Fortini, P., Rossi, O., Carrozzino, F., Raspaglio, G., Cox, L.S., Lane, D.P., Abbondandolo, A., and Dogliotti, E. (1996). Two pathways for base excision repair in mammalian cells. J Biol Chem *271*, 9573-9578.

Fukui, T., Yamauchi, K., Muroya, T., Akiyama, M., Maki, H., Sugino, A., and Waga, S. (2004). Distinct roles of DNA polymerases delta and epsilon at the replication fork in Xenopus egg extracts. Genes Cells *9*, 179-191.

Garg, P., and Burgers, P.M. (2005). DNA polymerases that propagate the eukaryotic DNA replication fork. Crit Rev Biochem Mol Biol *40*, 115-128.

Gari, K., Decaillet, C., Stasiak, A.Z., Stasiak, A., and Constantinou, A. (2008). The Fanconi anemia protein FANCM can promote branch migration of Holliday junctions and replication forks. Mol Cell *29*, 141-148.

Ge, X.Q., and Blow, J.J. (2010). Chk1 inhibits replication factory activation but allows dormant origin firing in existing factories. J Cell Biol *191*, 1285-1297.

Hanada, K., Budzowska, M., Davies, S.L., van Drunen, E., Onizawa, H., Beverloo, H.B., Maas, A., Essers, J., Hickson, I.D., and Kanaar, R. (2007). The structure-specific endonuclease Mus81 contributes to replication restart by generating double-strand DNA breaks. Nat Struct Mol Biol *14*, 1096-1104.

Hashimoto, Y., Chaudhuri, A.R., Lopes, M., and Costanzo, V. (2010). Rad51 protects nascent DNA from Mre11-dependent degradation and promotes continuous DNA synthesis. Nat Struct Mol Biol *17*, 1305-1311.

Hassa, P.O., and Hottiger, M.O. (2008). The diverse biological roles of mammalian PARPS, a small but powerful family of poly-ADP-ribose polymerases. Front Biosci *13*, 3046-3082.

Heyer, W.D., Ehmsen, K.T., and Liu, J. (2010). Regulation of homologous recombination in eukaryotes. Annu Rev Genet *44*, 113-139.

Heyer, W.D., Li, X., Rolfsmeier, M., and Zhang, X.P. (2006). Rad54: the Swiss Army knife of homologous recombination? Nucleic Acids Res *34*, 4115-4125.

Higgins, N.P., Kato, K., and Strauss, B. (1976). A model for replication repair in mammalian cells. J Mol Biol *101*, 417-425.

Hoeijmakers (2009). DNA damage, aging, and cancer. N Engl J Med.

Holm, C., Covey, J.M., Kerrigan, D., and Pommier, Y. (1989). Differential requirement of DNA replication for the cytotoxicity of DNA topoisomerase I and II inhibitors in Chinese hamster DC3F cells. Cancer Res *49*, 6365-6368.

Interthal, H., Chen, H.J., Kehl-Fie, T.E., Zotzmann, J., Leppard, J.B., and Champoux, J.J. (2005). SCAN1 mutant Tdp1 accumulates the enzyme--DNA intermediate and causes camptothecin hypersensitivity. EMBO Journal *24*, 2224-2233.

Jackson, D.A., and Pombo, A. (1998). Replicon clusters are stable units of chromosome structure: evidence that nuclear organization contributes to the efficient activation and propagation of S phase in human cells. J Cell Biol *140*, 1285-1295.

Jiricny, J. (2006). The multifaceted mismatch-repair system. Nat Rev Mol Cell Biol *7*, 335-346.

Kannouche, P., and Stary, A. (2003). Xeroderma pigmentosum variant and error-prone DNA polymerases. Biochimie *85*, 1123-1132.

Kannouche, P.L., Wing, J., and Lehmann, A.R. (2004). Interaction of Human DNA Polymerase eta with Monoubiquitinated PCNA; A Possible Mechanism for the Polymerase Switch in Response to DNA Damage. Mol Cell *14*, 491-500.

Kaplan, D.L., Davey, M.J., and O'Donnell, M. (2003). Mcm4,6,7 uses a "pump in ring" mechanism to unwind DNA by steric exclusion and actively translocate along a duplex. J Biol Chem *278*, 49171-49182.

Katou, Y., Kanoh, Y., Bando, M., Noguchi, H., Tanaka, H., Ashikari, T., Sugimoto, K., and Shirahige, K. (2003). S-phase checkpoint proteins Tof1 and Mrc1 form a stable replication-pausing complex. Nature *424*, 1078-1083.

Kim, J.K., Patel, D., and Choi, B.S. (1995). Contrasting structural impacts induced by cis-syn cyclobutane dimer and (6-4) adduct in DNA duplex decamers: implication in mutagenesis and repair activity. Photochem Photobiol *62*, 44-50.

Koster, D.A., Croquette, V., Dekker, C., Shuman, S., and Dekker, N.H. (2005). Friction and torque govern the relaxation of DNA supercoils by eukaryotic topoisomerase IB. Nature *434*, 671-674.

Koster, D.A., Palle, K., Bot, E.S., Bjornsti, M.A., and Dekker, N.H. (2007). Antitumour drugs impede DNA uncoiling by topoisomerase I. Nature *448*, 213-217.

Krogh, B.O., and Symington, L.S. (2004). Recombination proteins in yeast. Annu Rev Genet *38*, 233-271.

Lehmann, A.R. (2005). Replication of damaged DNA by translesion synthesis in human cells. FEBS Lett *579*, 873-876.

Lindahl, T. (1993). Instability and decay of the primary structure of DNA. Nature *362*, 709-715.

Liu, L.F. (1989). DNA topoisomerase poisons as antitumor drugs. Annu Rev Biochem *58*, 351-375.

Lopes, M. (2009). Electron microscopy methods for studying in vivo DNA replication intermediates. Methods Mol Biol *521*, 605-631.

Lopes, M., Cotta-Ramusino, C., Liberi, G., and Foiani, M. (2003). Branch migrating sister chromatid junctions form at replication origins through Rad51/Rad52-independent mechanisms. Molecular Cell *12*, 1499-1510.

Lukas, C., Falck, J., Bartkova, J., Bartek, J., and Lukas, J. (2003). Distinct spatiotemporal dynamics of mammalian checkpoint regulators induced by DNA damage. Nat Cell Biol *5*, 255-260.

Luke-Glaser, S., Luke, B., Grossi, S., and Constantinou, A. (2010). FANCM regulates DNA chain elongation and is stabilized by S-phase checkpoint signalling. EMBO J *29*, 795-805.

Mahaney, B.L., Meek, K., and Lees-Miller, S.P. (2009). Repair of ionizing radiation-induced DNA double-strand breaks by non-homologous end-joining. Biochem J *417*, 639-650.

Malanga, M., and Althaus, F.R. (2004). Poly(ADP-ribose) reactivates stalled DNA topoisomerase I and Induces DNA strand break resealing. J Biol Chem *279*, 5244-5248.

Marinsek, N., Barry, E.R., Makarova, K.S., Dionne, I., Koonin, E.V., and Bell, S.D. (2006). GINS, a central nexus in the archaeal DNA replication fork. EMBO Rep *7*, 539-545.

Masai, H., Matsumoto, S., You, Z., Yoshizawa-Sugata, N., and Oda, M. (2010). Eukaryotic chromosome DNA replication: where, when, and how? Annu Rev Biochem *79*, 89-130.

Masutani, C., Kusumoto, R., Iwai, S., and Hanaoka, F. (2000). Mechanisms of accurate translesion synthesis by human DNA polymerase eta. EMBO J *19*, 3100-3109.

Messner, S., Altmeyer, M., Zhao, H., Pozivil, A., Roschitzki, B., Gehrig, P., Rutishauser, D., Huang, D., Caflisch, A., and Hottiger, M.O. (2010). PARP1 ADP-ribosylates lysine residues of the core histone tails. Nucleic Acids Res *38*, 6350-6362.

Mimitou, E.P., and Symington, L.S. (2008). Sae2, Exo1 and Sgs1 collaborate in DNA double-strand break processing. Nature *455*, 770-774.

Mimitou, E.P., and Symington, L.S. (2009). Nucleases and helicases take center stage in homologous recombination. Trends Biochem Sci *34*, 264-272.

Minca, E.C., and Kowalski, D. Multiple Rad5 activities mediate sister chromatid recombination to bypass DNA damage at stalled replication forks. Mol Cell *38*, 649-661.

Modrich, P. (2006). Mechanisms in eukaryotic mismatch repair. J Biol Chem *281*, 30305-30309.

O'Connell, B.C., Adamson, B., Lydeard, J.R., Sowa, M.E., Ciccia, A., Bredemeyer, A.L., Schlabach, M., Gygi, S.P., Elledge, S.J., and Harper, J.W. (2010). A genome-wide camptothecin sensitivity screen identifies a mammalian MMS22L-NFKBIL2 complex required for genomic stability. Mol Cell *40*, 645-657.

O'Connor, T.R., Boiteux, S., and Laval, J. (1989). Repair of imidazole ring-opened purines in DNA: overproduction of the formamidopyrimidine-DNA glycosylase of

Escherichia coli using plasmids containing the fpg+ gene. Ann Ist Super Sanita *25*, 27-31.

Paques, F., and Haber, J.E. (1999). Multiple pathways of recombination induced by double-strand breaks in Saccharomyces cerevisiae. Microbiol Mol Biol Rev *63*, 349-404.

Pellicioli, A., Lucca, C., Liberi, G., Marini, F., Lopes, M., Plevani, P., Romano, A., Di Fiore, P.P., and Foiani, M. (1999). Activation of Rad53 kinase in response to DNA damage and its effect in modulating phosphorylation of the lagging strand DNA polymerase. Embo J *18*, 6561-6572.

Petermann, E., Woodcock, M., and Helleday, T. (2010). Chk1 promotes replication fork progression by controlling replication initiation. Proc Natl Acad Sci U S A *107*, 16090-16095.

Pommier, Y. (2006). Topoisomerase I inhibitors: camptothecins and beyond. Nature Reviews Cancer *6*, 789-802.

Postow, L., Crisona, N.J., Peter, B.J., Hardy, C.D., and Cozzarelli, N.R. (2001). Topological challenges to DNA replication: conformations at the fork. Proc Natl Acad Sci U S A *98*, 8219-8226.

Pouliot, J.J., Yao, K.C., Robertson, C.A., and Nash, H.A. (1999). Yeast gene for a Tyr-DNA phosphodiesterase that repairs topoisomerase I complexes. Science *286*, 552-555.

Pursell, Z.F., Isoz, I., Lundstrom, E.B., Johansson, E., and Kunkel, T.A. (2007). Yeast DNA polymerase epsilon participates in leading-strand DNA replication. Science *317*, 127-130.

Raschle, M., Knipscheer, P., Enoiu, M., Angelov, T., Sun, J., Griffith, J.D., Ellenberger, T.E., Scharer, O.D., and Walter, J.C. (2008). Mechanism of replication-coupled DNA interstrand crosslink repair. Cell *134*, 969-980.

Redon, C., Pilch, D.R., Rogakou, E.P., Orr, A.H., Lowndes, N.F., and Bonner, W.M. (2003). Yeast histone 2A serine 129 is essential for the efficient repair of checkpoint-blind DNA damage. EMBO Rep *4*, 678-684.

Robertson, A.B., Klungland, A., Rognes, T., and Leiros, I. (2009). DNA repair in mammalian cells: Base excision repair: the long and short of it. Cell Mol Life Sci *66*, 981-993.

Rogakou, E.P., Pilch, D.R., Orr, A.H., Ivanova, V.S., and Bonner, W.M. (1998). DNA double-stranded breaks induce histone H2AX phosphorylation on serine 139. J Biol Chem *273*, 5858-5868.

Rothstein, R., Michel, B., and Gangloff, S. (2000). Replication fork pausing and recombination or "gimme a break". Genes Dev *14*, 1-10.

Rouleau, M., Patel, A., Hendzel, M.J., Kaufmann, S.H., and Poirier, G.G. (2010). PARP inhibition: PARP1 and beyond. Nat Rev Cancer *10*, 293-301.

Schultz, N., Lopez, E., Saleh-Gohari, N., and Helleday, T. (2003). Poly(ADP-ribose) polymerase (PARP-1) has a controlling role in homologous recombination. Nucleic Acids Res *31*, 4959-4964.

Shiloh, Y. (1997). Ataxia-telangiectasia and the Nijmegen breakage syndrome: related disorders but genes apart. Annu Rev Genet *31*, 635-662.

Stewart, L., Redinbo, M.R., Qiu, X., Hol, W.G., and Champoux, J.J. (1998). A model for the mechanism of human topoisomerase I. Science *279*, 1534-1541.

Stillman, B. (2008). DNA polymerases at the replication fork in eukaryotes. Mol Cell *30*, 259-260.

Stojic, L., Mojas, N., Cejka, P., Di Pietro, M., Ferrari, S., Marra, G., and Jiricny, J. (2004). Mismatch repair-dependent G2 checkpoint induced by low doses of SN1 type methylating agents requires the ATR kinase. Genes Dev *18*, 1331-1344.

Su, T.T. (2006). Cellular responses to DNA damage: one signal, multiple choices. Annu Rev Genet *40*, 187-208.

Sugasawa, K. (2010). Regulation of damage recognition in mammalian global genomic nucleotide excision repair. Mutat Res *685*, 29-37.

Sugasawa, K., Ng, J.M., Masutani, C., Iwai, S., van der Spek, P.J., Eker, A.P., Hanaoka, F., Bootsma, D., and Hoeijmakers, J.H. (1998). Xeroderma pigmentosum group C protein complex is the initiator of global genome nucleotide excision repair. Mol Cell *2*, 223-232.

Sugasawa, K., Okamoto, T., Shimizu, Y., Masutani, C., Iwai, S., and Hanaoka, F. (2001). A multistep damage recognition mechanism for global genomic nucleotide excision repair. Genes Dev *15*, 507-521.

Sugimura, K., Takebayashi, S., Taguchi, H., Takeda, S., and Okumura, K. (2008). PARP-1 ensures regulation of replication fork progression by homologous recombination on damaged DNA. J Cell Biol *183*, 1203-1212.

Swann, P.F., Waters, T.R., Moulton, D.C., Xu, Y.Z., Zheng, Q., Edwards, M., and Mace, R. (1996). Role of postreplicative DNA mismatch repair in the cytotoxic action of thioguanine. Science *273*, 1109-1111.

Takahashi, T.S., Wigley, D.B., and Walter, J.C. (2005). Pumps, paradoxes and ploughshares: mechanism of the MCM2-7 DNA helicase. Trends Biochem Sci *30*, 437-444.

Takeda, D.Y., and Dutta, A. (2005). DNA replication and progression through S phase. Oncogene *24*, 2827-2843.

Teicher, B.A. (2008). Next generation topoisomerase I inhibitors: Rationale and biomarker strategies. Biochem Pharmacol *75*, 1262-1271.

Tissier, A., Frank, E.G., McDonald, J.P., Iwai, S., Hanaoka, F., and Woodgate, R. (2000). Misinsertion and bypass of thymine-thymine dimers by human DNA polymerase iota. EMBO J *19*, 5259-5266.

Trenz, K., Smith, E., Smith, S., and Costanzo, V. (2006). ATM and ATR promote Mre11 dependent restart of collapsed replication forks and prevent accumulation of DNA breaks. EMBO Journal *25*, 1764-1774.

Tuduri, S., Crabbe, L., Conti, C., Tourriere, H., Holtgreve-Grez, H., Jauch, A., Pantesco, V., De Vos, J., Thomas, A., Theillet, C.*, et al.* (2009). Topoisomerase I suppresses genomic instability by preventing interference between replication and transcription. Nat Cell Biol *11*, 1315-1324.

Wang, J.C. (2002). Cellular roles of DNA topoisomerases: a molecular perspective. Nat Rev Mol Cell Biol *3*, 430-440.

Wang, L., Lin, C.M., Brooks, S., Cimbora, D., Groudine, M., and Aladjem, M.I. (2004). The human beta-globin replication initiation region consists of two modular independent replicators. Mol Cell Biol *24*, 3373-3386.

Wang, Z.Q., Auer, B., Stingl, L., Berghammer, H., Haidacher, D., Schweiger, M., and Wagner, E.F. (1995). Mice lacking ADPRT and poly(ADP-ribosyl)ation develop normally but are susceptible to skin disease. Genes Dev *9*, 509-520.

Ward, J.F. (1988). DNA damage produced by ionizing radiation in mammalian cells: identities, mechanisms of formation, and reparability. Prog Nucleic Acid Res Mol Biol *35*, 95-125.

Wasko, B.M., Holland, C.L., Resnick, M.A., and Lewis, L.K. (2009). Inhibition of DNA double-strand break repair by the Ku heterodimer in mrx mutants of Saccharomyces cerevisiae. DNA Repair (Amst) *8*, 162-169.

Weterings, E., and van Gent, D.C. (2004). The mechanism of non-homologous end-joining: a synopsis of synapsis. DNA Repair (Amst) *3*, 1425-1435.

Wu, Y., Kantake, N., Sugiyama, T., and Kowalczykowski, S.C. (2008). Rad51 protein controls Rad52-mediated DNA annealing. J Biol Chem *283*, 14883-14892.

Yang, Y.G., Cortes, U., Patnaik, S., Jasin, M., and Wang, Z.Q. (2004). Ablation of PARP-1 does not interfere with the repair of DNA double-strand breaks, but compromises the reactivation of stalled replication forks. Oncogene *23*, 3872-3882.

Zechiedrich, E.L., and Cozzarelli, N.R. (1995). Roles of topoisomerase IV and DNA gyrase in DNA unlinking during replication in Escherichia coli. Genes Dev *9*, 2859-2869.

Zhang, Y.W., Regairaz, M., Seiler, J.A., Agama, K.K., Doroshow, J.H., and Pommier, Y. (2011). Poly(ADP-ribose) polymerase and XPF-ERCC1 participate in distinct pathways for the repair of topoisomerase I-induced DNA damage in mammalian cells. Nucleic Acids Res.

Zhu, Z., Chung, W.H., Shim, E.Y., Lee, S.E., and Ira, G. (2008). Sgs1 helicase and two nucleases Dna2 and Exo1 resect DNA double-strand break ends. Cell *134*, 981-994.

7. ACKNOWLEDGEMENTS

I would like to thank Prof. Massimo Lopes for giving me the opportunity to do my PhD in his lab, and especially for the stimulating discussions, the ideas and the scientific freedom he gave me. He has not only been an amazing teacher and mentor, but also a great source of inspiration and a great friend.

I am very grateful to my thesis committee members, Prof. Michael Hengartner, Dr. Vincenzo Costanzo and Dr. Angelos Constantinou for their inputs and commitment to my PhD committee.

Furthermore I would like to thank Prof. Joe Jiricny for giving me the opportunity to work his great institute.

I would also like to thank the members of the Lopes Lab, Kai, Cindy, Akshay, Isabella and Judith for their support, discussions and for the great working atmosphere in the lab. Special thanks to Raquel, for the wonderful technical support that I from her received during my PhD.

I would like to express my gratitude to Yoshi, Rodrigo and Danielle for the great collaboration and discussions with them.

Furthermore I would like to thank my friends and colleagues at IMCR, in particular, Javi, Martin and Kim.

Last but not least, I would like to thank my parents, Rita and Pranab Ray Chaudhuri for their continuous support throughout.

Dear Nitika, thanks for being there by my side always and for all the support you gave me!

CURRICULUM VITAE

Surname: **Ray Chaudhuri**

Name: **Arnab**

Date of birth: **25.08.1980**

Place of birth: **Kolkata**

Nationality: **Indian**

Education:

10th grade: Central Board of Secondary Education (CBSE). Faculty Higher Secondary School, Guwahati, India. 1997

12th grade: Central Board of Secondary Education (CBSE). Hariyana Vidya Mandir, Kolkata, India. 1999

Bachelor of Science: (Microbiology, Chemistry, Zoology).Garden City College of Science And Management Studies, Bangalore University, Bangalore, India. 2002

Master of Science (Medical) in Biochemistry: Kasturba Medical College, Mangalore, Manipal Academy of Higher Education (Now Manipal University), India. 2005

Master thesis: Purification of Glyceraldehyde 3-Phosphate Dehydrogenase from Ehrlich Ascites Carcinoma cells. Group of Prof Manju Ray, Indian Association for the Cultivation of Science (IACS), India. 2004

PhD at Institute of Molecular Cancer Research, University of Zürich.
Project: Uncovering the Structural Determinants of DNA Replication Stress Induced by Topoisomerase Inhibition. Dec 2007-present.

Professional experience:

Sept 2005 – Feb 2006 Junior Scientist, Manipal Acunova, Bangalore, India

June 2006 – Sept2007 Research Fellow with Dr. B.S. Patro, Bio-Organic Division Bhabha Atomic Research Centre, Mumbai, India.

Fellowship and Awards:

EMBO Short Term Fellowship 2008 to visit CRUK, Clare Hall for a period of 3 months.

Future of Science award 2011 from Keystone Symposia awards committee to attend the Keystone symposia meeting on DNA replication and recombination.

Publications:

Yoshitami Hashimoto, **Arnab Ray Chaudhuri**, Massimo Lopes & Vincenzo Costanzo.(2010) Rad51 protects nascent DNA from Mre11-dependent degradation and promotes continuous DNA synthesis. **Nature Structural and Molecular Biology**. doi:10.1038/nsmb.1927